The Effect of Netropsin on One-electron Oxidation of DNA

A Thesis
Presented to
The Academic Faculty

By

Lezah Wilette Roberts

In Partial Fulfillment
Of the Requirements for the Degree
Doctorate of Philosophy in Chemistry

Georgia Institute of Technology
August 2005

The Effect of Netropsin on One-electron Oxidation of DNA

Approved by:

Dr. Gary B. Schuster, (Advisor)
College of Chemistry and Biochemistry
Georgia Institute of Technology

Dr. Donald Doyle
College of Chemistry and Biochemistry
Georgia Institute of Technology

Dr. Laren Tolbert
College of Chemistry and Biochemistry
Georgia Institute of Technology

Dr. Roger Wartell
College of Biology
Georgia Institute of Technology

Dr. Nicholas Hud
College of Chemistry and Biochemistry
Georgia Institute of Technology

Date Approved: May 27, 2005

Dedication

I dedicate this to my parents William and Hazel Roberts who have always been supportive of me and keep encouraging me from day to day. It is because of them I am the person I am today. I wish I could give back half of what they given me. I hope to the kind of parent they are to me. I thank you and I love you very much!

I would also like to dedicate this to my sisters Yvette Roberts and Ardria Cooper. Growing up with you has been a blessing. You are very special to me.

I thank God for my family.

Acknowledgements

I would like to thank my Savior Jesus Christ. All things are made possible through Him and I could not succeed without Him in my life. Thank You Lord!!!!

I would like to thank my advisor, Dr. Gary B. Schuster, for giving me the opportunity to work in his research laboratory. He has been very patient with me and I have learned a great deal under his guidance. He has opened up an area of chemistry that I was not aware of when I first started at GA Tech. I greatly appreciate all the support he has given me through the years and I just want to say THANK YOU.

I would like to thank the Schuster group members past and present who have helped me during the years. There help has meant a lot. Even though at times I didn't see eye to eye with them, I like them all and cherish the time I have spent with them. I also thank them for putting up with my moodiness. I would like to thank Valerie Sartor for training me when I first joined the group. Merci Valerie for all your help. I would like to thank Anthony Dotse and Ibrahim Abdou for helping me with my synthesis. Thank you Dr. Edna Boone for being there when I had a question and for being my friend and who is still there when I need her. Cheers Miss Edna! To Dr. Rochelle Fisher Bradford, thank you for all your advice and for being a good friend. You are a good friend and I missed having you in the lab. Thank you for your support. To Dr. Susi Coons Moore you are a great friend thank you for your help, advice and support. We got through those lit exams together. I will always remember those times. Gracias! To Dr. Genara Andrade, you were a mess and I will always remember hanging out and going to the gym. Thank you for

being a friend and all your support. I will remember it always. To Ms. Chiko Umeweni thank you for being a friend and for your energy. Everything will work our out. Thank you for your spirit. To Ms. Thabisile Ndlebe thank you for being a great friend. I will miss you dearly. It was great hanging out with you and getting to know you. Keep in touch, God has great things in store for you and I wish you all the happiness in the world. To Ms. Gozde Guler it was fun knowing you Good luck on everything and stay bubbly. To Sriram Kanvah, Abraham Joy and Chuseng Liu, thank you for all your help when I needed it.

To Mamie Gaskin and Karen Tyree, thank you for your support and encouragement through the years.

To Robert Crummie Sr., Mrs. Snow, Mrs. Martin, Usher Board #3, Young Adult Choir and rest of the Mount Calvary Family: thank you for making me a part of your church home.

I would like to thank my family for all their support and my brother-in-law, James Cooper III for all his help.

To all my friends in other departments, you have made Tech just a little bit better and I thank you for your support. To Ms. Monique Hite thank you for the encouragement and I pray God will bless you in everything you do.

Memoriam

In Memory of Mrs. Cheryl R. Crummie. We started GA Tech together and even though we didn't finish together we were and will always be friends. You are in a better place and I miss you very much. Thank you for your strength. Even when you were sick, I never saw you complain. Thank you for bringing me to Mount Calvary and giving me a Church home. It is strange not seeing you there. You were a Godly woman and someone to look up too and I pray that I can be more like you in my spiritual journey. There were so many things I wanted to say so I will say this now I love you and I will see you again.

Your Sister in Christ,

Lezah

Table of Contents

List of Tables

List of Figures

List of Schemes

List of Abbreviations

A	Adeinine
AQ	Anthtaquinone
BET	back electron transfer
C	Cytidine
^{o}C	degrees Celsius
CD	Circular Dichroism
CV	Cyclic Voltammetry
D_2O	Deuterated water
DNA	Deoxy-ribonucleic acid
DPEA	diisopropyl ethyl amine
EA	Electron acceptor
ED	Electron donor
ET	electron transfer
ε	extinction coefficient
G	Guanine
ΔG	Change in Gibbs Free Energy
I	Inosine
kcal	kilocalories
M	molar
mol	moles

NaPi	Sodium Phosphate
NHE	Normal Hydrogen Electrode
nm	nano meters
NMR	Nuclear Magnetic Resonance Spectroscopy
$^1O_2$	singlet oxygen
O_2	Molecular oxygen
PAGE	Polyacrylamide Gel Electrophoresis
SSB	Single strand breaks
T	Thymine
T_m	Melting temperature
TQ	Naphthacenedion
UAQ	Uridine linked anthraquinone
UV-vis	Ultraviolet-Visible Spectroscopy
V	volts

Abstract

One electron oxidation of DNA has been studied extensively over the years. When a charge is injected into a DNA duplex, it migrates through the DNA until it reaches a trap. Upon further reactions, damage occurs in this area and strand cleavage can occur. Many works have been performed to see what can affect this damage to DNA. Netropsin is a minor groove binder that can bind to tracts of four to five A:T base pairs. It has been used in the studies within to determine if it can protect DNA against oxidative damage, caused by one-electron oxidation, when it is bound within the minor groove of the DNA. By using a naphthacenedione derivative as a photosensitizer, several DNA duplexes containing netropsin binding sites as well as those without binding sites, were irradiated at 420 nm, analyzed, and visualized to determine its effect on oxidative damage. It has been determined netropsin creates a quenching sphere of an average of $5.8 * 10^8$ Å whether bound to the DNA or not. Herein we will show netropsin protects DNA against oxidative damage whether it is free in solutions or bound within the minor groove of a DNA duplex.

Chapter I: DNA

Introduction

DNA, Deoxyribonucleic acid, is vital for the survival of living organisms. Its functions include the production of proteins as well as passing genetic information from one generation to another[1]. It is involved in cellular reproduction by replication, transcribes RNA which in turn is translated to proteins.

Damage to DNA can cause many problems to the living organism and can start a chain of events for cellular death[2]. When DNA is damaged and the damage is not repaired, mutations can occur in the DNA strand. When DNA is mutated, it can cause problems with transcription and translation, causing various diseases and protein deficiencies. For example these mutations lead to incorrect transcription of RNA. The incorrect RNA strand in turn is translated into the incorrect amino acids causing the synthesis of incorrect enzymes. These enzymes could be lethal to the cell by not performing its primary function of the appropriate metabolic reaction. Damage to the DNA can also affect the genetic information it stores.

DNA can be damaged by physiological surroundings as well as during the course of performing important biological processes [3]. It is susceptible to be oxidative damaged by ionizing radiation, metabolic process products and UV light. The exposure of mammalian and bacterial cells to UV light above 320 nm, where DNA is invisible (

260 nm, Figure 1-1), can cause endogenous molecules to act as sensitizers which may lead to photosensitized reactions within cells[4-6]. The photosensitized reactions can lead to DNA damage and the caused damage leads to mutations in the DNA which changes the DNA chemically[7].

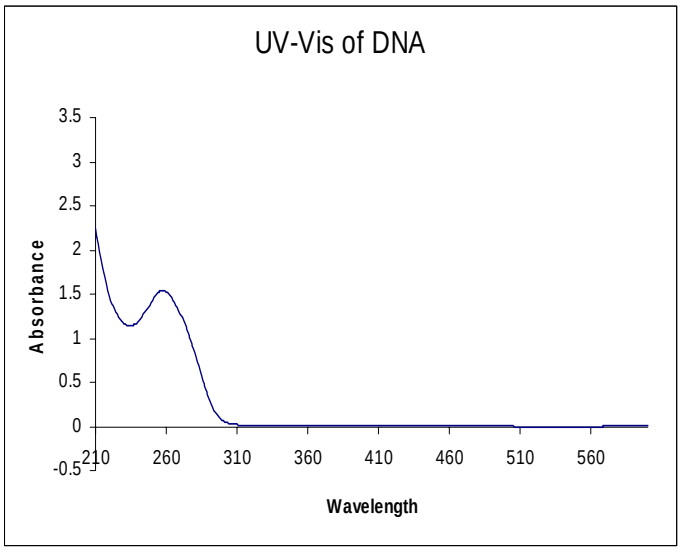

Figure 1- 1. The UV-Vis absorbance spectrum of DNA strand with a peak maximum of ~ 260 nm.

One of the reactions responsible for the interactions with DNA and photosensitizer is electron transfer. Electron transfer reactions are responsible for numerous biological processes[8]. To mimic these processes, scientists have studied electron transfer between synthetic compounds and DNA. Through these experiments it has been found the π,π interaction between the stacked bases of DNA provides a pathway for charge transport. Several research groups have undertaken the task of elucidating the

mechanism of DNA damage by monitoring how charge propagates through the DNA[9]. The study of one-electron oxidative damage of DNA has flourished and a growing interest has not only led to the elucidation of the mechanism but also expanded into an array of other studies. These studies include understanding how changing different parameters and environmental influences such as, backbone modifications[10], base modifications[11], base pair mismatches[12], base bulges[13], as well as adding outside factors such as proteins[14] affect the charge's migration.

A way to mimic how oxidative damage occurs in DNA is to use photo-active molecules that can be excited in order to introduce a charge into the DNA to promote electron transfer. DNA's unique structure and the way charge propagates through DNA have brought up the possibility of using it in electronic devices[15,16]. Therefore understanding how charge propagates through duplex DNA has attracted scientists from diverse disciplines. Before we can understand how DNA is damaged, understanding the structure of DNA is important.

DNA Structure

DNA is made up of four monomers called nucleotides that are covalently linked together to form oligomers. The monomers can combine to create numerous arrays of sequences and each possible DNA sequence determines genetic characteristics, protein synthesis and gene function[7]. Each nucleotide is made up of three different moieties, a 2-deoxyribose sugar, a phosphate group and a planar aromatic heterocyclic base (Figure 1-2). The 2-deoxyribose sugar is a cyclic molecule that contains two free hydroxyl groups located on the 5′ carbon and the 3′ carbon. There is no hydroxyl group on the sugar at the 2′ as in a ribose therefore the sugar moiety is a 2-deoxyribose. In DNA, these hydroxyl

groups are called the 5′ and the 3′ hydroxyls. It is the hydroxyl groups that give a DNA oligomer its designation of 5′ and 3′ end.

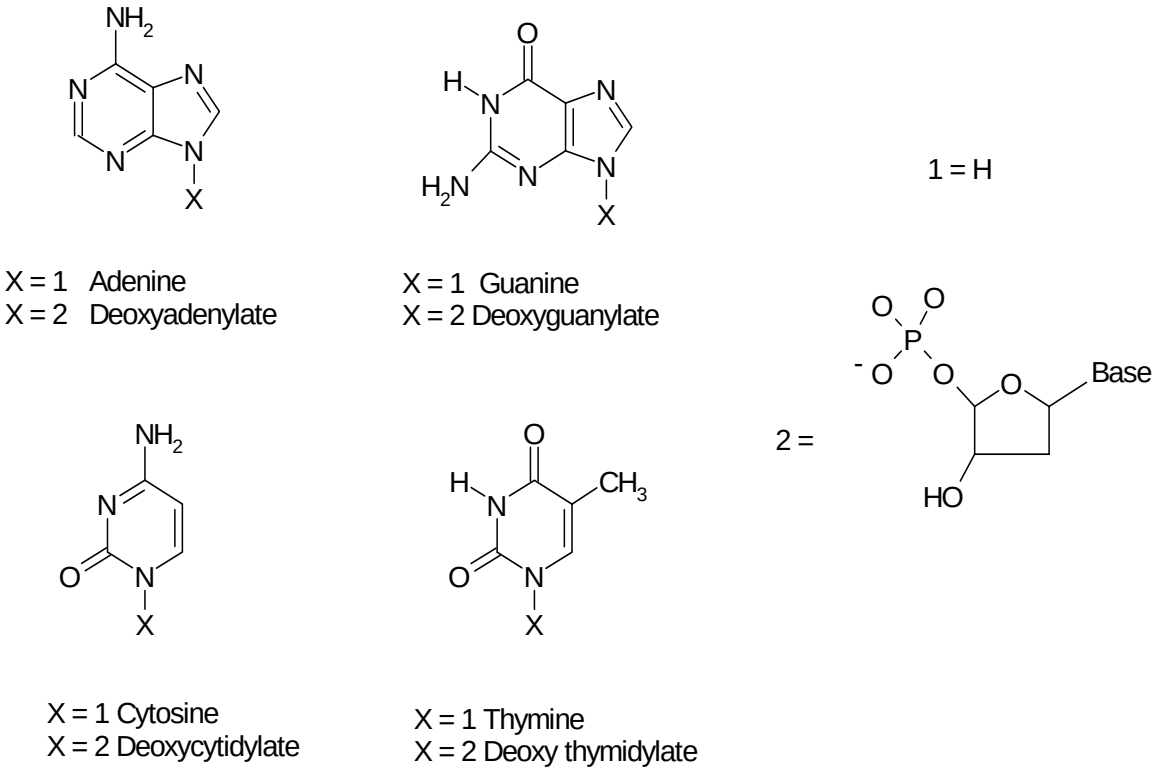

Figure 1-2. The DNA bases. When x = 1 the structures represent the bases. When x = 2 the structures represent the nucleotides as found in DNA.

The negatively charged phosphate group is covalently linked to the 5′ hydroxyl on the 2-deoxyribose sugar. These phosphate groups link one nucleotide monomer to another joining the 5′ end of one nucleotide to the 3′ hydroxyl of another end creating phosphodiester bonds (Figure 1-3).

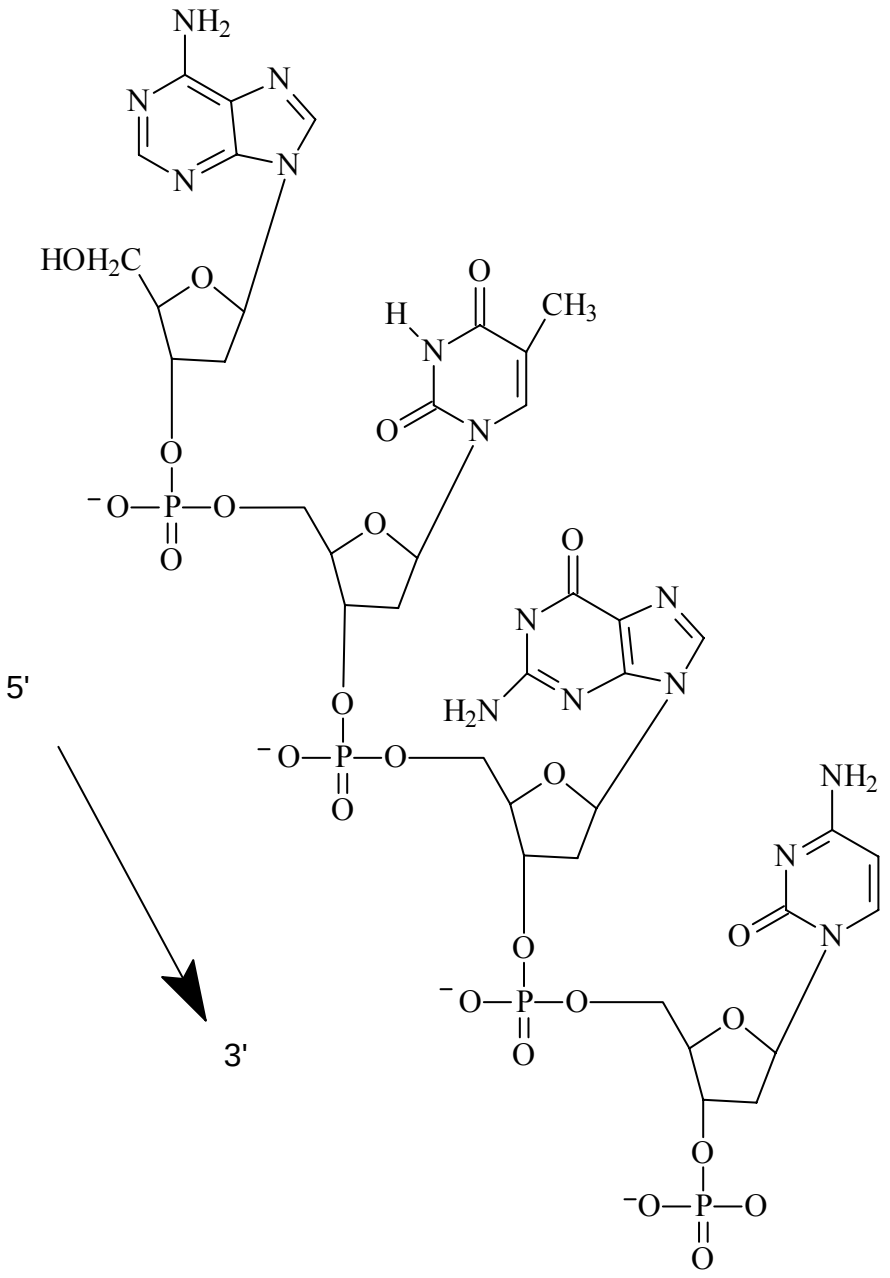

Figure 1-3. The four DNA nucleotides connected by phosphodiester bonds in a DNA strand.

There are four bases that make one nucleotide monomer different from the other. These bases are adenine (A), cytosine (C), guanine (G), and thymine (T). Adenine and guanine are a part of the purine family of compounds and cytosine and thymine are a part of the pyrimidine family. The bases are covalently linked with a glycosidic bond to the carbon-1 (C-1) position also known as the anomeric carbon of the 2-deoxyribose sugar. It is oriented in the β position where it is on the same side of the sugar as the 5′ carbon[17]. The bases form complementary pairs to one another[18]. The G is the natural complement to C and A the complement to T (Figure 1-4). The G:C base pair have three hydrogen bonds while A:T base pairs contain only two and the pairing of these bases is called Watson-Crick base pairing. The G has an acceptor:donor:donor (a:d:d) functional groups while C has a d:a:a functional groups to make them H bond to one another. The A has a d:a groups that pair with the a:d groups of T.

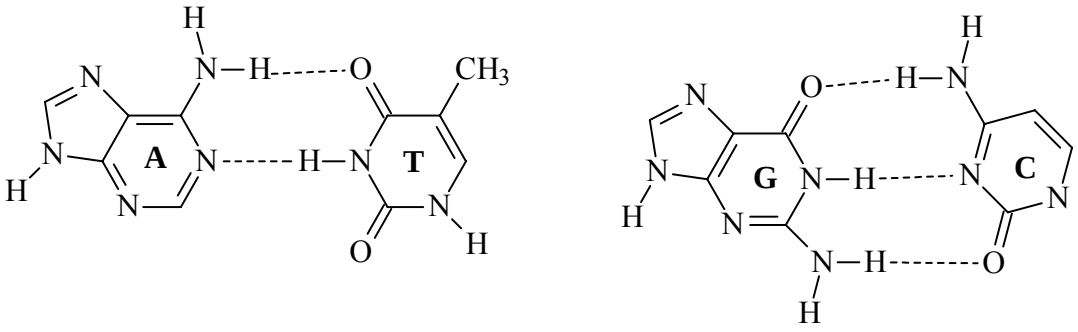

Figure 1-4. Watson and Crick base pairs. A:T and G:C are complementary as found in DNA duplexes.

In the cell DNA is naturally found as a duplex (Figure 1-5) also referred to as double stranded DNA. The helical structure of DNA was first elucidated by Watson and Crick in 1953 using X-ray fiber diffraction and the chemical evidence of base complementarities[19]. The oligomers form a double helix in which the two strands run anti-parallel to one another, the 5′ end of one strand to the 3′ end of the other. These anti-parallel strands are complementary to one another and are held together by hydrogen bonding between donor (d) and acceptor (a) groups on the bases. The base complementarity makes DNA strands complementary [7]to one another. Because of its helical structure, the two strands cannot be separated without the helix being unwound[7].

When the DNA exists in a double helix, the phosphate and sugar moieties make up its backbone while the bases make up the inner region of the duplex. The bases form a structure that resembles the rungs of a ladder. The bases also make this inner area of the duplex is hydrophobic. The outer region is hydrophilic due to the negatively charged backbone of alternating phosphate and sugar groups. DNA is considered an acid because in physiological conditions, its backbone is totally ionized. Due to its negative charges, positive ions are needed to counter act the charges. In a physiological environment, proteins, polyamines and metal ions such as sodium keep the two strands from repelling one another.

The helix is wound around an imaginary axis to form a right handed or left handed structure. The bases are positioned perpendicular to the imaginary axis and the spacing of the strands creates two grooves that have uneven dimensions. One of the grooves is known as the minor groove the other is known as the major groove. The

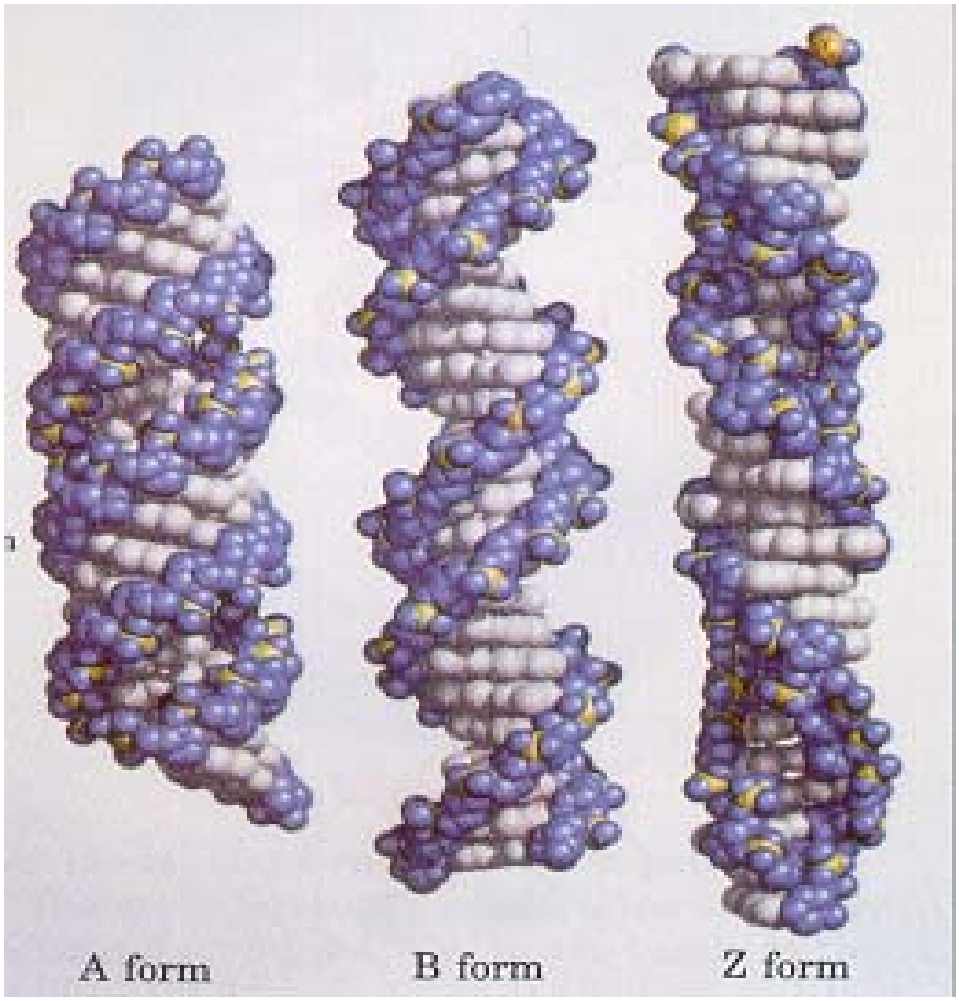

Figure 1-5. Space filled model of different forms of DNA, A form, B form, and Z form.[20]

minor groove is the area between the complementary strands where the bases act as the floor of the groove and the backbone acts as the wall. The major groove is also between the complementary strands but the parts of the strands are not complementary to one another. The bases act as the ceiling and the backbones are the walls. This groove is also typically bigger than the minor groove depending on the conformation of the DNA.

Double stranded DNA exists in several forms and can create several different conformations; A, B, and Z-form. These are the major forms of DNA duplexes. The A-form DNA has a right handed helical structure, Z-form which has a left handed helical structure, and the most common form B-form DNA also has a right handed structure (Figure 1-5). The three different forms differ from one another not only by their left or right handedness but by the differences in minor groove width, pitch and rise (Table 1-1). It is these differences that give each form of DNA different heights and widths as well as the diameter of the axis as seen in table 1-1 (Figure 1-6). The three different forms also exist under different conditions. There are also different other types of DNA structures such as four way junctions, hairpins, cruciform, and triplexes structures. During the course of the studies here in, the focus will remain on B-form DNA of different sequences.

Table 1-1 A table giving the parameters of each major form of DNA. Data was obtained from reference 20.

Conformation	**A**	**B**	**Z**
Rise per base Pair (Å)	2.3	3.4	3.8
Diameter (Å)	25.5	23.7	18.4
Base pair per Turn	11	10.4	12
Pitch per turn	25	35.4	45.6
Base tilt	19^{o}	1^{o}	9^{o}
Major Groove	Narrow/Deep	Wide/Deep	Flat
Minor Groove	Broad/Shallow	Narrow/Deep	Narrow/Deep

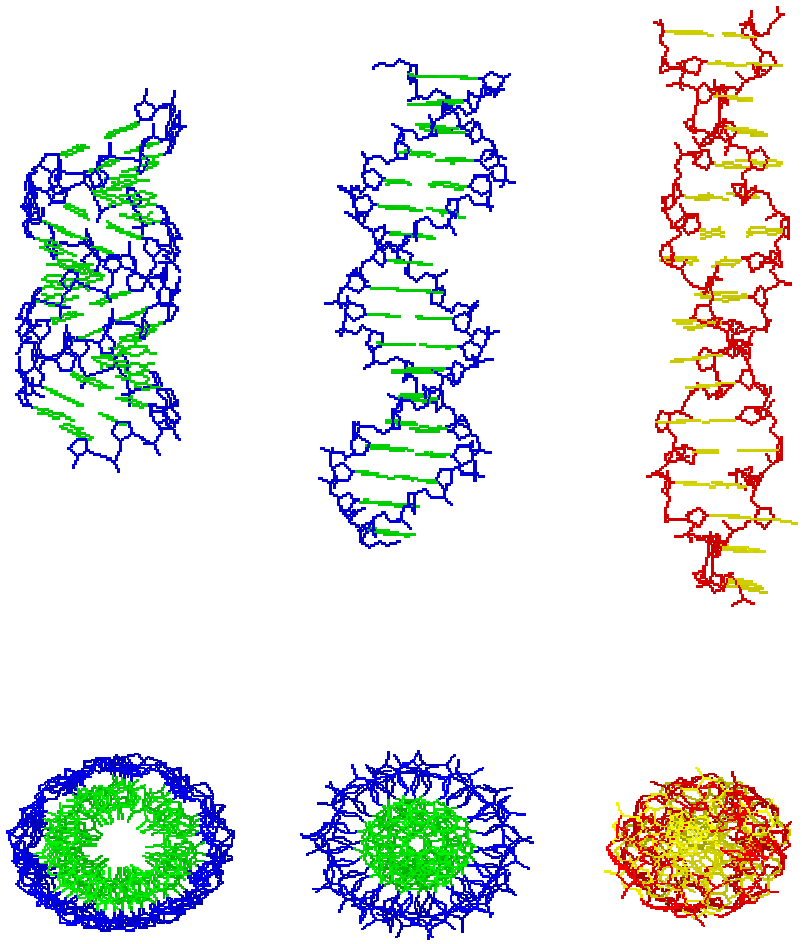

Figure 1-6. A hyperchem rendering of the three major forms of DNA A, B and Z-form respectively. Below is another view showing the differences in the diameter of the axis for the different forms.

Conclusion

DNA can be damaged can be caused by several different processed one of which is photosensitization. Through out this study we have concentrated on the damage caused by photosensitized reaction. During the course of this report the author will discuss types of DNA damage and how damage occurs; netropsin and why it may be possible that it can protect DNA form oxidative damage; preliminary experiments leading up to the main study; as well as the effect of netropsin affects one-electron oxidation of DNA.

References

(1) Avery, O., MacLeod, C., McCarty, M. *J. Expt. Med* **1944**, *79*, 137-157.

(2) Kochevar, I. E., Dunn, D. A., *In Bioorganic Photochemistry* **1990**, 1, 273-315.

(3) Gasper, S. M., Armitage, B., Shui, X., Hu, G. G., Yu, C., Schuster, G. B., Williams, L. D. *J. Am. Chem. Soc.* **1998**, *120*, 12402-12409.

(4) Becker, D., Sevilla, M. D. *Adv. Rad. Biol.* **1993**, *17*, 121-180.

(5) Cheng, K. C., Cahill, D. S., Kasai, H., Nishimura, S., Loeb, L. A. *J. Biol. Chem* **1992**, *267*, 166-172.

(6) Heelis, P. F., Hartman, R. F., Rose, S. D. *Chem. Soc. Rev.* **1996**, 289.

(7) Voet, D., Voet, J. G. *Biochemistry*; 2nd ed.; John Wiley & Sons, INC: New York.

(8) Ly, D., Sanii, L., Schuster, G. B. *J. Am. Chem. Soc.* **1999**, *121*, 9400-9410.

(9) Armitage, B. *Chem. Rev.* **1998**, *98*, 1171-1200.

(10) Barnett, R. N., C. L. Cleveland, A. Joy, U. Landman, and G. B. Schuster *Science* **2001**, *294*, 567-571.

(11) Kanvah, S., Schuster, G. B. *J. Am. Chem. Soc.* **2004**, *126*, 7341-7344.

(12) Schlientz, N., Schuster, G. B. *J. Am. Chem. Soc.* **2003**, *125*, 15732-15733.

(13) Boone, E., Schuster, G. B. *Nucleic Acids Res.* **2002**, *30*, 830-837.

(14) Rajski, S. R., and J. K. Barton. *Biochemistry*, **2001** 40 5556–5564.

(15) Seeman, N. C. *J. Theor. Biol.* **1982**, *99*, 237-247.

(16) Seeman, N. C., Kallenbach, N. R. *Annu. Rev. Biophys. Biomol. Struct.* **1994**, *23*, 53-86.

(17) Bloomfield, V. A., Crothers, D. M., Tinoco Jr., Ignacio *Nucleic Acids: Structures, Properties, and Functions*; University Science Books: Sausalito, CA, 2000.

(18) Chargaff, E. *Experientia* **1950**, *6*, 201-209.

(19) Watson, J. D., Crick, F. H. C. *Nature (London)* **1953**, *171*, 737-738.

(20) Lehninger, A. L., Nelson, D. L., Cox, M. *Principles of Biochemistry*; 2nd ed.; Worth Publishers: New York, 1993.

Chapter II: Charge Transfer

DNA's importance has led scientists in the direction of understanding how damage affects the cell as well as understanding the mechanism of damage. Countless studies have been performed to understand what causes damage, the areas where damage most likely occurs, as well as the effect on the DNA structure. These studies have led to the development of methods to study the mechanism of charge migration through DNA by monitoring the damage at certain bases. By using past experiments as precedence, the effect on oxidative damage can be observed when certain parameters are changed such as base modifications and the addition of small binding molecules.

DNA Damage

Damaged DNA, if not repaired, can lead to mutagenesis, carcinogenesis, aging as well as cell death[1-3]. There are several mechanisms which can lead to cleavage of the DNA sugar-phosphate backbone. Some involve interactions with intermediates such as singlet oxygen ($^1O_2$) and radicals, other involve direct interaction with the excited state of a photosensitizer or with its radical. These species interact at reactive sites on the nucleotide in the DNA strand which in turn leads to single strand breaks (SSB)[4]. These cleavage sites are more commonly located on the sugar moiety (Figure 2-1).

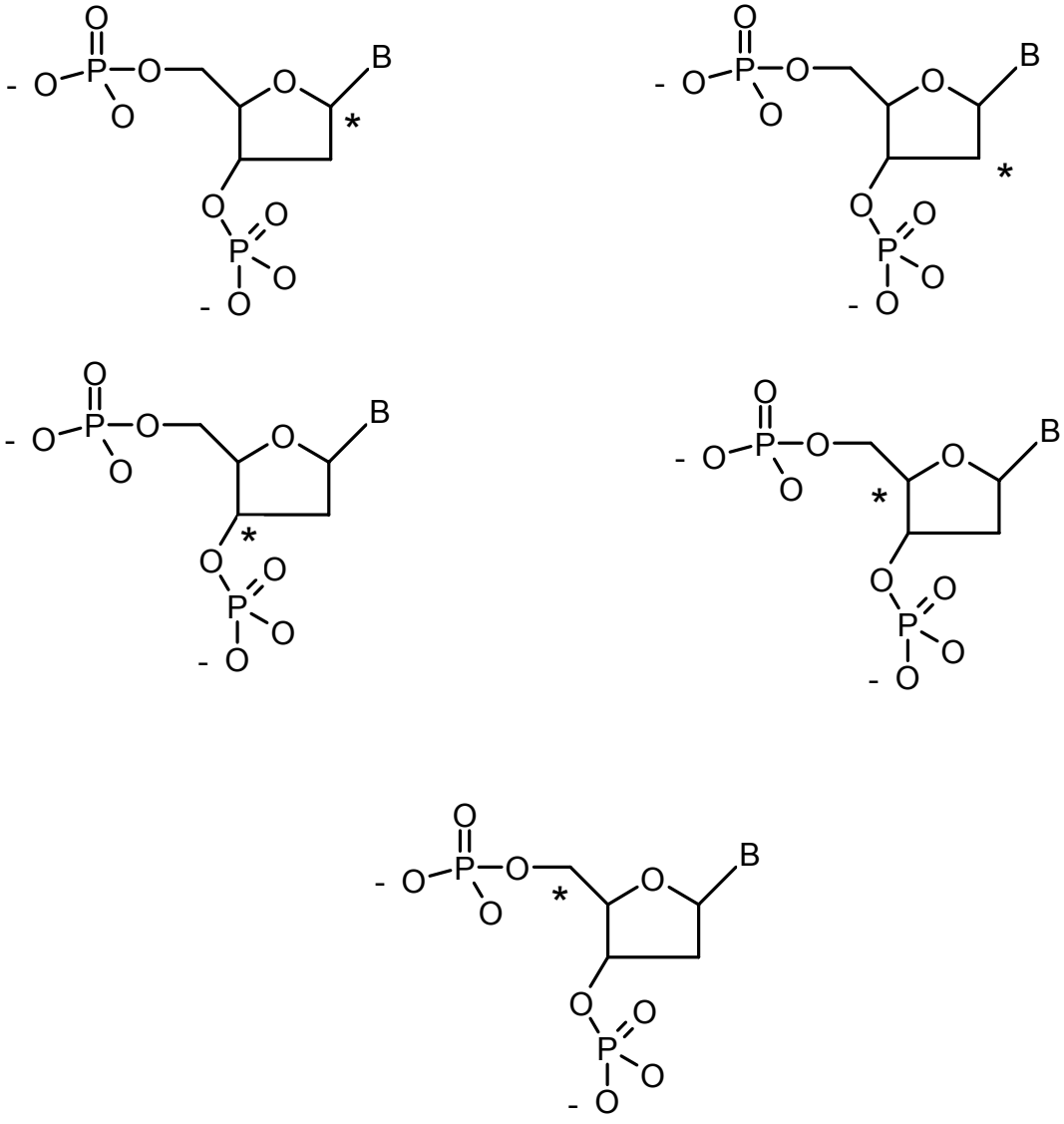

Figure 2-1. Sites of reaction. The sites of reaction for single strand break on a DNA nucleotide mostly occurring on the sugar moiety. The symbol (*) represents the sites of reactivity.

There are several different types of SSB. The first types of breaks occur with no further treatment and cleavage occurs spontaneously after initial reaction with DNA. This type of SSB is referred to as a frank strand break and can form under neutral conditions. These breaks are analyzed by techniques, such as neutral agrose gel electrophoresis, under neutral experimental conditions[4]. Another type of SSB sites are alkali labile sites. Theses sites require treatment by alkaline denaturing conditions after the reaction at the cleavage site occurs. The next type is thermal labile sites which require treatment by heat to cause cleavage. Some sites may even require treatment by both heat and alkaline denaturing. These types of breaks are analyzed with techniques such as denaturing polyacrylamide electrophoresis (PAGE) which separate the DNA by size and charge[4,5].

Reactions Leading to Damage

There are several reactions that can lead to DNA damage. The first is reaction with singlet oxygen ($^1O_2$). It is formed by energy transfer between the excited state of a photo-active molecule, photosensitizer, to the ground state of molecular oxygen (O_2). $^1O_2$ reacts primarily with the guanine (G) nucleotides[6]. This is most likely due to G being more susceptible to damage. All types of SSB can be produced by $^1O_2$ under the right conditions and these cleavage sites can be enhanced with the addition of D_2O making the lifetime of the $^1O_2$ longer[7].

The second mechanism is hydrogen abstraction. Hydrogen abstraction from the sugar can occur by reaction with OH· radical[8]. The photosensitizer reacts with O_2 in an electron transfer reaction to form superoxide (O_2^-) which in turn creates the hydroxyl radical by an iron-catalyzed process[9]. Hydrogen abstraction can also occur by n,π*

excited states of the photosensitizer with the DNA as well as the photosensitizer being involved in reactions which creates other radical species that undergo H abstraction.

Electron transfer is the last mechanism. This involves the transfer of an electron directly from the DNA to the excited photosensitizer. This charge transfer usually occurs depending on the reduction potential of the sensitizer and the oxidation potential of the bases[10]. In order for electron transfer to occur, the ΔG of the reaction (ΔG_{rxn}) should be negative and ΔG_{rxn} can be predicted by using the Weller equation[10]. Researchers have used this information to design and conduct logical studies on electron transfer through DNA.

Electron transfer from the base can also occur in a two step process as proposed by Berg in 1978. The first step is electron transfer from to the photosensitizer to an O_2 followed by electron transfer from the base to the photosensitizer creating the base radical cation[4].

Reaction with Guanine

Usually electron transfer reactions involving DNA and a photosensitizer occur between the photosensitizer and the guanine nucleotide because guanine has the lowest oxidation potential of 1.29 V vs. NHE at pH 7 (Table 2-1)[11]. Although this is the measured oxidation potential, there have been studies that suggest lower oxidation potential when G is in DNA on the range of 1.10-1.24 V vs. NHE[12-14]. One electron oxidation of G forms a radical cation, $G^{+}\cdot$, which in turn reacts with H_2O or O_2 which leads to damage of the DNA strand with further treatment by hot base[5]. Guanine can also be ionized by multiphoton excitation which can also cause the formation to the guanine radical cation to cause SSBs.

Table 2-1. Oxidation Potentials of the DNA bases as reported in literature[11]

Bases	E_{ox} (V) vs. NHE
Guanosine	1.29
Adenosine	1.42
Cytidine	1.6
Thymidine	1.7

.

Studying Charge Migration Through DNA

The low oxidation potential of guanine has made it ideal for monitoring long range migration of the radical cation through the DNA duplex. When $d(G)_n$ (n=2 or 3) are together, the oxidation potential of the 5′ G of the step is even lower than that of a single G in the DNA duplex[15]. This increase in reactivity leatds to selective damage predominantly at the 5′ G of a d(GG) step. This has been explained using ab initio calculations showing the electrostatic interactions between the electron rich N7 of the 3′ G being localized directly below the six-membered ring of the 5′ G is responsible for the 5′ selectivity[16].

When a charge is injected into the DNA it creates a “hole” in the DNA and this hole or radical cation travels through the DNA until it reaches a point of low energy d(GG) step. When the radical cation reaches this step it is trapped and a reaction with

water or O_2 leads to damage to the DNA strand occurring predominantly at the 5′ G. By placing d(GG) steps at different places along a DNA strand, charge migration can be monitored by observing the amount of oxidative damage at the 5′ G.

Researchers use photo-activated compounds to mimic the sensitizers that cause damage to DNA *in vivo*. The molecules are commonly referred to as photocleavers or photosensitizers. Photosensitizers are technically defined as "compounds whose excited states can initiate a series of chemical reactions which ultimately lead to a chemical reaction". This simply means that these molecules, when excited by light, react to form reactive intermediates such as radicals and carbocations which in turn reacts with DNA and leads to strand cleavage. They can also react directly with the DNA. The photosensitizers can be covalently linked at the end of the DNA strand or intercalated within the DNA duplex where it can π stack with the DNA bases[17-19]. They can also be free in solution and intercalate anywhere within the DNA duplex. In both cases, the compounds are able to π stack with the DNA bases giving it the ability to undergo electron transfer reaction with the bases. It is preferred to have the photosensitizer covalently linked to the DNA in order to know where the charge originates. This is important in the cases for determining the distance of charge migration. Figure 2-2 shows a simple schematic of a charge transfer experiment between a covalently linked photosensitizer and a DNA duplex containing GG steps.

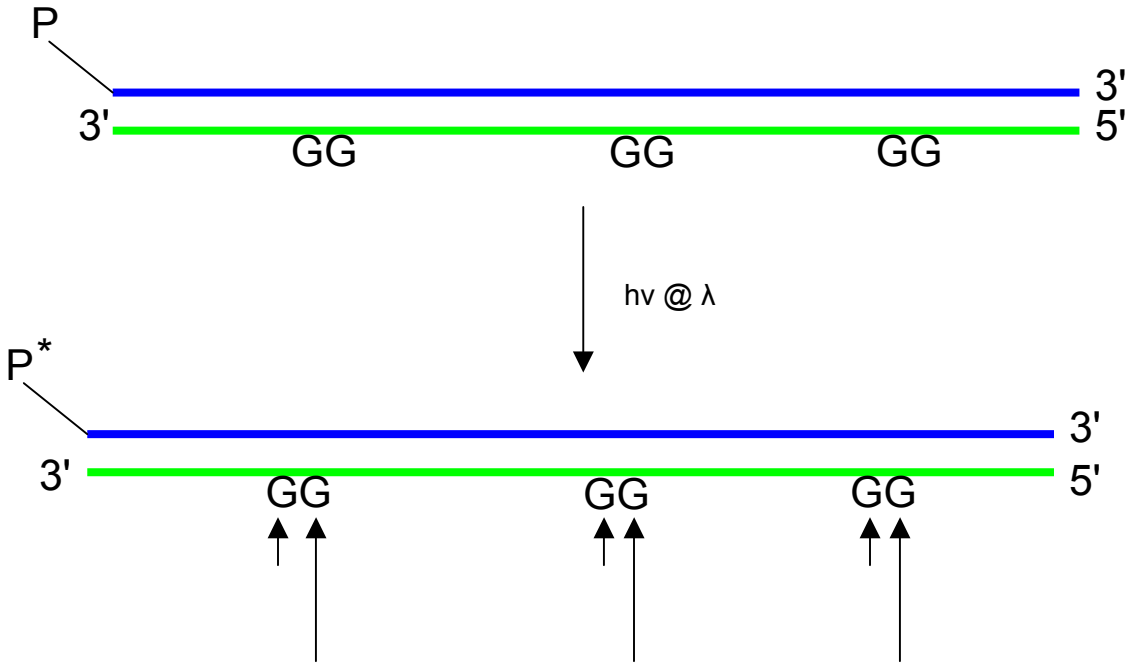

Figure 2-2 A basic scheme of what occurs during charge transfer experiments. P is the photosensitizers and the arrows indicate the amount of reaction at the GG steps after irradiation showing the 5′G of the GG step is more reactive.

The photo-active compounds can act as either electron acceptors (EA), or H abstractors depending on the structure of the photosensitizer[20]. A good photosensitizer should not be consumed by the reaction that they catalyze. These compounds should be able to be excited at a unique wavelength where the other components in the system are invisible. The photosensitizers typically have absorbencies at wavelengths higher than 300 nm where the DNA is invisible and cannot absorb the light. In the case of electron transfer, once the excitation of the photosensitizer occurs, an electron from the DNA, electron-donor (ED), is moved into the empty ground state orbital of the photosensitizer, electron-acceptor (EA) and creates a radical anion and cation pair between the EA-ED.

The radical cation migrates through the DNA duplex until it encounters an area of low energy. In the DNA strand this is the d(GG) steps. Once it reaches this area it is trapped and reacts with H_2O or O_2. When this occurs a series of reactions take place and imidazalone and oxazalone are formed[5,9]. The DNA cleavage occurs after treatment with hot piperidine. The piperidine reacts with formed damaged products to create strand cleavage to the DNA (Figure 2-3). The strand cleavage at this juncture is analyzed by electrophoresis and visualized with autoradiography.

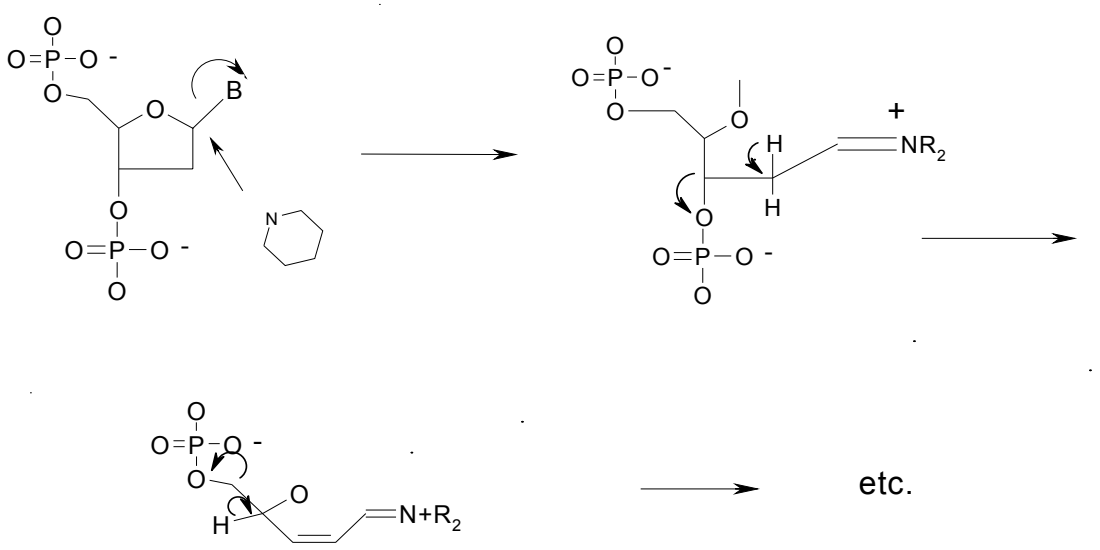

Figure 2-3. The mechanism when damaged DNA reacts with piperidine to cause strand cleavage.

This donor-acceptor type system is illustrated in figure 2-4 with anthraquinone (AQ) as the photosensitizer. An electron transfer occurs causing the formation of a

radical cation and anion pair. Following, several events can occur; back electron transfer (BET) giving the original species or cation migration, or the quenching of the radical by other species in the reaction. The radical anion is eventually quenched with O_2 and the EA is regenerated.

Mechanisms of Charge Transfer

Over the years the study of the DNA structure and oxidation of DNA have led to studies to understand the mechanism of long range charge transfer through DNA by studying how the radical cation propagates through duplex DNA. Over time several mechanisms of long range charge transfer through DNA have been reported.

The first mechanism proposed by Barton et al stated the DNA acts as a molecular wire creating a "π-way" for the migration of the radical cation[21]. This mechanism was based on the electron transfer theory of superexchange. Giese et al have followed this proposal by suggesting that superexchange does occur but when this mechanism occurs it is sequence dependent[22,23]. Jortner et al concluded the charge migrates by superexchange as well as by a hopping mechanism[24]. Although there have been different theories of the mechanism in which this action occurs, over the years the most widely excepted mechanism comes from the Schuster group. This theory is the phonon-assisted polaron-like hopping mechanism[23,25,26]. This theory coupled the molecular wire theory with the hole hopping theory. This mechanism involves the charge being delocalized over the bases causing the DNA to form a self-trapped distortion to support the charge. This

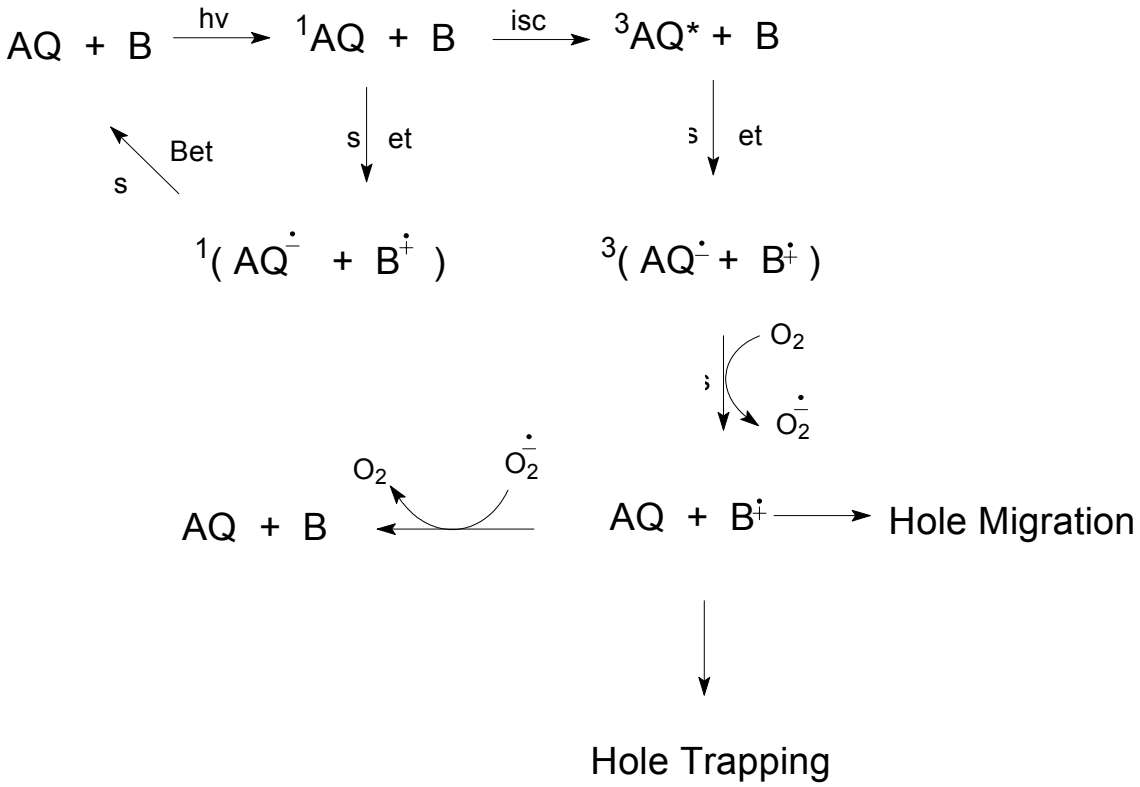

Figure 2-4. Reaction pathways for electron transfer in AQ linked DNA.

charge is characterized as a polaron. A polaron is a radical ion self-trapped by structural distortion of its containing medium[27] (Figure 2-5)[28]. Polarons travel by tunneling or is thermally assisted by a phonon. The polaron within the DNA travels by the assistance of phonons introduced to the DNA by UV excitation.

When the positive charge is on a base it delocalizes over neighboring bases and move along the DNA in an accordion type motion. Once it reaches an arear of low energy, it is trapped or partially trapped and upon further reaction, damage at that base occurs. It is unknown how many bases make up the polaron at one time. The polaron-like hopping mechanism can be generalized to explain prior theoretical and experimental results that contradict one another.

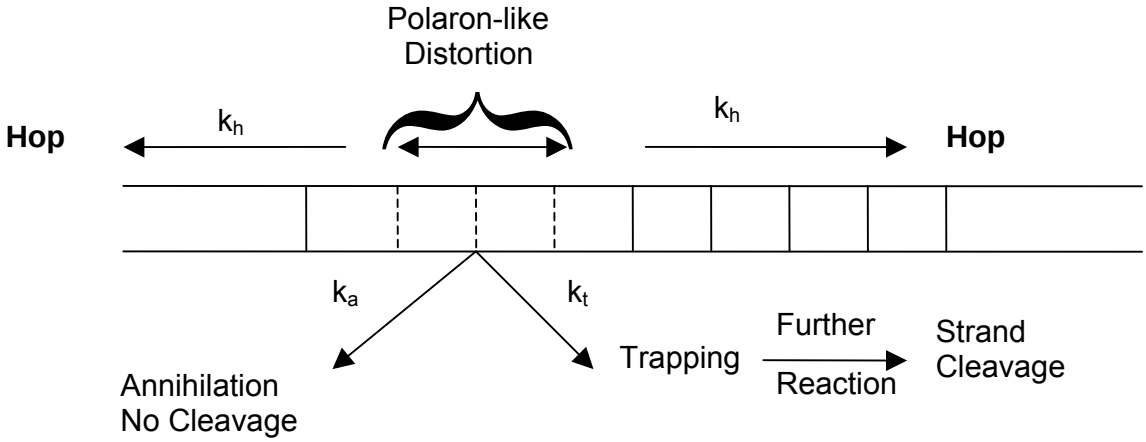

Figure 2-5. Schematic for the polaron hopping mechanism proposed by Schuster showing the different pathways the radical cation can take when injected into the DNA.

Photosensitizers

The Schuster group uses different photosensitizer to study charge transfer through DNA, anthraquinone based compounds, AQ and UAQ, and a naphthacenedione compound (TQ) (Figure 2-6). They have done extensive studies that have focused on different types of anthraquinone (AQ) photosensitizers and how they interact with DNA[17]. Most experiments use a covalently linked AQ that is linked to the 5′ terminus of the sugar moiety, to promote electron transfer. The AQ has a short two carbon linker and an electron- withdrawing group linked to the 2 position of the AQ aromatic ring. By placing the AQ at this position the origin of ET is known and the position of the photosensitizer is known to ensure controlled experiments. The AQ π-stacks with the DNA bases and does not disturb structure of the DNA, more specifically base stacking and H bonding.

The AQ is excited at a wavelength of 350 nm to the singlet state then undergoes intersystem crossing to the triplet state. When the intersystem crossing occurs, the electrons have the same spin keeping it from falling back down to the ground state. An electron from the neighboring base is transferred to the half-filled orbital creating the radical anion-cation pair. A uridine linked AQ is also used in order to place AQ anywhere in the DNA strand and it intercalates at the 3′ side of the base.

Another charge injector, TQ, was also designed and synthesized for charge transfer experiments. It was designed in order to conduct experiment that require excitation of the photosensitizers at wavelengths higher than 400 nm. The TQ has a structure similar to AQ with an addition of a fourth fused aromatic ring. The UV-Vis

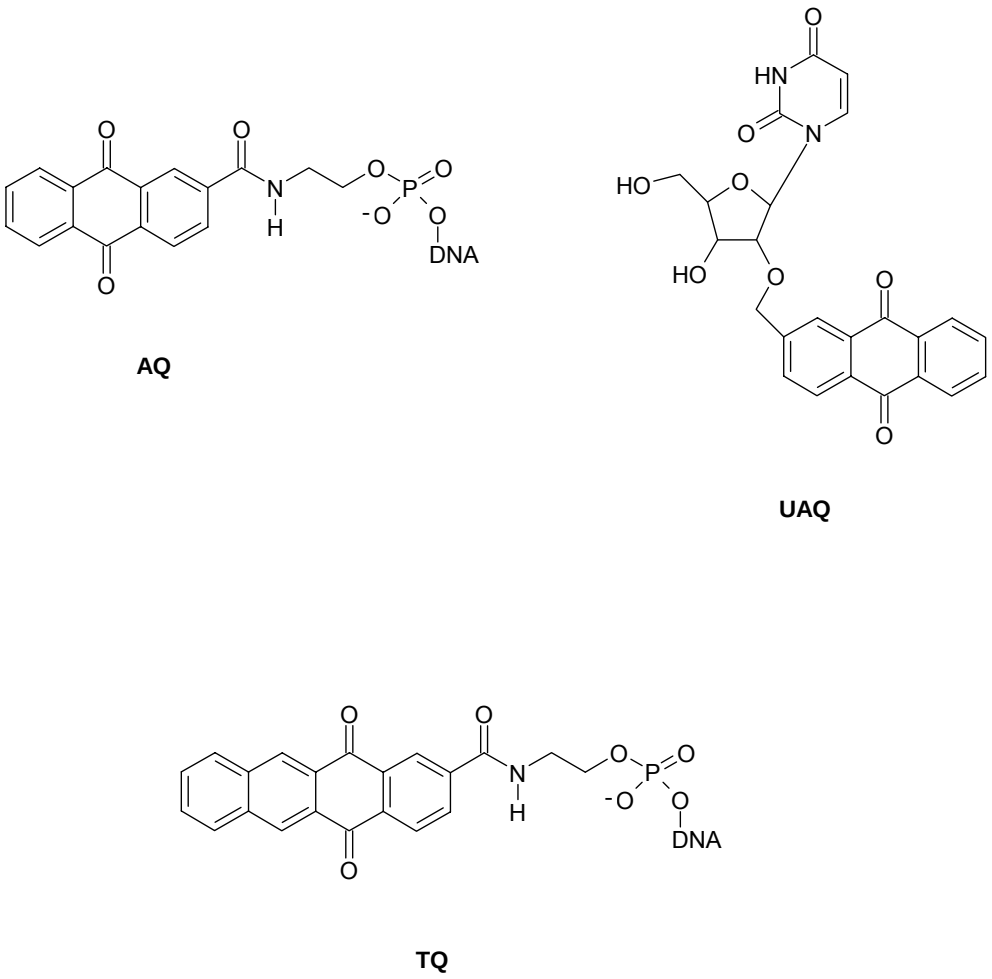

Figure 2-6. The structures of the photosensitizers used for the introduction of the radical cation into duplex DNA.

absorbance spectrum shows a maximum of ~ 400 nm (Figure 2-7) but in the case of TQ linked DNA, the absorbance is red shifted to ~ 420 nm. The TQ has been analyzed theoretically as well as experimentally to determine if it would be a suitable charge injector.

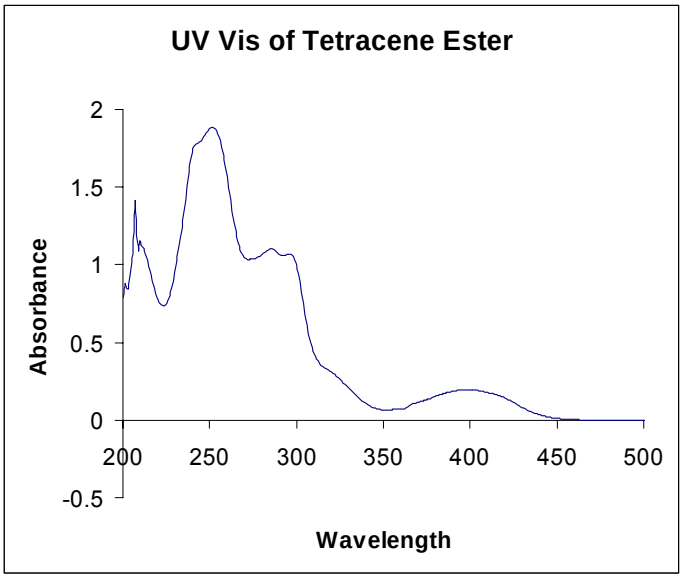

Figure 2-7. The UV-Vis spectrum of the TQ ester in acetonitrile.

The phosphoramidites of the AQ and TQ charge injectors are synthesized for coupling to the DNA strand by phosphoramidite chemistry. The syntheses of these compounds have been previously reported and will be discussed briefly here in[17,29].

AQ Synthesis

The synthesis of the AQ phophoramidite **1** involves a two step synthesis starting with the commercially available anthraquinone-2-chloride. The chloride is reacted with

ethanol amine in dry methylene chloride to yield the AQ amide **2**. The amide was then reacted with with 2-cyanoethyl diisopropyl chlorophosphoramidite in dry methylene chloride and DPEA to produce molecule **1** (Scheme 2-1).

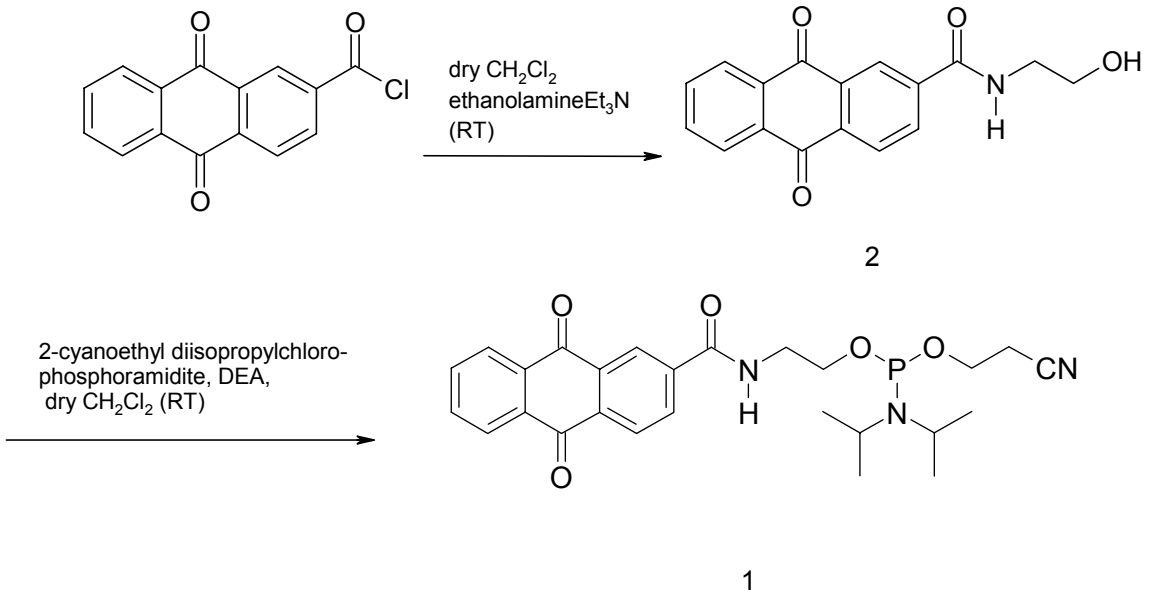

Scheme 2-1. Synthetic scheme for AQ photosensitizer.

TQ Synthesis

Synthesis of the TQ phosphoramidite **3** involved a multi-step process derived from several resources to give the known starting material, aldehyde **4** (Scheme 2-2 and Scheme 2-3)[30-32].

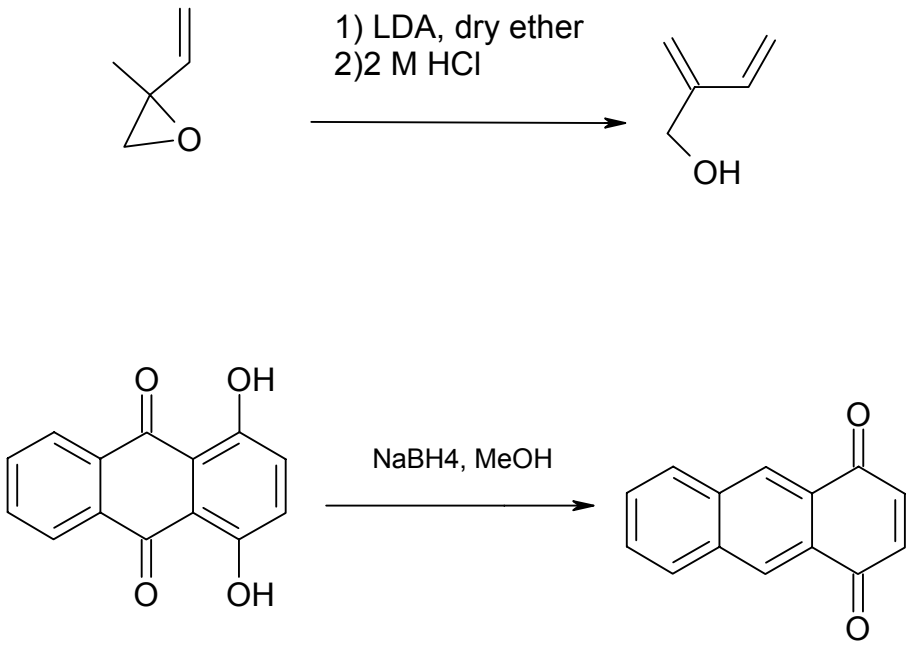

Scheme 2-2 Synthesis scheme of the starting materials for the TQ photosensitizer.

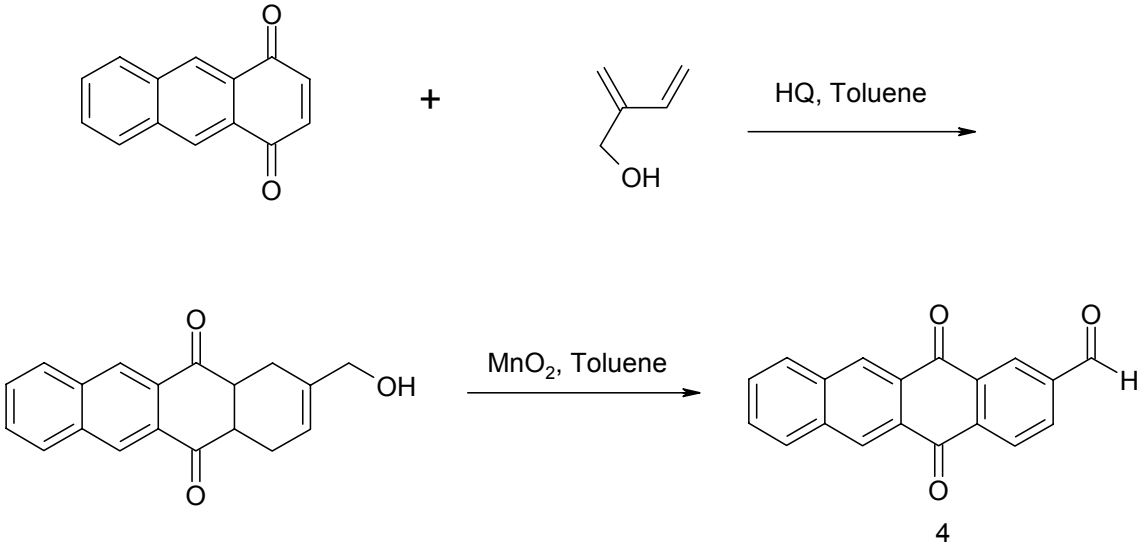

Scheme 2-3 Synthesis for the TQ aldehyde 4 starting material.

The synthesis was described in detail elsewhere (Scheme 2-4). Compound **4** was oxidized by chromium trioxide to yield the carboxylic acid **5** in a 42% yield[33]**.** This was indicated by the disappearance of the aldehyde peak at ~10.2 ppm and the product having a molecular weight value of 302 amu by mass spectroscopy. Acid **5** was refluxed in thionyl chloride to yield acid chloride **6** and was immediately used to prevent conversion back to the acid. The acid chloride was dissolved in dry methylene chloride and reacted with ethanolamine in dry methylene chloride to produce the TQ amide **7** in a 55% yield. The target compound **3**, TQ phosphoramidite, was obtained by reacting **7** with 2-cyanoethyl diisopropyl chlorophosphoramidite in dry methylene chloride and DPEA. Column purification was performed to yielded the product in a 95% yield[17].

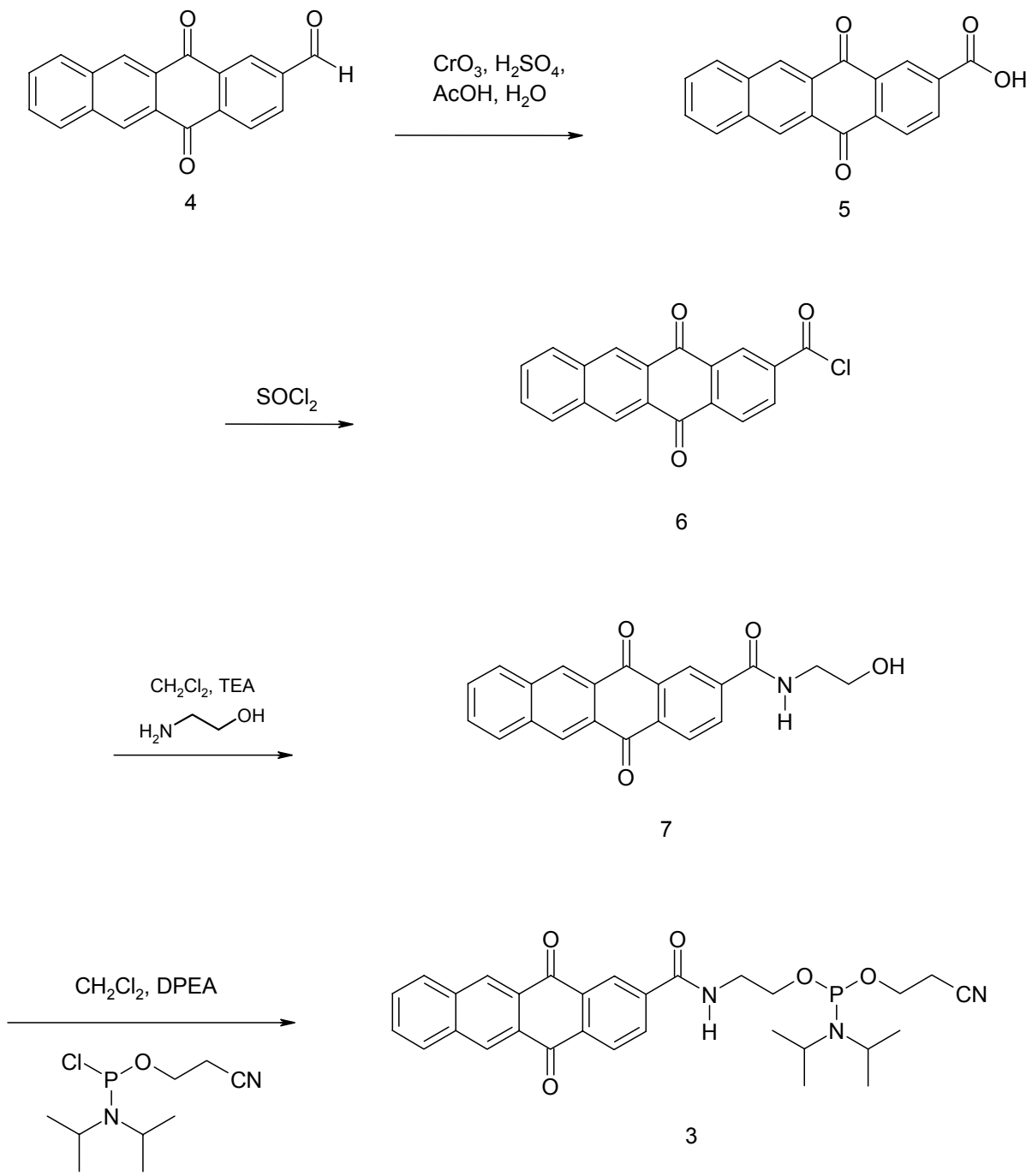

Scheme 2-4 The synthetic scheme for the TQ photosensitizer.

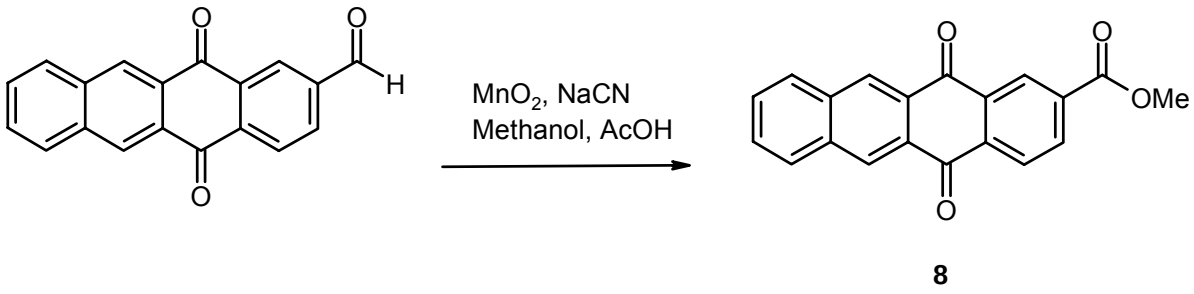

8

Scheme 2-5 Synthetic scheme for the TQ ester for reduction potential measurements.

The reduction potential of the TQ ester **8** was measured during the course of this study using cyclic voltammetry to determine the reduction potential of the TQ (Figure 2-8). The ester was synthesized[34] (Scheme 2-5) and dissolved in acetonitrile solution with 0.1 M tetrabutylammonium hexafluorophosphate as the electrolyte. The solution was purged with nitrogen to remove the oxygen. A platinum electrode was used as the working electrode versus silver chloride as the reference and several measurements were taken at several sweep rates. This was to insure that the observed potential was the true reduction potential. The voltammogram showed a reversible curve (Figure 2-8). The reduction potential was observed to be –0.88 V vs NHE. This reduction potential along with data previously reported gave new values for ΔG_{ET} for each base with TQ (Table 2-

2). By using the Weller equation[35], calculations were performed again to give more accurate ΔG_{ET} values for TQ. Using the

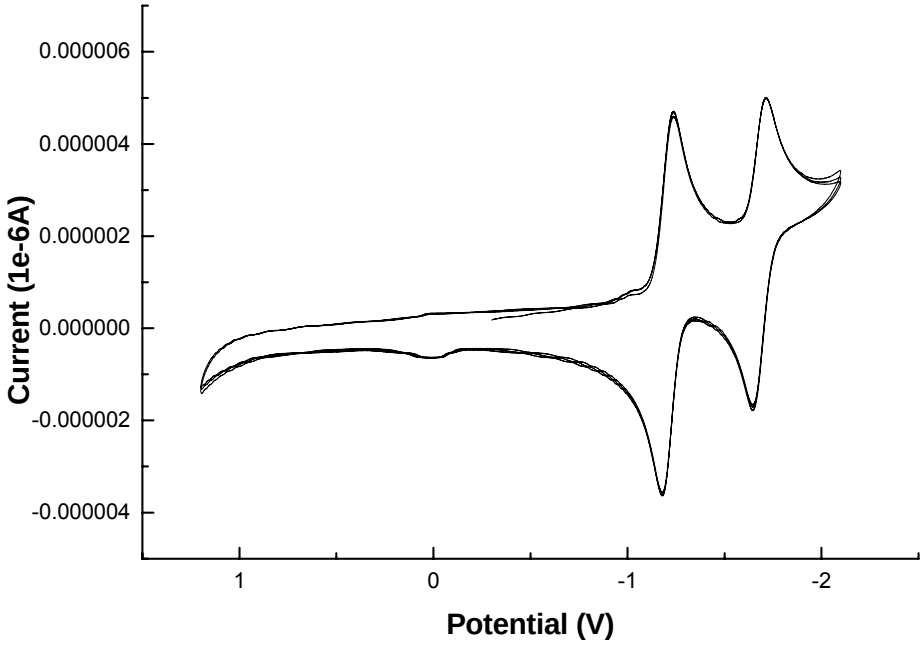

Figure 2-8. The cyclic voltammogram of the TQ ester in acetonitrile.

triplet energy and reduction potential of the photosensitizer and the oxidation potentials of the bases, the ΔGs were calculated. Although T and C have positive ΔG, because of base pairing TQ was an adequate charge injector for our purposes.

Table 2-2. The Gibbs Free Energy of the electron transfer reaction between TQ and the four DNA bases calculated by using the Weller equation.

Bases	**ΔG**
Guanosine	-0.26
Adenosine	-0.13
Cytidine	0.05
Thymidine	0.15

AQ vs. TQ

The structures of AQ and TQ are similar, therefore they should perform the same function in the case of charge injection. They have different photo-physical properties causing differences in charge injection efficiencies. These differences are summarized in table 2-3. Prior theoretical and experimental findings show the TQ can act as an efficient photosensitizer[29]. Charge transfer experiments with AQ-linked DNA and TQ-linked DNA have been performed yet they were performed using different irradiation sources. A comparison is difficult and could not be performed due to irradiation conditions

differences and differences in extinction coefficients, a more controlled experiment was performed using a rayonet chamber with lamps of a specific wavelength for both duplexes as opposed to using the rayonet chamber for the AQ-linked DNA and 150 watt light source using a filter for the TQ-linked DNA as done previously[16].

The DNA duplex used in this experiment can be found in figure 2-9 with X representing either AQ or TQ. This duplex was also used in experiments reported later in chapters. The AQ containing duplex was irradiated with 350 nm lamps and the TQ containing duplex was irradiated with 420 nm lamps for 15 and 30 min. The A-C experimental lanes contain the TQ-DNA samples and lanes D-F contain the AQ-DNA samples (Figure 2-10). The experiments contained two dark control experimental lanes, A and D, in which the sample was not exposed to the lamps. Experimental lanes B and E contain the samples irradiated for 15 min and lanes C and F are the experimental lanes for samples irradiated for 30 min. The TQ linked DNA and the AQ DNA are similar with a AQ seemingly more efficient for charge injection. Damage is seen at the 5' G of the d(GG) steps as expected. There was less damage seen in the case of the TQ-linked DNA. There is no way to conclusively say the AQ is more efficient than the TQ because of the difference of the lamps and extinction coefficients. TQ is an ideal photosensitizer for the experiments it was designed for.

```
X 5'-AACTGGCCTTTTCCGGTCGC-3'
  3'-TTGACCGGAAAAGGCCAGCG-5'

      X = TQ or AQ
```

Figure 2-9. The DNA duplex used for the TQ vs AQ experiments.

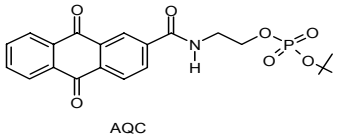

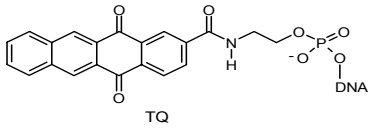

Table 2-3 Comparison of the photophysical properties of AQ and TQ photosensitizers.

Variable	**AQ**	**TQ**
Extinction Coefficient	6700 mol^{-1} cm^{-1}	4500 mol^{-1} cm^{-1}
Reduction Potential	-0.82 V	-0.88 V
Triplet Energy	2.76 eV	2.37 eV

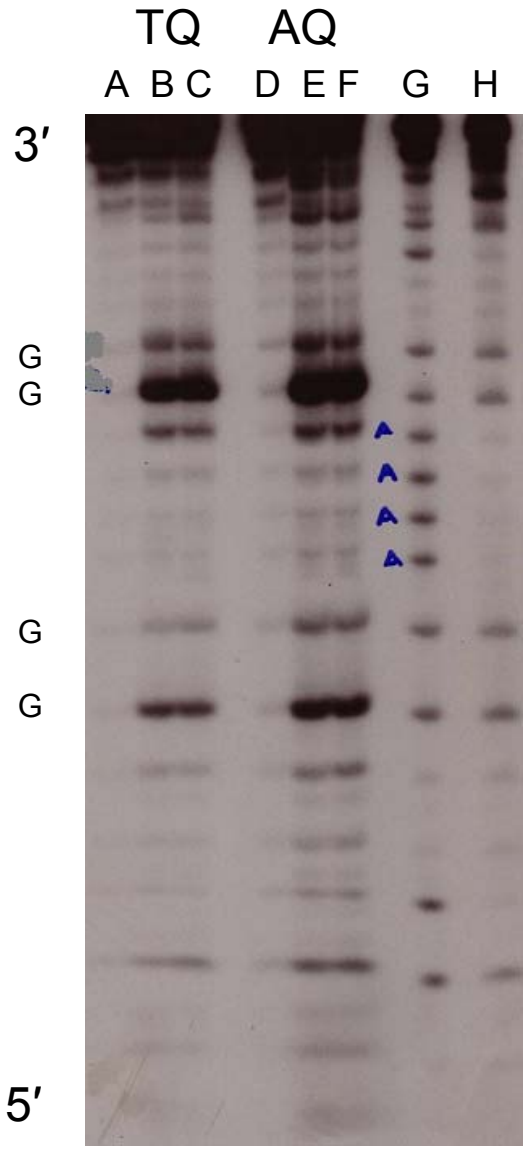

Figure 2-10 The autoradiogram of TQ-linked DNA and AQ-linked DNA irradiated for 15 and 30 min. The AQ samples were irradiated with 350 nm lamps and TQ samples were irradiated with 420 nm lamps. Lanes A and D are the experimental lanes for the dark control samples. Lanes B and E are the lanes for samples irradiate for 15 min. Lanes C and F are the experimental lanes for samples irradiated for 30 min. Lanes G and H are the A/G and T sequencing lanes respectively.

Conclusion

There are different studies done with charge migration. The study of sequence dependence, bases modification and mismatched pairs have been studied yet there have not been experiments involving small molecules binding to the minor groove of the DNA. The TQ charge injector was synthesized specifically to determine the effect of minor groove binders on oxidative damage of DNA. Its absorbance allows excitation where the DNA and the minor groove binder are invisible and are well out the range of the lamp's absorbance spectrum, 420 nm +/- 20 nm. During the course of this report we will discuss the effect of the minor groove binder, netropsin on one-electron oxidation of DNA.

Materials and Methods

1,4-Anthraquinone. In a dried round bottom flask, 10 g (41.6 mmol) of quinizarin was dissolved in 200 ml methyl alcohol and stirred vigorously at 0 oC. While stirred 5 g (132 mmol) sodium borohydride was added slowly and the solution was refluxed for twenty-four hours. It was then poured into 300 ml of water and acidified with hydrochloric acid. 1,4-anthraquinone precipitated out and removed by filtration, washed with water and dried under vacuum. The product was a dark orange color. It was then purified by column chromatography with methylene chloride in a 90% yield. ^{1}HNMR values correspond with those found in literature. ^{1}HMR (300 MHz, DMSO-d_6) δ 6.86 (s, 2 H, aromatic), 7.45 (m, 2H, aromatic), 7.84 (m, 2 H, aromatic) and 8.34 (s, 2H, aromatic). MS (EI, 70 eV) *m/z* 208.

2-Hydroxymethyl-1,3-Butadiene. In a three-neck flask dried under nitrogen, 42 ml of 2.0 M lithium diisopropylamide was dissolve in 100 ml of ethyl ether. 6.3 ml of 2-methyl-2-vinyloxirane was added dropwise to the solution. As soon as refluxed had ceased, the solution was poured into 2 M HCl. The organic and aqueous layers were separated and the aqueous layer was washed twice with 5% sodium bicarbonate and then dried over magnesium sulfate. The solvent was then removed under vacuum. The product was run through a short silicon column with methylene chloride (CH_2Cl_2), solvent was removed under vacuum and product was used immediately.

2,3-(3-methylhydroxy-3-cyclohexene)-1,4-anthraquinone. A mixture of 2 g (9.6 mmol) of 1,4-anthraquinone, 1.5 g (17.9 mmol) of butadiene and 80 mg of hydroquinone were placed in a dried round bottom flask and dissolved in 100 ml of toluene. The reaction mixture was heated under reflux for two days. The solution was cooled and concentrated down to yield a dark crude material. The material was purified by column chromatography with a 50:50 solution of CH_2Cl_2 and benzene to obtain starting material and side products. Ethyl ether was then used to obtain the product as a light yellow material in 50% yield. ^{1}HMR (300 MHz, DMSO-d_6) δ 3.30 (d, 4H, methylene), 3.50 (d, 2H, methane), 3.80 (d, 2H, methylene), 5.60 (d, 1H, vinyl), 7.78 (d of d, 2H, aromatic), 8.28 (d of d, 2 H, aromatic) and 8.60 (s, 2H, aromatic). Further oxidation to the aldehyde confirmed the product was synthesized. MS (EI, 70 eV) *m/z* 292.

5,12-dihydro-5,2-dioxo-2-Naphthacenecarboxylate aldehyde (4). Using a Dean Stark apparatus, 1.4 g (4.8 mmol) of alcohol and 4.1 g of manganese dioxide was dissolved in 100 ml of toluene and heated to reflux for two hours. The hot solution was then run through Celite; and, the Celite was then washed with methylene chloride. The washings and product were combined and the solvent was removed. This product was purified by column chromatography with methylene chloride to yield 960 mg of yellow solid in 70% yield. The ^{1}HNMR data corresponds to literature values 17. ^{1}HNMR (300MHz, CDCl3-d1) d 7.75 (m, 2H, aromatic), 8.15 (m, 2H, aromatic), 8.30 (d of d, 1H, aromatic), 8.57 (d, 1H, aromatic), 8.92 (m, 3H, aromatic), 10.2 (s, 1H, aromatic), MS (EI, 70 evV) *m/z* 286.

5, 12-dihydro-5, 12-dioxo-2-Naphthacenecarboxalate (8),. In a round bottom flask, 84 mg (0.29 mmol) of aldehyde, 549 mg (1.56 mmol) of MnO_2 and 28 mg of acetic acid were dissolved in 80 mL of methanol. With stirring, 76.6 mg of NaCN was added; and, the reaction mixture was stirred overnight. The mixture was passed through Celite and purified by column chromatography with methylene chloride to yield 76 mg of yellow material in 83% yield. ^{1}H NMR (300 MHz, $CDCl_3$-d_1) δ 4.0 (s, 3H, methyl), 7.70 (d, 2H, aromatic), 8.19 (d, 2H, aromatic), 8.40 (d, 2H, aromatic), 8.85 (d, 2H, aromatic) 9.00 (s, 1H, aromatic), MS (EI, 70 eV) *m/z* 316.

5,12-dihydro-5,2-dioxo-2-Naphthacenecarboxylic Acid (5). A 900 mg (3.0 mmol) portion of aldehyde was dissolved in a 50:50 mixture of acetic acid and acetone and cooled to 0^{o}C in an ice bath. A chromic acid solution containing 2.2 g (22 mmol) of chromium trioxide, 3.5 g sulfuric acid, 11 mL acetic acid, and 7 mL of water was prepared and this solution was slowly added to the aldehyde and stirred for six hours. The solution was poured into water and the acid precipitated out of solution. The product was removed by filtration, then washed with water and dried to yield 443 mg of yellow solid in 49% yield. ^{1}H NMR (300MHz, DMSO-d_6) δ 7.80 (d of d, 2H, aromatic), 8.30 (d of d, 2H, aromatic), 8.40 (d, 2 H, aromatic) 8.78 (s, 1H, aromatic), 8.89 (d, 2H, aromatic) MS (EI, 70 eV) *m/z* 302.

5,12-dihydrox-5,12-dioxo-2-(2'-hydroxyethyl)-Naphthacenecarboxamide (7). For the reaction, 500 mg (1.7 mmol of acid was dissolved in thionyl chloride and refluxed for three hours. Thionyl chloride was distilled off and the product remained as a residue.

The acid chloride **(6)** was dried under vacuum and was used immediately. Under nitrogen, the acid chloride was dissolved in 20 mL of methylene chloride. 0.4 mL (6.6 mmol) o ethanolamine and 0.24 mL (1.8 mmol) of triethylamine was dissolved in 80 mL of methylene chloride. The acid chloride solution was then added form a cloudy green solution. The solution was stirred overnight and filtered. The collected solid was recrystallized with isopropyl alcohol to yield 322 mg of the amide as a pale yellow solid in 55% yields. 1H NMR (300MHz, DMSO-d_6) δ 3.38 (t, 2H, aromatic), 8.25 – 8.38 (m, 4H, aromatic), 8.70 (s, 1H, aromatic). (The ^{1}H NMR data corresponds with the data found for the AQ amide, difference was the aromatic proton region). MS (EI, 70 eV) *m/z* 345.

Tetracene Quinone-2-Phosphoramidite (3). In a three-neck round bottom flask, 350 mg (1.0 mmol) of amide was dissolved in 20 mL dry methylene chloride. To the solution, 0.7 mL diisopropylethylamine and 0.44 mL of 2-cyanoethyldiisopropychlorophosphoramidite were added to 90 mL of dry methylene chloride. The amide solution was added drop by drop to the 90 mL solution. After addition of the amide, the solution became a clear brown color and was stirred at room temperature for 1 hour. The solution was poured into a mixture of 12 mL of ethylacetate and 1.2 mL of triethylamine (TEA). The mixture was washed twice with sodium bicarbonate and twice with brime. The product was then dried over sodium sulfate; and, the solvent was removed under vacuum. The product was purified by column chromatography using a solution of 45:45:10, hexane, ethyl acetate to triethyl amine solvent system, respectively. This produced 520 mg in a 95% yield. Comparison with

the NMR data of the AQ and mass spectroscopy supports the synthesis of the TQ phosphoramidite. ^{1}H NMR (300 MHz, CDCl3-d_1) δ 1.2 (d of d, 12H, methyl), 2.55 (d of d, 2H, methylene), 3.60 – 3.70 (m, 2H, methane), 3.75 – 3.80 (m, 2H, methylene), 3.86 – 3.97 (m, 4H, methylene), 7.1 (br.t, 1H, amide), 7.7 (d of d, 2H, aromatic), 8.05 – 8.13 (m, 2H, aromatic), 8.40 (d of d 2H, aromatic) 8.65 (s, 1H, aromatic) 8.85 (d, 2H, aromatic). MS (EI, 70 eV) *m/z* 444. ^{31}PNMR (400 MHz, $CDCl_3$-d_1) d 149.17.

Cyclic Voltammetry.

The ester reduction potential was measured by using a 0.1 M solution of tetrabutylammonium hexafluorophosphate as the electrolyte. Once the background was measured, the ester was added to be form a final 0.1 M concentration of ester and electrolyte. The sweep range was from -2000 mV - 1500 mV. Sweep rates varied from 100 mV - 1000 mV/s.

UV-Vis Spectroscopy. A solution of 16 mg of the tetracene ester and acetonitrile was prepared to make a 5 μM solution. A blank of 990 μL acetonitrile was measured and 10 μL of the ester solution was added. Using the absorbance at 400 nm, the extinction coefficient was calculated to be 4200 L/mol cm. The samples were analyzed using a Hewlett Packard 8453 UV-Vis Spectrophotometer.

References

(1) Kanvah, S., Schuster, G. B. *J. Am. Chem. Soc.* **2004**, *126*, 7341-7344.

(2) Demple, B., Harrison, L. *Annu. Rev. Biochem.* **1994**, *63*, 915-948.

(3) Loft, S., Poulsen, H. E. *J. Mol. Med.* **1996**, *74*, 297-312.

(4) Kochevar, I. E., Dunn, D. A. In *Bioorganic Photochemistry* 1990; Vol. 1, p 273-315.

(5) Armitage, B. *Chem. Rev.* **1998**, *98*, 1171-1200.

(6) Boon, P. J., Cullis, P. M., Symons, M. C. R., Wren, B. W. *J. Chem. Soc. Perkin Trans.* **1984**, *2*, 1393-1399.

(7) Merkel, P. B., Kearns, D. R. *J. Am. Chem. Soc.* **1972**, *94*, 1029-1031.

(8) Oneil, P., Fielden, E. M. *Adv. Radiat. Biol.* **1993**, *17*, 53-120.

(9) Burrows, C. J., Muller, J. G. *Chem. Rev.* **1998**, *98*, 1109-1151.

(10) Rehm, D., Weller, A. *Isr. J. Chem.* **1970**, *8*, 259.

(11) Steeken, S., Jovanovic, S. V. *J. Am. Chem. Soc.* **1997**, *119*, 617-618.

(12) Brabec, V., Dryhurst, G. *J. Electroanal. Chem.* **1978**, *89*, 161-173.

(13) Brabec, V. *Biophys. Chem* **1979**, *9*, 289-297.

(14) Johnston, D. H., Cheng, C. -C, Campbell, K. J., Thorp, H. H. *Inorg. Chem.* **1994**, *33*, 6388-6390.

(15) Schuster, G. B. *Acc. Chem. Res.* **2000**, *33*, 253-260.

(16) Prat, F., Houk, K. N., Foote, C. S. *J. Am. Chem. Soc.* **1998**.

(17) Gasper, S. M., Schuster, G. B. *J. Am. Chem. Soc.* **1997**, *119*, 12762-12409.

(18) Bhattacharya, P. K., Barton, J. K. *J. Am. Chem. Soc.* **2001**, *123*, 8649-8656.

(19) Lewis, F. D., Letsinger, R. L., Wasielewski, M. R. *Acc. Chem. Res.* **2000**, *34*, 159-170.

(20) Gasper, S. M., Armitage, B., Shui, X., Hu, G. G., Yu, C., Schuster, G. B., Williams, L. D. *J. Am. Chem. Soc.* **1998**, *120*, 12402-12409.

(21) Turro, N. J., Barton, J. K. *Science* **1993**, *262*, 1025-1029.

(22) Giese, B., Wessely, S., Spormann, M., Lindemann, U., Meggers, E., Michel-Beyerle, M. E. *Agnew. Chem. Int. Ed.* **1999**, *38*, 996-998.

(23) Meggers, E., Michel-Beyerle, M. E., Giese, B. **1998**, *120*, 12950-12955.

(24) Jortner, J., Bixon, M. Langenbacher, T., Michel-Beyerle, M. E. *Proc. Natl. Acad. Sci. USA* **1998**, *95*, 12759-12765.

(25) Ly, D., Sanii, L., Schuster, G. B. *J. Am. Chem. Soc.* **1999**, *121*, 9400-9410.

(26) Armitage, B. A., Yu, C., Devadoss, C., Schuster, G. B. *J. Am. Chem. Soc.* **1994**, *116*, 9847-9859.

(27) Henderson, P., Jones, D., Hampikian, G., Kan, Y., Schuster, G. B. *Proc. Natl. Acad. Sci. USA* **1999**, *96*, 8353-8358.

(28) Sartor, V., Schuster, G. B. *J. Am. Chem. Soc.* **1999**, *121*, 11027-11033.

(29) Roberts, L. W., Schuster, G. B. *Org. Lett.* **2004**, *6*, 3813-3816.

(30) Gupta, D. N., Hodge, P., Khan, N. *J. Chem. Soc., Perkin Trans. 1* **1981**, 689-696.

(31) Riley, R. G., Silverstein, R. M. *J. Org. Chem.* **1974**, *39*, 1957-1958.

(32) Cormier, R. A., Connolly, J. S., Pelter, L. S. *Synth. Commun.* **1992**, *22*, 2155-2164.

(33) Heilbron, S. I., Jones, E. R. H., Sondheimer, F. *J. Chem. Soc.* **1948**, 604-607.

(34) Corey, E. J., Gilman, N. W., Ganem, B. E. *J. Am. Chem. Soc.* **1968**, *90*, 5616-5617.

(35) Breslin, D. T., Schuster, G.B. *J. Am. Chem. Soc.* **1996**, *118*, 2311-2319.

Chapter III: Minor Groove Binder : Netropsin

Minor Groove Binders

Minor groove binders are small natural and synthetic materials that have an affinity to bind to the minor groove of a DNA duplex. Most binders have a preference for certain sequences such as A_4 regions or A_nT_n regions. These are known as their binding sites. Through studies of the naturally occurring compounds, groups have made efforts to synthesize binders that will recognize certain sequence segments.

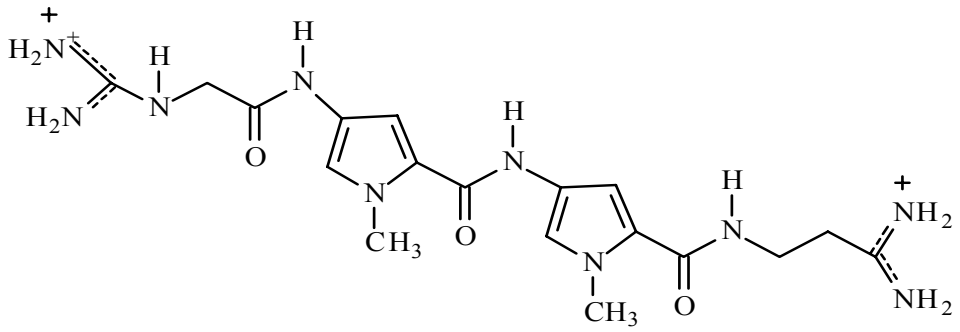

Figure 3-1. Netropsin Structure

Several binders have been studied extensively over the past several decades. Among these are netropsin, distamycin A, and Hoechst 33258[1,2]. Netropsin is one of the most investigated DNA binders to date and is the main focus of this report (Figure 3-1). The other binders mentioned here in have also been used as support for the results seen for netropsin.

Netropsin

Netropsin was isolated from *Streptomyces netropsis* in 1951 by A. C. Finlay for Pfizer Company[3]. It is characterized as an antibiotic drug and has shown anti-viral and anti-tumor activity. Its crescent structure contains two pyrrole rings connected by amide groups, and end groups of an amidinium group and a guanadinium group giving netropsin dicationic character (Figure 3-1).

Over the years scientists have performed extensive studies to determine netropsin's behavior in the presence of DNA[4-6]. There have been many reports of its mode of binding as well as its binding properties that differ because of the various experimental techniques used. The reports all agree netropsin is a non-intercalative drug that bind within the minor groove with an affinity for tracts of 3 to 5 A:T base pairs. It binds mostly to double helical DNA and some RNA: DNA hybrids[6]. Netropsin has a crescent shape making it structurally favorable to bind in the minor groove of the DNA and when bound, it does not disturb the Watson-Crick base pairing and barely disturbs the DNA structure itself[7,8] (Figure 3-2). This is supported by NMR studies using a synthetic oligomer with AATT binding site. It also displaces the water molecules within the minor groove in an exothermic reaction[9]. When bound within the minor groove, it

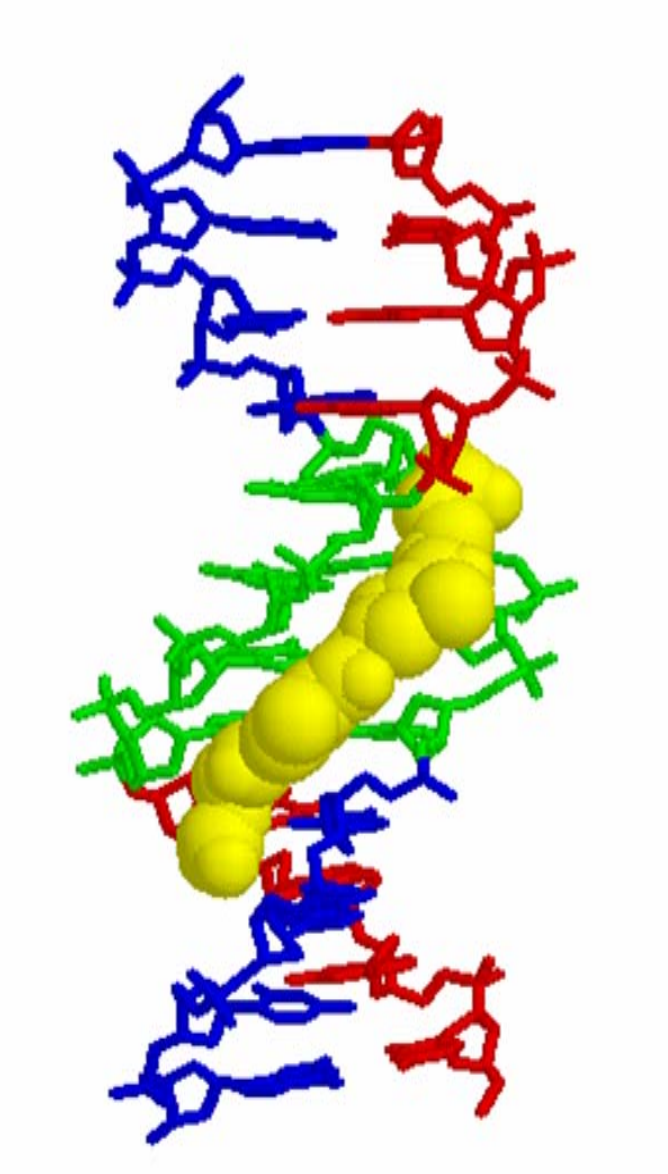

Figure 3-2 Rendering of a space filled molecule of netropsin bound to the minor groove of a DNA duplex.[10]

interferes with transcription and replication processes by blocking RNA and DNA polymerase.

NMR, footprinting, and X-ray crystallization experiments have been used to evaluate the modes of binding not only on natural occurring oligonucleotides but synthetic oligonucleotides as well[11-13]. Netropsin binds in a 1:1 mode, netropsin to DNA binding site. In other words only one netropsin fits in the minor groove per binding site[14]. Although there is room for more than on molecule of netropsin, the positive charges at each end deter another netropsin molecule form binding once one is bound within the groove. Netropsin binds to all combinations of A:T base pairs with the strongest affinity for AAAA:TTTT sequences[2]. Each combination seems to interact with netropsin in different ways. These different binding modes seem to be due to the different lengths of the hydrogen bonding sites varying from A to T. Its amide hydrogens lie towards the DNA and form hydrogen bonds with the 2-oxygen atom of the thymidine and the 3-nitrogen of the adenine. In the case of a tract of AATT the amide hydrogens and hydrogens from the guanidinium and amidinium groups stabilize the DNA:netropsin complex[15]. Each amide hydrogen creates bonds to the appropriate base and the neighboring base of the complementary base on the other strand. These hydrogen bonds are believed to be the primary mode of binding of the netropsin to the DNA. The two positively charged ends interact with the phosphate groups as well as their hydrogens creating bonds with the bases. Netropsin also exhibit van der Waals interactions with the DNA. Yet it has been concluded from circular dichroism (CD) experiments that the positively charged ends have little to do with the binding process of netropsin to DNA.

Netropsin is deterred from binding areas where G is present because of G's exocyclic amine group that sits in the minor groove. The amine group collides with the hydrogen on the CH_3 group of the pyrrole ring and inhibits the netropsin from binding in the areas where G is present. In case where inosine replaces guanine, netropsin is able to bind because of the absence of the amine.

Amounts of free netropsin in equilibrium with the DNA-netropsin complex are in very small amounts; therefore it is hard to obtain an equilibrium constant for binding of this complex system. The ones that have been measured have averaged around 10^9 M^{-1} yet there have been equilibrium constants of netropsin:DNA complexes ranging from 10^5 to 10^9 M^{-1} [8,16]. The equilibrium constants also seem dependent the binding site. Several reported different binding constants based on the sequence combination and the number of A:T base pairs at the binding site. Wartel et al. examined the binding constants of netropsin using different type of AT binding sites[6]. Values also seem to vary because of the different techniques used to acquire them. Some have used CD and monitored the induced Cotton effect of netropsin when in the presence of DNA. When netropsin is free in solution, it gives no CD signal and bound to DNA, the CD spectrum of DNA changes and absorbance peaks attributed to netropsin are observed[17]. Though there has been some speculation that netropsin changes B-form DNA to A-form DNA, further investigation such as NMR studies, have shown netropsin has little effect on the DNA conformation or structure.

NMR spectroscopy can also be used to determine the binding of netropsin to DNA. The shift of the H-3 protons of thymine is decreased when in the presence of non-

intercalative binders. By the shifts of the pertinent peaks, it can be understood where the netropsin is binding and what it is binding to.

The effect of netropsin on T_m has been studied using UV melting to determine binding constants[17]. When netropsin is bound to duplex DNA, the temperature of melting will increase, stabilizing the DNA duplex. Netropsin has been seen to stabilize duplexes increasing the T_m to 10 ^oC. Calculations can be performed to determine binding constants based on the T_m data. Tm changes are also useful in determining if netropsin is bound to a duplex and was use in this study to verify netropsin binding.

Netropsin has a UV absorption spectrum displaying an absorbance maximum of 240 and 296 nm (Figure 3-3). It has an $\varepsilon_{295} = 21500$. When is bound to DNA, it changes the DNA absorbance spectrum by red shifting the absorbance maxima. It is reported to give an absorbance past 320 nm. These are other indications of netropsin binding. Other thermodynamic data for netropsin binding to DNA include a reported binding free energy of -12.3 kcal/mol and binding entropy of calculated to be 10.3 cal/degree[9].

Studies involving netropsin have branched off into other research areas. The most common area has been using netropsin as the lead compound for the development of other minor groove binders[18,19]. This new compounds are synthesized to be specific for certain base sequences. Many researchers have based their minor groove binding molecules on how netropsin binds within the groove and have used this information for their purposes. There have even been modifications to help recognize sites containing guanines. There have also been modifications that create binders that recognize longer binding sites. Dervan et al. has synthesized molecules that actually bind to the minor groove and extend to the major groove.

Studies dealing with oxidative damage of DNA have also been reported in literature. Netropsin has been used in experiments to deliver compounds that cause oxidative damage. Its ability for specific binding has given researchers the ability to covalently link the netropsin to a compound such a pyrene. Once linked the netropsin binds to its binding site and the pyrene is able to intercalate within the DNA duplex.

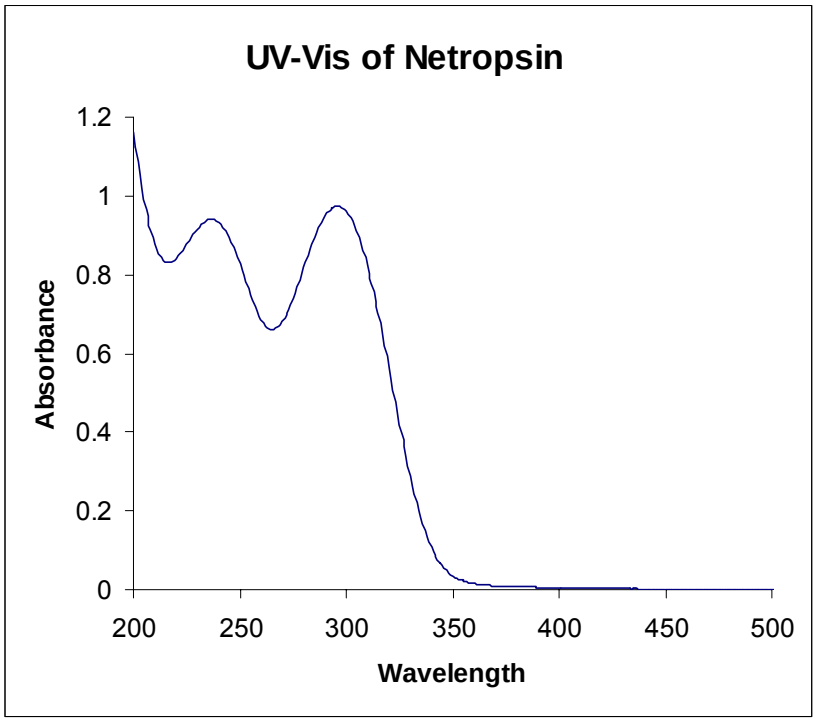

Figure 3-3. UV-Vis specutrum of netropsin of netropsin in water.

Upon intercalation, the pyrene is excited and is able to cause damage to the DNA at its intercalation site[20].

Though this type of research has been done, there seems to be no literature reporting how netropsin would affect charge transfer through a DNA duplex. If a covalently linked electron acceptor was linked to a DNA duplex to initiate charge migration, how would a netropsin molecule in a remote area affect the results of charge migration? Charge migration seems to move through the bases by π-stacking. Netropsin sits in the minor groove and does not π-stack with the bases. Although there are hydrogen bonds and van der Waals interactions, was this enough to have an effect on the charge migration? Will the displacement of the water have anything to do with the results? Will the positive charged molecule serve the same the purposes as the sodium ions?

Cyclic Voltammetry

In order to answer these questions and understand possible results, not only must the binding mode of netropsin be understood but also certain electrochemical properties such as oxidation potential. Oxidative damage occurs at the 5′ G of the GG steps because G has the lowest oxidative potential. The potential seems to lower in the presence of two or three G. Therefore it was important to discern where netropsin's potential fell in the scheme of the four bases. The peak potential was determined using cyclic voltammetry consisting of a three electrode system. The measurements were taken in 0.1 M solution of tetrabutylammonium tetrafluoroborate as the electrolyte in nanopure water. A platinum electrode was used as the auxiliary electrode, a carbon electrode was the working electrode, and Ag/AgCl was used as the reference electrode. The experiment was run at several different sweep rates to ensure accuracy. The potential was measured

and converted to vs. NHE measurements to correspond with the E_{ox} for the four DNA bases. The voltammogram displayed a non-reversible curve that displayed a peak potential of 0.938 mV vs. Ag/AgCl (Figure 3-4). The conversion of the value gave a potential of 1.18 V vs. NHE. The experiment was also performed with platinum as the working electrode and the same results were observed.

Charge Transfer Experiments

Preliminary experiments were performed using AQ linked DNA to determine if charge transfer experiments were worth being pursued (Figure 3-5, Table 3-1). The results of these experiments were reported in earlier communications and can be see in figure 3-5. The results seen in the experimental lanes containing DNA and netropsin in a 1:1 ratio were interesting. The oxidative damage seen at the 5′ G of the DNA strand decreased compared to the control lane where there is clearly damage at the proximal and distal d(GG) steps of most of the strands. Upon initial examination four strands were examined. The first experimental change performed was to change the DNA sequence. Examining the sequences in use, there were possibilities of more than one binding site. It was imperative to have only one site in order to control the placement of the netropsin. It was also important in order to determine the effects on the GG step before the binding site as well as after the binding site. By using these duplexes there was no way to determine this because of the possibility of the netropsin binding before either GG steps. After determining from the result which binding site duplex, DNA B, was more efficient for DNA migration, a new strand was synthesized for further investigation with a naphthacendione photosensitizer in plane of the AQ (results found elsewhere). This was determined by literature results of the best netropsin site and also by determining how

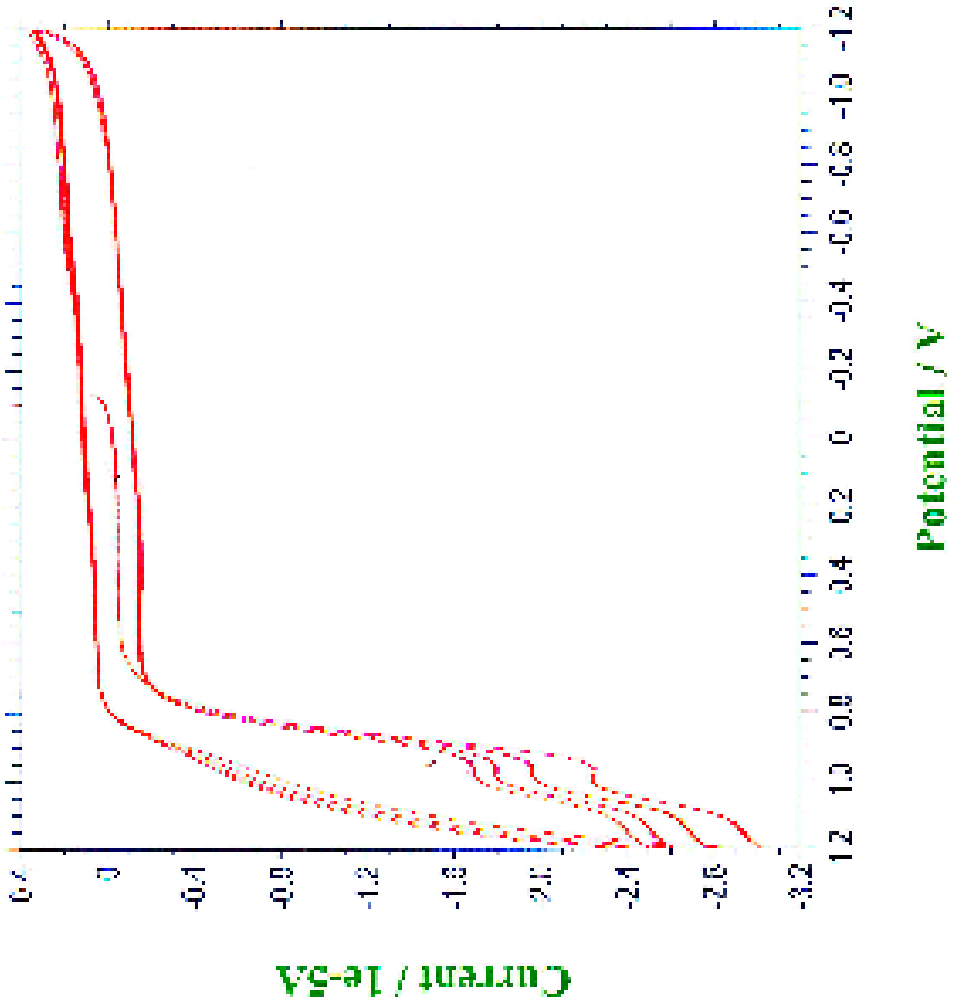

Figure 3-4 Oxidation wave of netropsin in 0.1 M as the electrolyte in water purged with nitrogen at a sweep rate of 100 mV/s.

much damage was seen in the proximal and distal GG steps. The AQ was linked to an adenine due to past experiment of charge injection efficiency[21]. Both strands were labeled and the results are seen figure 3-5. The concentration of netropsin was varied from 0.5:1 netropsin to DNA to 5:1 netropsin to DNA. As the concentration of netropsin increased, the amount of oxidation damage decreased. This was a somewhat a surprising result but it could be explained by the peak potential of netropsin being less than that of the four DNA bases. Although the result seemed conclusive, questions were raised that made the rethinking of the experimental set up necessary.

The AQ photosensitizer absorbs at 350 nm and there is a small absorbance at around 350 nm for netropsin. There was a possibility netropsin was absorbing some of the light causing a decrease in oxidative damage in the DNA. The 350 nm lamps also have distribution curve of +20 nm on either side of the 350 nm wavelength. This increases the probability of the netropsin's absorbing of some of the light. To ensure this was not occurring, it was decided to use the TQ in place of the AQ. This way the DNA could be irradiated at 420 nm, where the DNA as well as the netropsin is invisible. In the upcoming chapter, the experiments and the results of the charge transfer study with netropsin as the minor groove binder will be reported and discussed in the next chapter.

Table 3-1 Sequences for preliminary studies with netropsin binding site DNA. *Labeled strand.

DNA	Sequences
DNA A	AQ-5′-CAAAGCCTTTTCCGTAGAAC-3′ 3′-GTTTCGGAAAAGGCATCTTG-5′*
DNA B	AQ-5′-CAAAGCCAAAACCGTAGAAC-3′ 3′-GTTTCGGTTTTGGCATCTTG-5′*
DNA C	AQ-5′-CAAAGCCTAATCCGTAGAAC-3′ 3′-GTTTCGGATTAGGCATCTTG-5′*
DNA D	AQ-5′-CAAAGCCATTACCGTAGAAC-3′ 3′-GTTTCGGTAATGGCATCTTG-5′*
DNA E	AQ-5′-CAAAGCCTATACCGTAGAAC-3′ 3′-GTTTCGGATATGGCATCTTG-5′*
DNA F	AQ-5′-CAAAGCCATATCCGTAGAAC-3′ 3′-GTTTCGGTATAGGCATCTTG-5′*

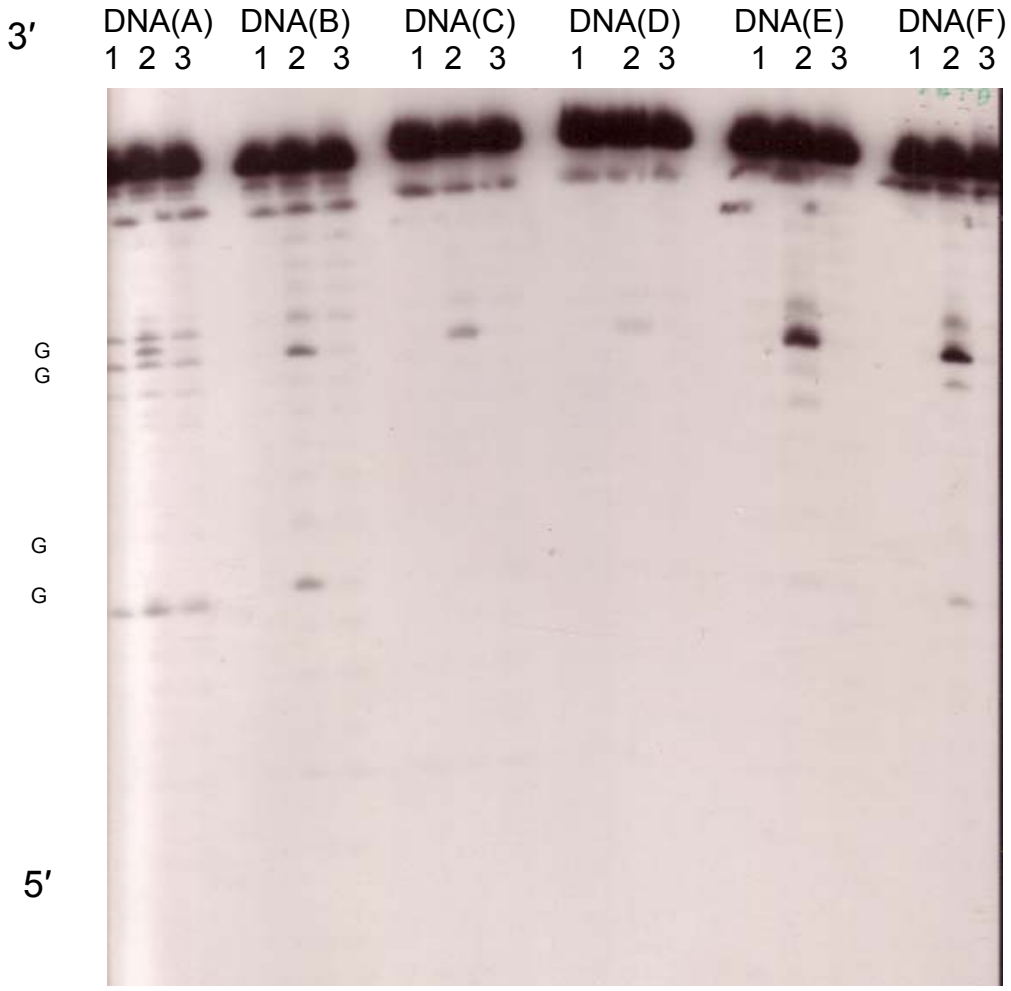

Figure 3-5 Autoradiogram of the six netropsin binding site duplexes (DNA A-F) with and without netropsin. Lanes one are the experimental lanes for the dark control samples. Lanes 2 are the light control lanes and experimental lanes 3 contain the samples with netropsin and in a 1:1.

Materials and Methods

Labeling of DNA. The DNA strand complement to the charge injector linked DNA was radiolabelled with γ-P^{32} labeled at the 5′ end. An aliquot of 5 μL of DNA was added to a micro centrifuge tube followed by 10 μL of water, 2 μL of NEBuffer for T4 Polynucleotide Kinase and 2 μL of T4 Polynucleotide Kinase enzyme. A 1 μL amount of γ-P^{32} was added to the sample. The samples were incubated 37 ^{o}C for 45 min. A volume of 10 μL of dye (bromophenol blue) was added to bring the mixture to 30 μL. The radiolabelled strands were purified on 20% denaturing PAGE which separates all labeled strands by size. Voltage to run the purification gel was set at 400 V. Visualized DNA bands were excised from the gel developed by using radiography on Kodak film. The DNA was incubated in 800 μL of standard elution buffer (0.5 M ammonium acetate (NH_4OAc), 10mM of magnesium acetate ($Mg(OAc)_2$), 1 mM EDTA, 0.1 % SDS) for no less than 4 h at 37 ^{o}C.

Precipitation of DNA. The tubes containing the DNA were centrifuged for a minute. The eluent was removed with a thin tip pipet and added to each tube. To each of the samples, 600 μL of cold ethanol and 1 μL of glycogen were added. The radioactivity of the eluent was checked with a Geiger counter to ensure the labeled DNA was present in the solution. The samples were vortexed for at least 30 seconds and placed in a below -80^{o}C freezer on dry ice for 30 minutes. The samples were centrifuged for 30 minutes and the supernatant was checked for activity and discarded. An aliquot of 100 μL of 80% ethanol was added; and, the samples were centrifuged five minutes. The supernatant was discarded and this was repeated once more. The samples were then dried on low heat for

twenty minutes or until dry. Nanopure water (20 μL) was added to the samples until they at least contained 10,000 counts per μL.

Hybridization. The unlabeled strand and its complement were added to a tube of solution to have a final concentration of 5 μM each. A sample for dark control (no light exposure), light control (no netropsin), netropsin containing DNA samples, and footprinting samples were prepared giving a total of 4 individual samples consisting of 20 μL of solution each. Each sample consisted of 2 μL of radiolabelled DNA (5 μM) each, of nonlabeled DNA and its complement, 10 mM of sodium phosphate ~ pH 7.0 (NaPi), and nanopure water to bring the solutions to 20 μL volume. The mixture was heated to 90 ^{o}C for five minutes and left in heating block to cool down slowly to room temperature to form the duplex.

AQ-DNA samples were irradiated in a Rayonet Chamber with 8 X 350 nm lamps for 30 min.

Cyclic Voltammetry.

Cyclic Voltammetry experiments were run on a CH Instruments model 660 Electrochemical Workstation with a carbon electrode system and also with a platinum electrode system. The netropsin peak was measured by using a 0.1 M solution of tetrabutylammonium tetrafluoroborate as the electrolyte in nanopure water. Once the background was measured, the netropsin was added to be form a final 0.1 M concentration of netropsin and electrolyte. The sweep range was from -2000 mV - 1500 mV. Sweep rates varied from 100 mV - 1000 mV/s.

References

(1) Baguley, B. C. *Mol. Cell. Biochem* **1982**, *43*, 167-181.

(2) Abu-Daya, A., Brown, P. M., Fox, K. R. *Nucleic Acids Res.* **1995**, *23*, 3385-3392.

(3) Finlay, A. C., Hochstein, F. A., Sobin, B. A., Murphey, F. X. *J. Chem. Soc.* **1951**, 341-343.

(4) Patel, D. J., Shapiro, L. *J. Biol. Chem.* **1986**, *261*, 1230-1240.

(5) Patel, D. J., Shapiro, L., Hare, D. *J. Biol. Chem.* **1986**, *261*, 1223-1229.

(6) Wartell R. M., L., J. E., Wells, R. D. *J. Biol. Chem.* **1974**, *249*, 6719-6731.

(7) Patel, D. J., Shapiro, L. *Biopoylmers* **1986**, *25*, 707-727.

(8) Singh, S., Kollman, P. A. *J. Am. Chem. Soc.* **1999**, *121*, 3267-3271.

(9) Marky, L. A., Blumenfeld, K. S., Breslauer, K. J. *Nucleic Acids Res.* **1983**, *11*, 2857-2870.

(10) Wang, J. *J. Biochem.* **1992**, *131*, 11823.

(11) Patel, D. J. *Proc. Natl. Acad. Sci. USA* **1982**, *79*, 6424-6428.

(12) Nunn C. M., G., E., Neidle, S. *Biochemistry* **1997**, *36*, 4792-4799.

(13) Armitage, B., Schuster, G. B. *Photochem. Photobiol.* **1997**, *66*, 164-170.

(14) Lah, J., Vesnaver, G. *Biochemistry* **2000**, *39*, 9317-9326.

(15) Coll, M., Aymami, J., Marel, G. A., van Boom, J. H., Rich, A. Wang, A. H. -J. *Biochemistry* **1989**, *28*, 310-320.

(16) Barawkar, D. A., Ganesh, K. N. *Biochem. Biophys. Res. Comm.* **1994**, *203*, 53-58.

(17) Gondeau, C., Maurizot, J. C., Durand, M. *Nucleic Acids Res.* **1998**, *26*, 4996-5003.

(18) Dervan, P. *Bioorg. Med. Chem.* **2001**, *9*, 2215-2235.

(19) Mrksich, M., Dervan, P. B. *J. Am. Chem. Soc.* **1993**, *115*, 9892-9899.

(20) Hartley, J. A., Webber, J., Wyatt, M. D., Bordenick, N., Lee, Moses *Bioorg. Med. Chem.* **1995**, *3*, 623-629.

(21) Sanii, L., Schuster, G.B. *J. Am. Chem. Soc.* **2000**, *122*, 11545-11546.

Chapter IV: DNA:Netropsin Experiments

Careful consideration was taken to design the DNA duplexes used throughout the effect of netropsin on oxidative damage. It was important to use DNA complexes that would insure controlled experiments with very few variables. The duplexes would include a photosensitizer for charge injection that can be irradiated at wavelengths were DNA and netropsin are invisible. They would have two GG steps to monitor the oxidative damage; and DNA containing 0 or 1 netropsin binding site to determine the effect on damage when netropsin is bound within the minor groove or free in solution.

The duplexes were characterized using several methods; mass spectroscopy, HPLC, UV-Vis spectroscopy, UV-melting spectroscopy and circular dichroism. Charge transfer experiments were performed by irradiating the samples and analyzing them by PAGE and visualization by autoradiography and Fuji phosphorimaging methods. The results of these experiments as well as the design process and methodology will be discussed in chapter.

DNA Design

Several DNA sequences were designed to determine the effect of netropsin on one-electron oxidation of DNA. Each duplex contained a photosensitizer either linked to the 5′ terminus of one of the DNA strand or at the 2′ carbon of the ribose sugar on a uridine base (Table 4-1). The first duplex, duplex1, was designed for optimal binding of netropsin as well as for the efficiency of charge injection and migration from the

proximal GG step to the distal GG step. The TQ photosensitizer was linked to an adenine to optimize the efficiency of charge injection. This reasoning was based on prior experiments where duplexes were designed with each base linked to the AQ photosensitizer[1]. The duplexes were irradiated and analyzed by gel electrophoresis and HPLC. Through the HPLC experiments, the quantum yield of reaction was calculated, and it was found linking an A to the AQ led to more efficient charge injection than linking AQ to the other bases. It was also seen the more adenines, such as a sequence of AQ-5′AA or AQ-5′AAA, made charge injection even more efficient. Two adenines were used in the TQ linked DNA. Two A's would optimize charge injection and reduce the time of irradiation. Placing three A's would create an unwanted netropsin binding site before the GG steps. This would cause problems in

Table 4-1. The DNA sequences used during the course of netropsin study.

DNA	Sequence
Duplex (1)	TQ 5′-AACTGGCCTTTTCCGGTCGC-3′ 3′-TTGACCGGAAAAGGCCAGCG-5′
Duplex (2)	TQ 5′-AACTGGCCAAGGCCTTTTCCAAGGCCTACG-3′ 3′-TTGACCGGTTCCGGAAAAGGTTCCGGATGC-5′
Duplex (3)	TQ 5′-AACTGGCCTTGTCCGGTCGC-3′ 3′-TTGACCGGAACAGGCCAGCG-5′
Duplex (4)	TQ 5′-AGCTGGCCTCGTCCGGTCGC-3′ 3′-TCGACCGGAGCAGGCCAGCG-5′
Duplex (5)	TQ 5′-AACTGGCCTTGTCCGGTCGC-3′ 3′-TTTTTTGACCGGAACAGGCCAGCG-5′
Duplex (6)	5′-CAA GAGGCCAAAACCGGACGC-3′ 3′-GTUAQCTCCGGTTTTGGCCTGCG-5′
Duplex (7)	5′-GCACGGTCGCTGTCCCTCGT-3′ 3′-CGTGCCAGCGACAGGGAGCA-5′
Duplex (8)	AQ 5′-AACTGGCCTTTTCCGGTCGC-3′ 3′-TTGACCGGAAAAGGCCAGCG-5′

interpreting the data. Duplex1 is composed of ss1 and ss2 with the ss1 strand containing the TQ charge injector linked to the 5′ end of the strand. Both strands contain two d(GG) steps in order for either strands, if necessary, to be radiolabelled and monitored for oxidative damage. A four A:T base pair sequence was placed in between the two d(GG) steps in order to act as the netropsin binding site. This was in order to see the effect of the netropsin on damage at the GG steps before and after the netropsin binding site. The d(AAAA) sequence was chosen as opposed to a combination such as ATAT because it has been previously reported netropsin binds more tightly d(5′AAAA) and d(5′AATT) tracts[2]. The four A sequence was used as opposed to the d(AATT) sequence because initial experiments, reported earlier in this report showed charge migration from the proximal to the distal d(GG) step was more efficient through the $d(A:T)_4$ segment than the d(AATT) segment. As shown in earlier experiments, a four A:T tract allows radical cation migration from the proximal to the distal GG step, shown by damage at the 5′ G of the distal d(GG) step[3]. A hyperchem 7.5 rendering in figure 4-1 depicts Duplex1.

Duplex2 was designed to determine if GG steps further away from the netropsin binding site would be affected by the presence of netropsin. This duplex possessed four GG steps in each strand. The netropsin binding site was placed between the second and the third GG steps in the duplex. It contains 30 base pairs as opposed to the 20 base pairs in duplex1. It was also designed with the adenine linked to the TQ and did not contain more than the one netropsin binding site, the 5′AAAA.

Two nonbinding duplexes were designed to use as control strands. The first, duplex3, was similar to duplex1. This duplex is duplex3. The difference between duplex1 and duplex3 is the exchange of an A:T base pair for a G:C base pair in the

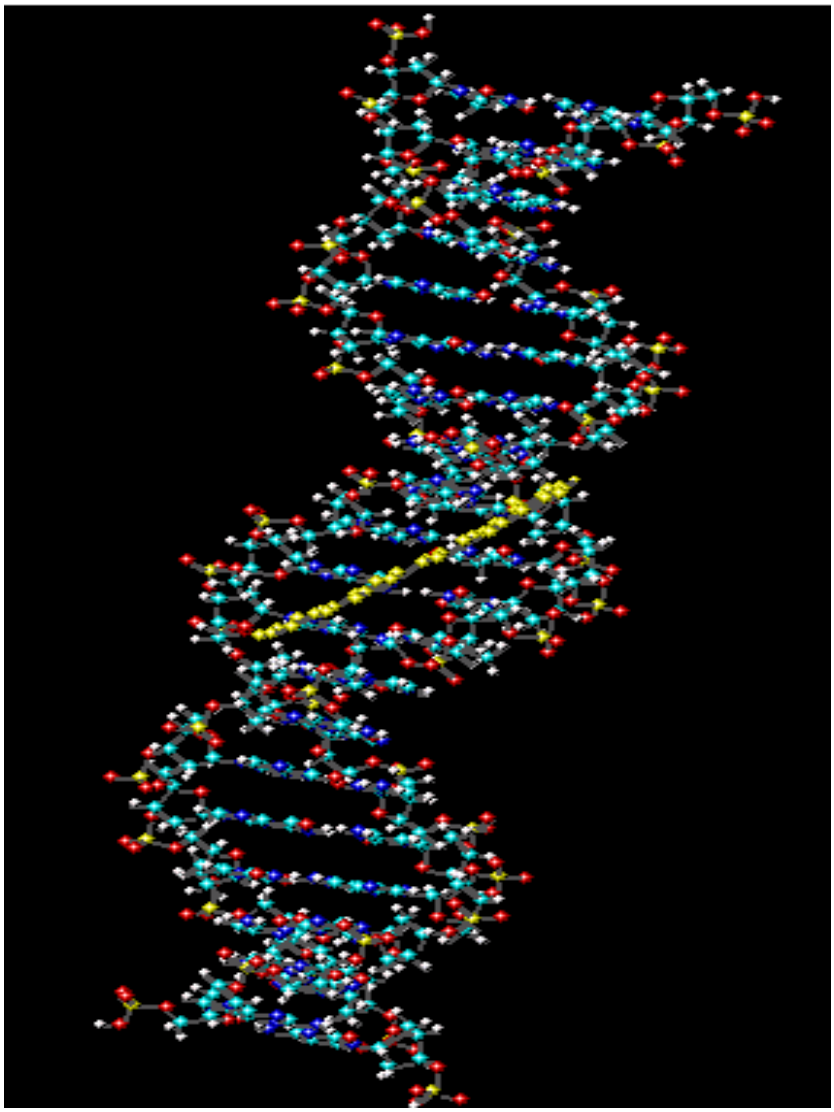

Figure 4-1. A hyperchem rendition of the duplex1 (binding site DNA) with netropsin (yellow molecule in the minor groove) placed in the minor groove at the $(A:T)_4$ binding site.

netropsin binding site. This was done in order to remove the netropsin binding site. By doing this, the netropsin has nowhere to bind within the duplex and duplex3 can be used as a control sequence and the change in chemical properties would be minimal. The purpose of this duplex was to determine whether the results that are observed from the binding site experiments with duplex1 were due to the binding of the netropsin within the minor groove.

The second nonbinding duplex, duplex4, was designed to ensure the possibility of the netropsin partially binding within the minor groove was not an option. There were not more than two A:T base pairs neighboring one another in this duplex. There have been recent reports of the possibility of netropsin partially binding to tracts as little as 2 A:T base pairs. The results from experiments with duplex4 would back up the result seen in duplex3. The first four bases in duplex4 were changed from that of duplex1 and duplex3. The A:T base pair linked to the TQ remained for charge injection efficiency and another G:C base pair was added to the binding site area to ensure no two A:T base pairs followed one another. The length of the duplex remained the same.

Duplex5 was designed to determine whether netropsin was coordinating with the TQ while not bound within the minor groove and quenching the TQ before charge injection could occur. By using an overhang sequence, it would hinder the netropsin form coordinating with the TQ and allowing charge injection to occur for charge migration. The sequence was identical to duplex3 except it had a four T overhang at the 3′ end of ss4. This strand is ss7. The ss3 strand remained the same as in duplex3. Four Ts were chosen because the thymine has the least charge injection efficiency of the four

bases in relation to TQ. Therefore the charge would still be injected into the duplex in order for charge migration to occur.

Duplex6 was designed for same purpose as duplex5. An UAQ photosensitizer was used in the place of the TQ in this DNA duplex. Although the AQ has an overlapping absorbance as the netropsin, this would indicate whether the effect on the damage was due to the quenching of the photosensitizer. If there was in fact damage seen when netropsin was in a 1:1 – 1:2 (DNA- netropsin) with DNA it could be assumed the netropsin was in some way coordinating with the charge injector. The UAQ was used because it can be placed anywhere within the DNA sequence and intercalates within the DNA duplex. This would ensure the netropsin could not possible coordinate with the AQ and cause quenching. The AQ linked uridine was placed as the third base in the DNA duplex. The duplex did contain netropsin binding site. Once the netropsin binding site was full, the remaining damage should remain the same with the titrating in of the netropsin.

Duplex7 was designed as a "sacrificial duplex." There has been speculation netropsin may be able to intercalate within the DNA duplex. If the netropsin was intercalating into the DNA, adding an excess amount of duplex7 in a mixture of duplex3 would give the netropsin a more suitable duplex to intercalate within. The duplex contained a number of G:C base pairs, a condition optimal for intercalation because DNA duplexes containing a number of G:C base pairs are known to be good for intercalation. This duplex does not contain a photosensitizers because its soul purpose is to act as deterrent for the netropsin not to bind to the TQ containing duplex. With this duplex in

the mixture with the nonbinding duplexes, any type of coordination between the DNA and the netropsin should be averted.

Characterization of DNA

Characteristics studies were performed on all DNA duplexes used during the course of this study. Individual DNA strands were also characterized to ensure the correct sequence was obtained from phosphoramidite based DNA synthesis. Samples were purified using High Performance Liquid Chromatography (HPLC). During purification, the UV absorbance spectra of the DNA peaks were observed. These spectra of the DNA peaks contained the characteristic DNA absorbance peak at ~ 260 nm. In cases where a charge injector was linked to the DNA such as an AQ or a TQ, a small peak at about 350 nm or 420 nm respectively appeared in the spectrum. These results were also supported by the measuring the UV spectrum on an UV-Vis spectrophotometer. The UV-Vis spectra of the DNA strands containing the photosensitizers also displayed the peaks at 350 nm and 420 nm exhibited (Figure 4-2). This along with HPLC traces was evidence the photosensitizers were covalently linked to the DNA and the DNA was pure. The absorbences obtained from the UV spectra were also used as a analytical technique along with a biopolymer calculator to determine the concentration of the DNA strand in solution.

The DNA sequences were submitted for mass spectral analysis to verify their correct mass and sequence. All experimental masses for each strand corresponded with the theoretical masses calculated. Some of the mass spectra can be seen in the Figures 4-3 and 4-4. Once the initial characteristics were examined, the duplexes were characterized by UV melting and circular dichroism (CD). These instruments were used to determine

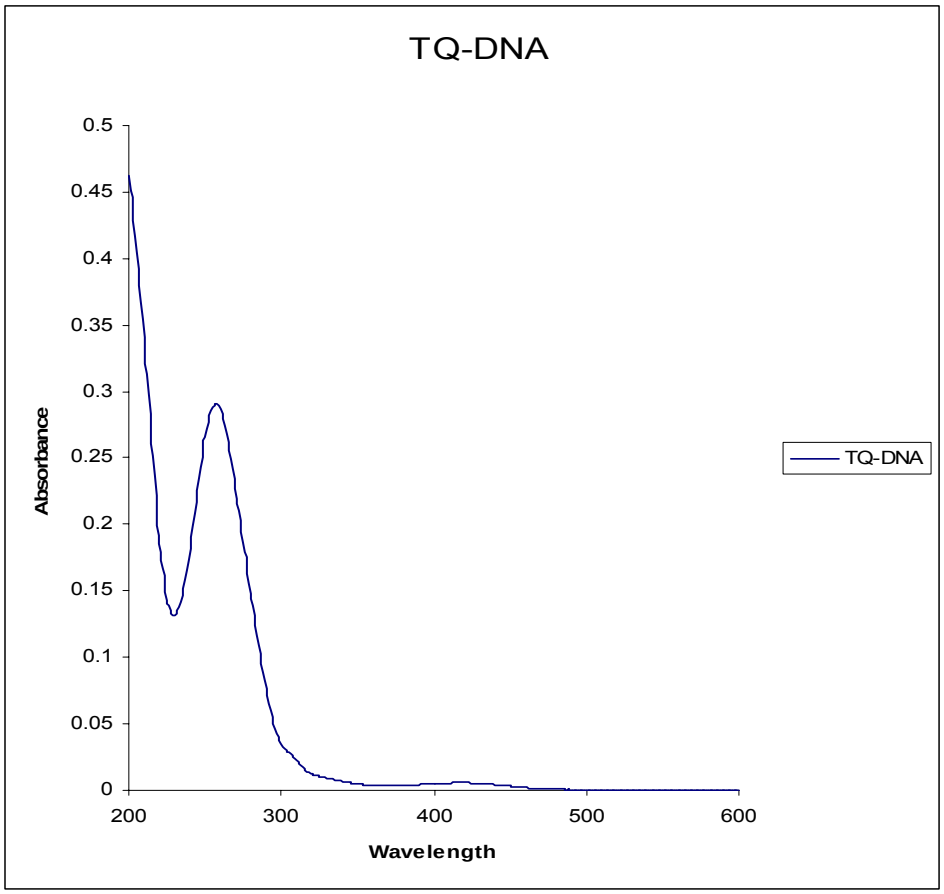

Figure 4-2. UV-Vis absorbance spectrum of TQ-linked DNA. This spectrum shows the characteristic DNA absorbance at 260 nm and an absorbance at ~ 420 nm indicating the presence of the TQ photosensitizer.

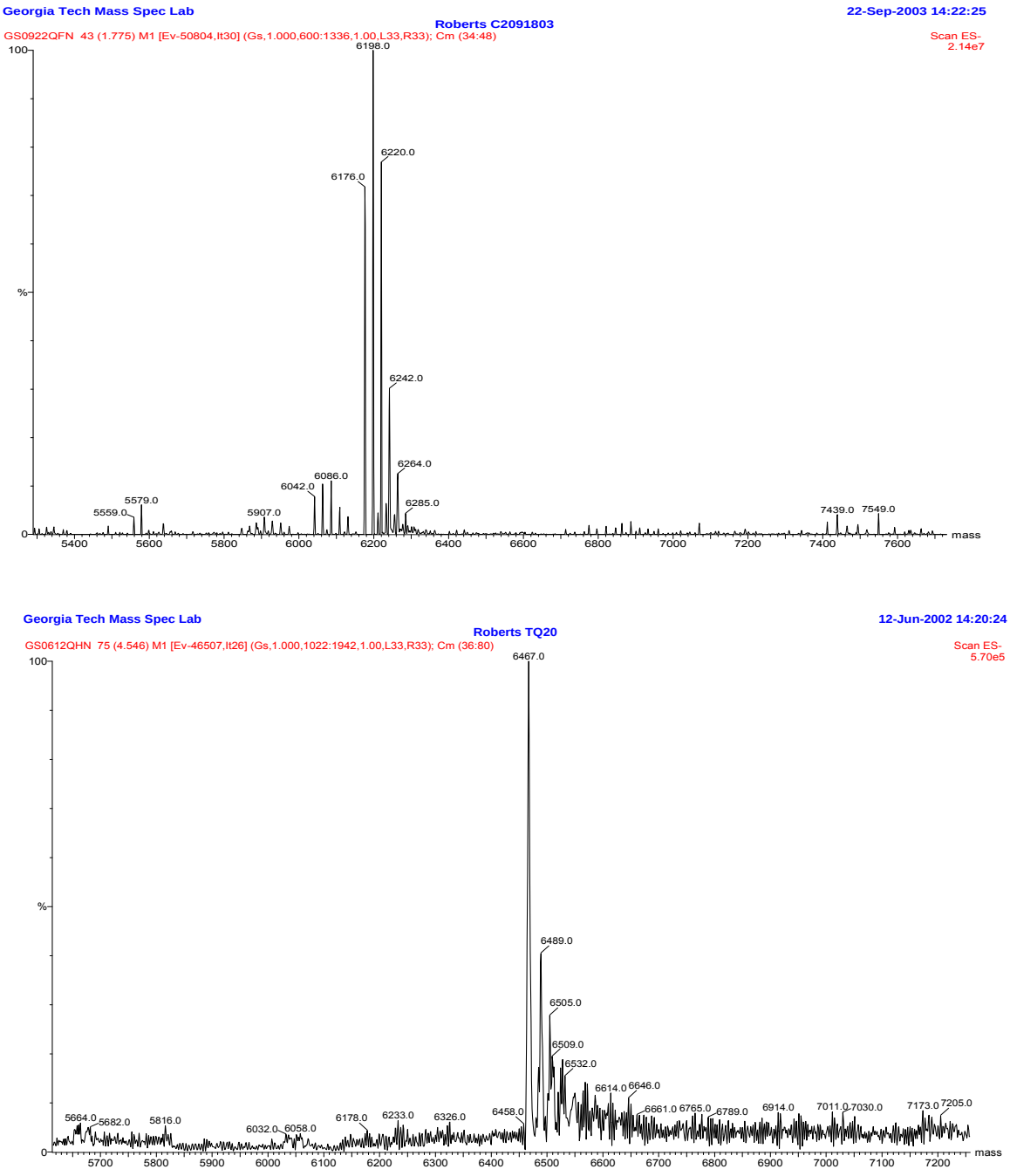

Figure 4-3 The electro spray mass spectrum of ss1 (above) and ss2 (below) of duplex1.

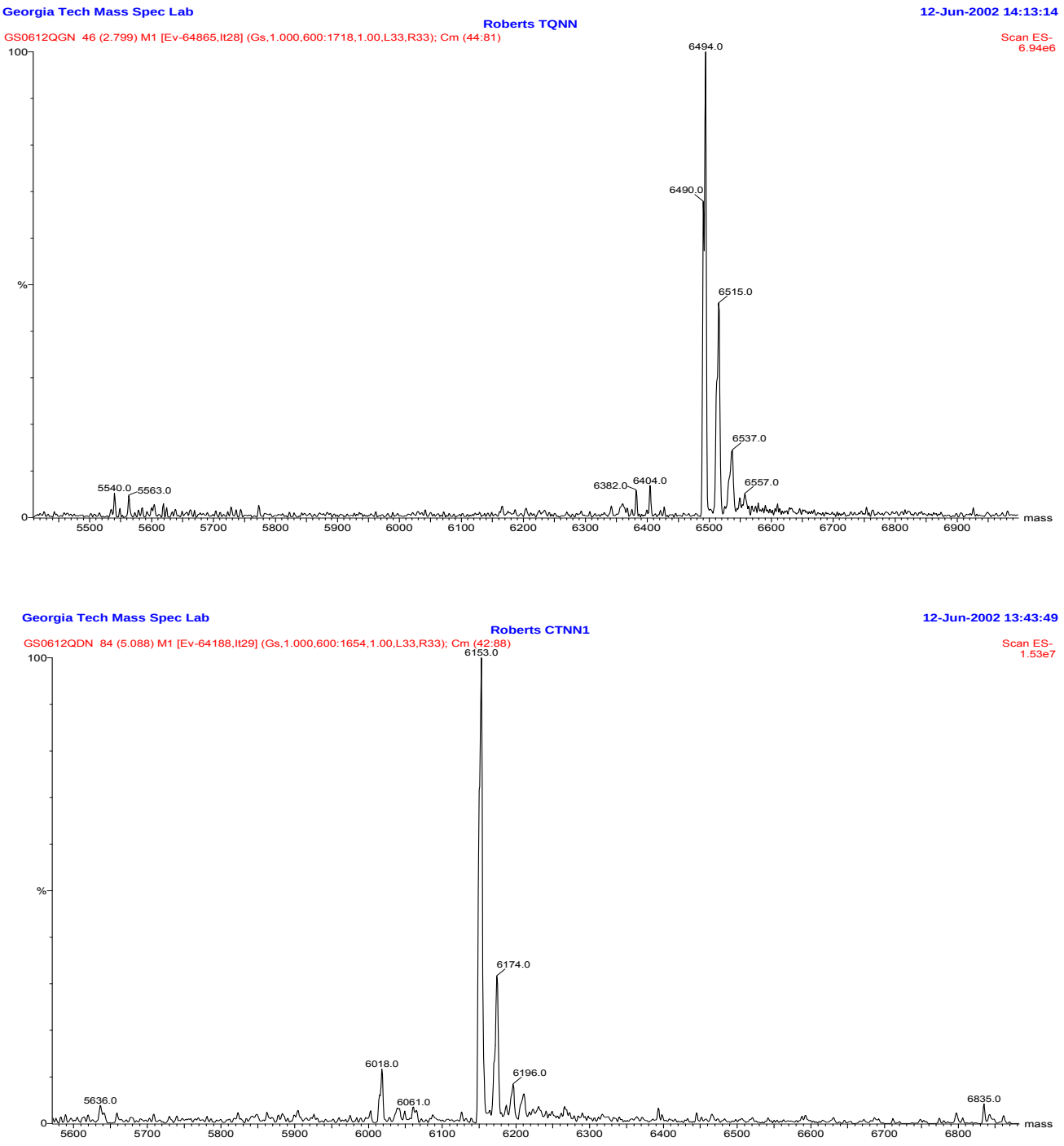

Figure 4-4. The electro spray mass spectra of ss5 (above) and ss6 (below) of duplex3.

if the DNA formed duplexes upon hybridization and also if the newly formed duplexes formed B-form DNA. The UV melting also determined if the duplex would be stable under experimental conditions and would the conditions need to be altered in order to sustain the DNA duplex. All of the duplexes were observed to be able to undergo experimental conditions and also for B-form DNA.

Proof of Netropsin Binding

UV melting experiments was used to determine whether or not netropsin was binding to the DNA duplex. A 2.5 μM solution of duplex1 and duplex3 were prepared without and with incubation with netropsin. The samples were placed inside the UV melting instrument and the curves for melting and cooling were recorded. The data from the curves were converted to first derivative plots and the peak values were taken as the melting temperatures of the duplexes. In the case of duplex1, the value for melting without netropsin was 63 ^{o}C. When netropsin is present in the sample, the melting temperature (T_m) increased to 74 ^{o}C (Figure 4-5). This was an 11 degree increase from the containing no netropsin sample showing the stabilization of the duplex by netropsin. These results show like stabilization behavior as seen in previously reported results for duplexes containing netropsin binding sites in the presence of netropsin[4]. This was evidence binding was occurring. The duplex3 sample was prepared in the same manner with and without netropsin. The sample containing no netropsin had a T_m of 64 ^{o}C, slightly higher than duplex1 but within experimental error. Not surprising due to the

change in the A:T base pair to G:C which adds only one H-bond to the duplex. The netropsin containing sample was also 64 ^{o}C (Figure 4-6). This indicated a lack of

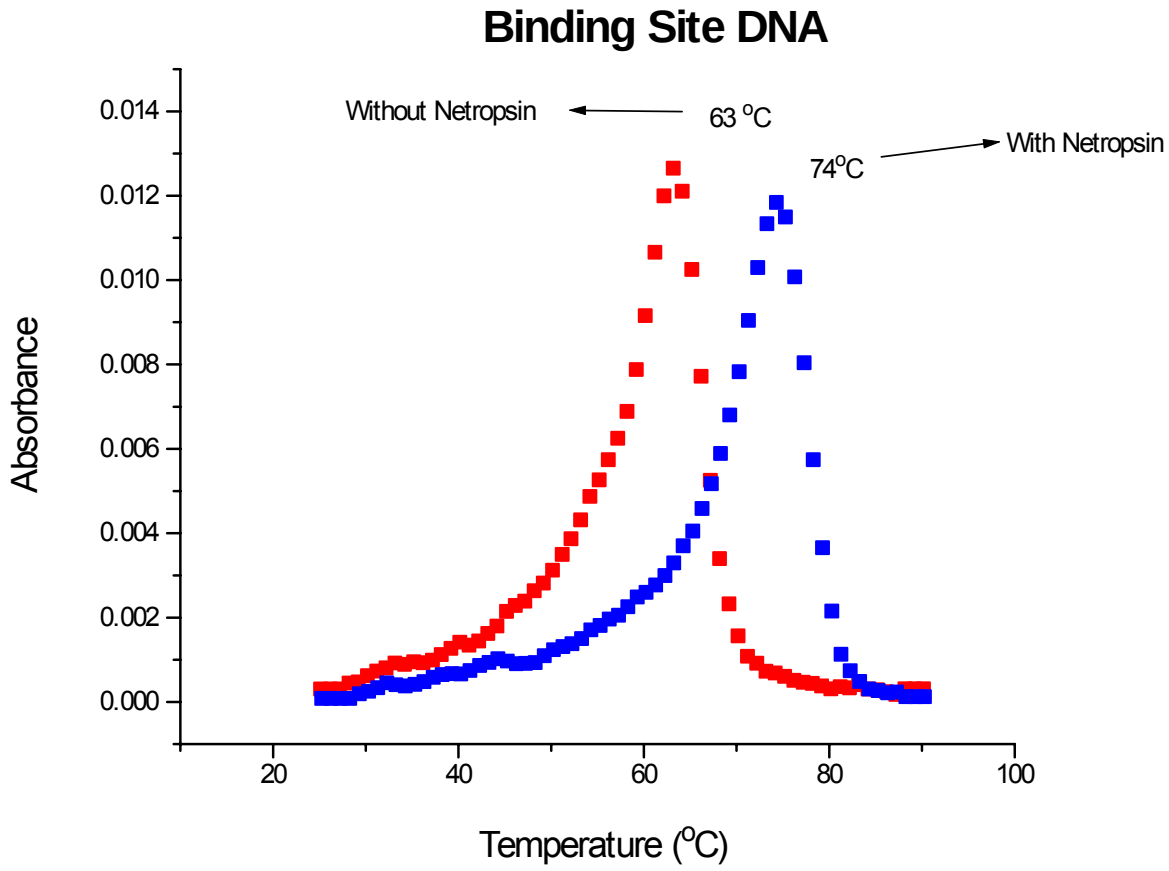

Figure 4-5. The first derivative plot of the melting curve for duplex1 without netropsin (red). The first derivative plot of the melting curve for duplex1 and netropsin in 1:1 (blue).

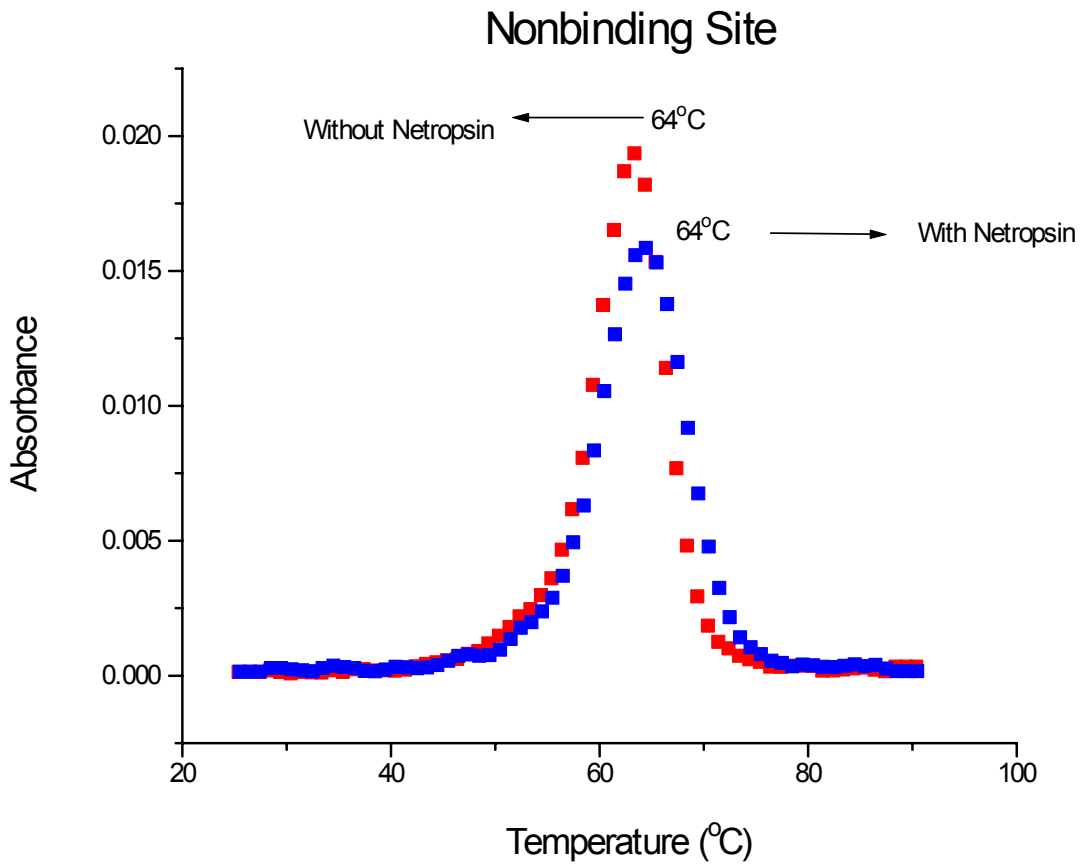

Figure 4-6 . The first derivative plot of the melting curve for duplex3 without netropsin (red). The first derivative plot of the melting curve for duplex3 and netropsin in 1:1 (blue).

stabilization of the duplex due to the presence of netropsin indicating no netropsin binding.

These samples were also used to record CD data. Netropsin does not have optical activity and should not give a CD signal when free in solution. When netropsin is bound to DNA it can be detected by CD because it is bound to the optically active compound. If netropsin is not bound in the DNA netropsin solution, the CD spectra of DNA alone and DNA-netropsin should look the same[4,5]. The samples were scanned from 200 to 400 nm. The duplex1 sample containing the netropsin spectrum shows clear added absorbencies at ~ 262 and past 300 nm unlike that of DNA and minor absorbencies at 240 and 296. This corresponds to literature values and indicates the binding of netropsin. The duplex3 sample containing netropsin CD spectrum showed no change from the dupex3 sample without netropsin spectrum. This was more evidence netropsin was binding to duplex1 and not duplex3 (Figure 4-7).

Foot printing experiments with DNase I were performed with duplexes 1 - 4 to determine not only if netropsin was binding but where netropsin was binding in the duplex. DNase I cleaves duplex DNA at every base except where there is a bound compound[6]. If there is nothing bound to the DNA, every base should show damage and places where there netropsin is bound there should be free from damage. The experiments included control samples that have varying amounts of DNase I to ensure proper experimental conditions, samples containing DNA and netropsin in 1:1 also with

varying amounts of DNase I, and samples containing DNA and netropsin in 1:2 with varying amounts of DNase I. Figure 4-8 shows the footprinting experiment performed

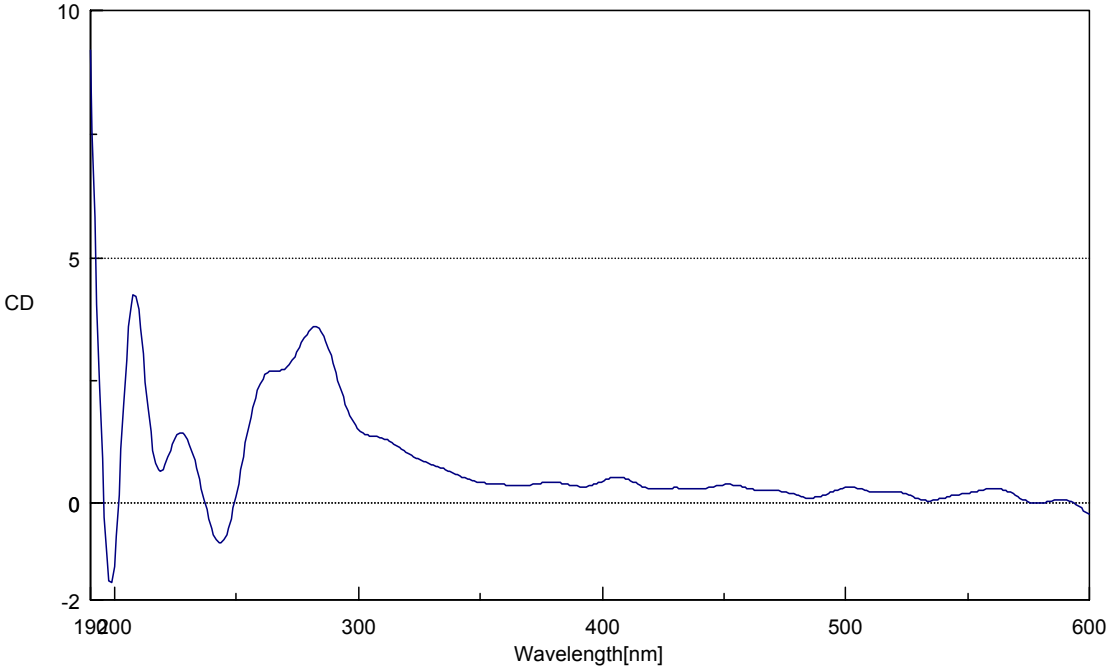

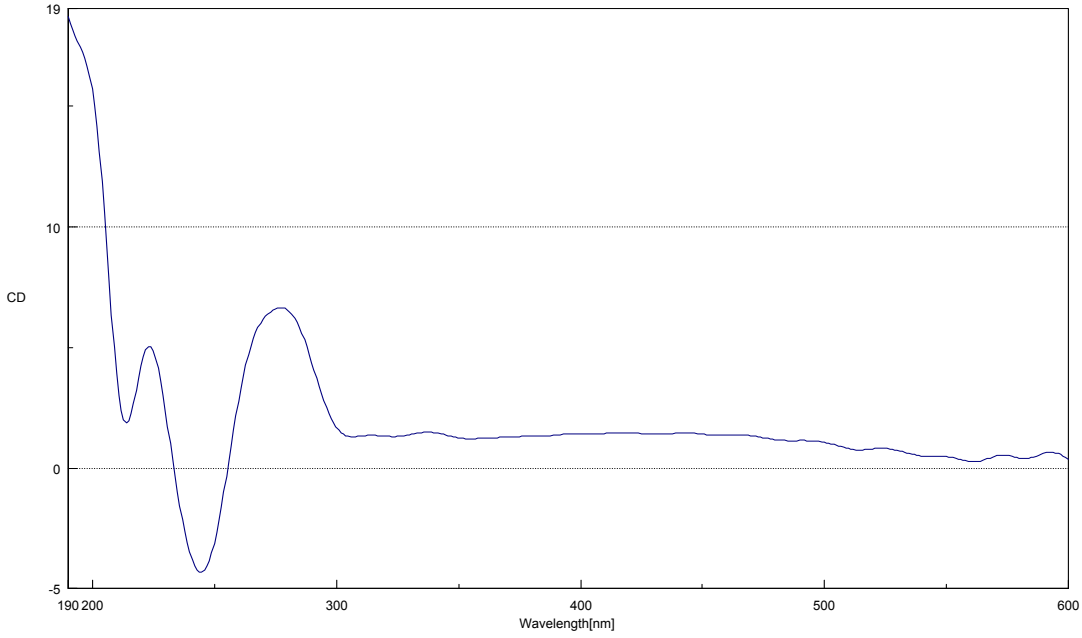

Figure 4-7. Above is the CD spectrum of duplex1 containing netropsin in a 1:1. Below is the CD spectra of duplex3 containing netropsin in a 1:1.

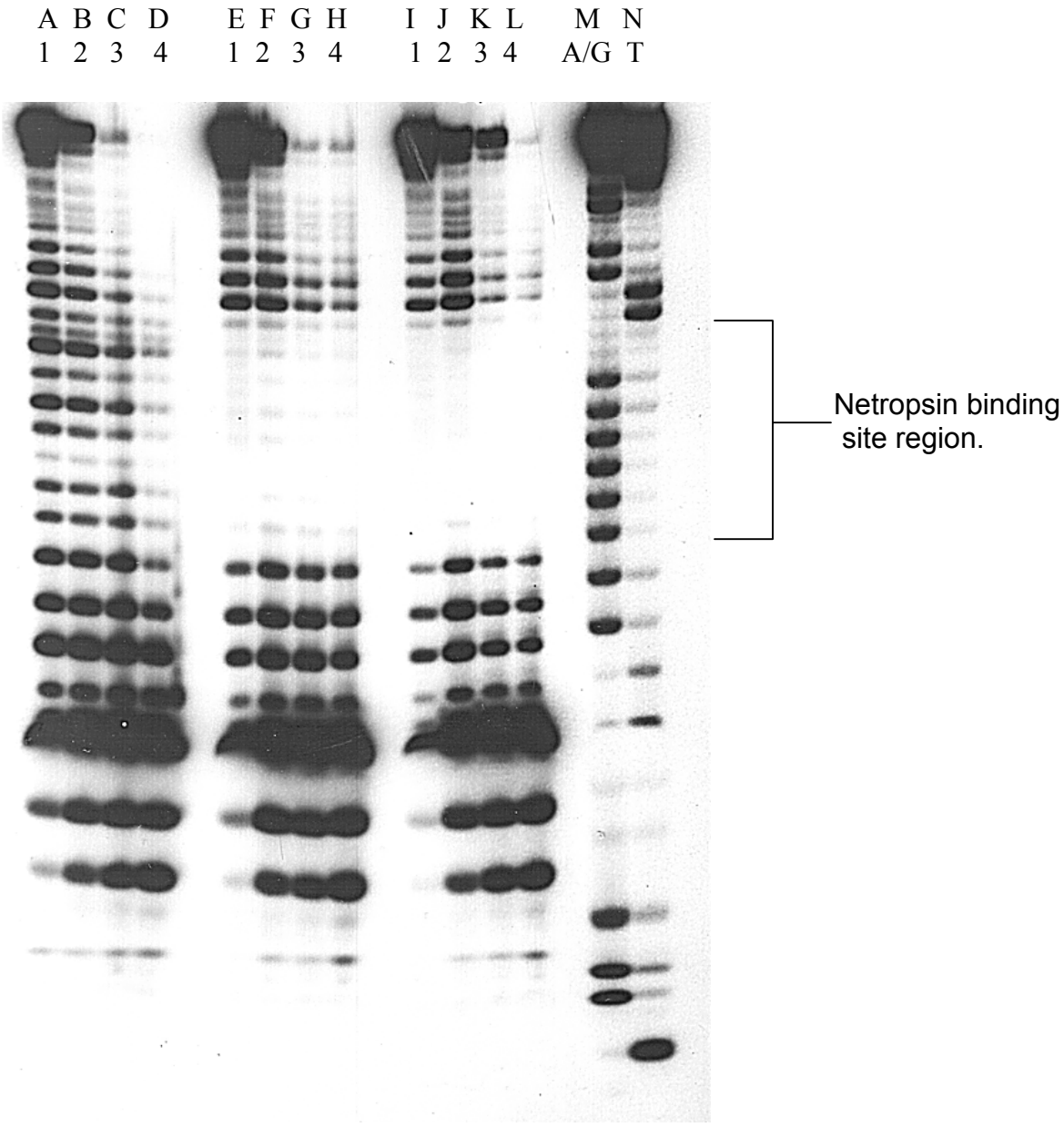

Figure 4-8 Autoradiogram of footprinting experiment for duplex2 using DNaseI. The first four lane are the control lanes with DNase I titrated in form 1 – 4 μL (1U/μL) in 1 μL increments. Experimental lanes E-H represent the duplex in a 1:1 with netropsin with DNase I titrated from 1-4 μL. Experimental lanes I-L contain samples with DNA and

netropsin in 1:2 with DNase ranging from 1-4 μL. Lanes M and N are the A/G and T sequencing respectively.

for duplex2. In lanes labeled A-D are the control lanes containing samples that do not contain netropsin with 1 – 4 μL of DNase I (1U/μM). These lane displayed damage at every base showing what should occur if there was no binding compound. Lanes E- H are the experimental lanes for DNA and netropsin in 1:1. As expected there was no damage seen in the netropsin binding site area as well as the a few bases on either side of the binding site. This indicated netropsin was bound in this area. The bases outside of the binding site were not damage because the DNaseI enzyme is a very large molecule and because of its size it was not able to cleave the bases near the binding site because the netropsin prevented it from being able to cleave those bases even though it was not bound there. Lanes I-L are the experimental lanes for samples containing DNA and netropsin in 1:2. Like those results seen for lanes E-H, there was no cleavage seen at the netropsin binding site. In these samples, netropsin was in excess and this experiment showed there were no additional binding sites present in duplex2. This was not only proof of netropsin binding but it was evidence the netropsin was binding at the proposed binding site. Lanes M and N are A/G and T sequencing respectively.

The footprinting experiment for nonbinding duplexes were performed the same way as for the binding duplexes. The only difference was the DNase I amounts ranged from 1 to 3 μL as opposed to 1 to 4 μL. The autoradiogram in figure 4-9 is the footprinting experiment duplex4. The three control lanes show the damage pattern for

duplex4. The experimental lanes containing the netropsin in 1:1 and 1:2 were identical to those of the control lanes. This was proof the netropsin was not binding in the case of duplex4 which were the expected results (Figure 4-9).

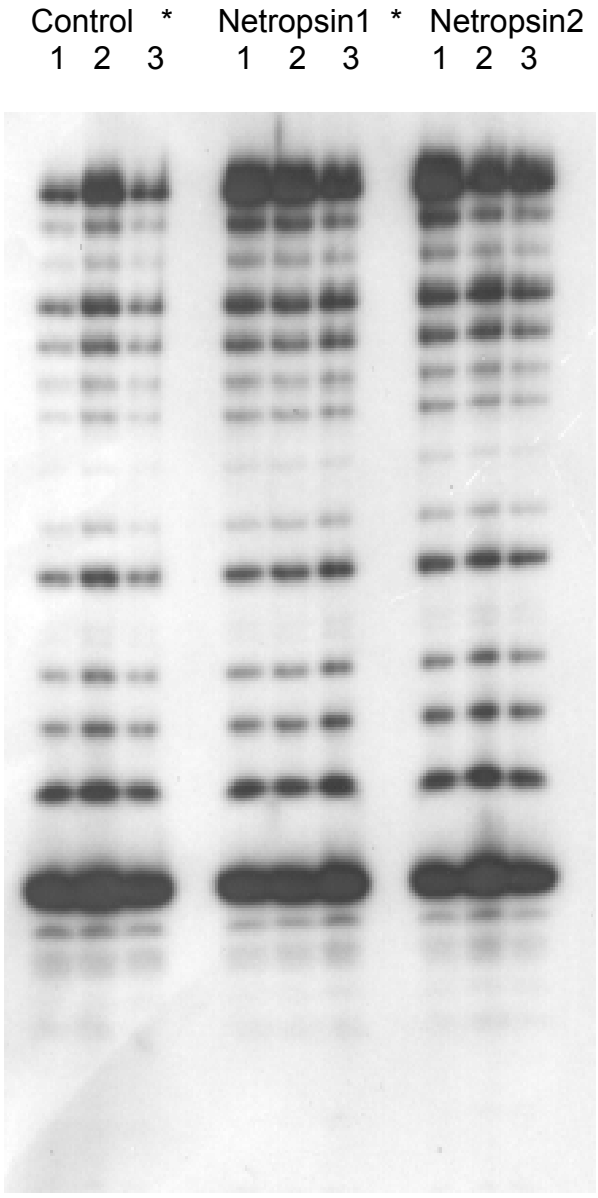

Figure 4-9 Autoradiogram of footprinting experiment for duplex4 using DNaseI. The first three lane are the control lanes with DNase I titrated in form 1 – 3 μL (1U/μL) in 1 μL increments. The second set of experimental lanes represents the duplex in a 1:1 with netropsin with DNase I titrated from 1-3 μL. The third set of experimental lanes contains

samples with DNA and netropsin in 1:2 with DNase ranging from 1-3 μL. The three sets of lanes are similar thereby showing netropsin is not binding.

Charge Transfer Experiments with Netropsin

Charge transfer experiments began by using duplex1 to determine the effect of netropsin on oxidative damage. Strand ss2 was radiolabeled using γ-P^{32} to label the 5′ end of the DNA strand. After purification of the labeled strand, several samples were prepared containing the labeled DNA strand with it complement strand ss1 and unlabeled ss2 for hybridization. After hybridization the netropsin was incubated with some of the duplex samples in a 1:1 for 30 min. The sample set consisted of a dark control containing only DNA, a dark control containing DNA and netropsin, two light control samples with DNA (15 and 30 min of exposure @ 420 nm), and two samples containing DNA and netropsin in a 1:1 (15 and 30 min of exposure @ 420 nm). The sample set, including the dark control samples, was treated with hot piperidine (@ 90 ^{o}C) followed by analysis and visualization by electrophoresis and autoradiography.

The experimental lanes, A and B, for the two dark control samples show little to no damage in their lanes (Figure 4-10). This indicates that all damage seen should be directly attributed to UV irradiation. This dark control was run with every experiment to ensure damage was caused by the exposure to UV light. Experimental lanes C and D were irradiated for 15 min. Lane C is the experimental lane for the DNA only sample and lane D represents the sample contains of DNA and netropsin in 1:1. Lane C displayed the expected results of damage at the proximal and distal GG step at the 5′ G. There was more damage at the proximal than the distal GG step. This was due to the rate of

trapping being faster than the rate of hopping in the case of a four A:T tract between the two GG steps. Lane D was quite different from lane C, there appeared to be decrease in damage at the proximal GG step. Lanes E and F were the same as C and D respectively

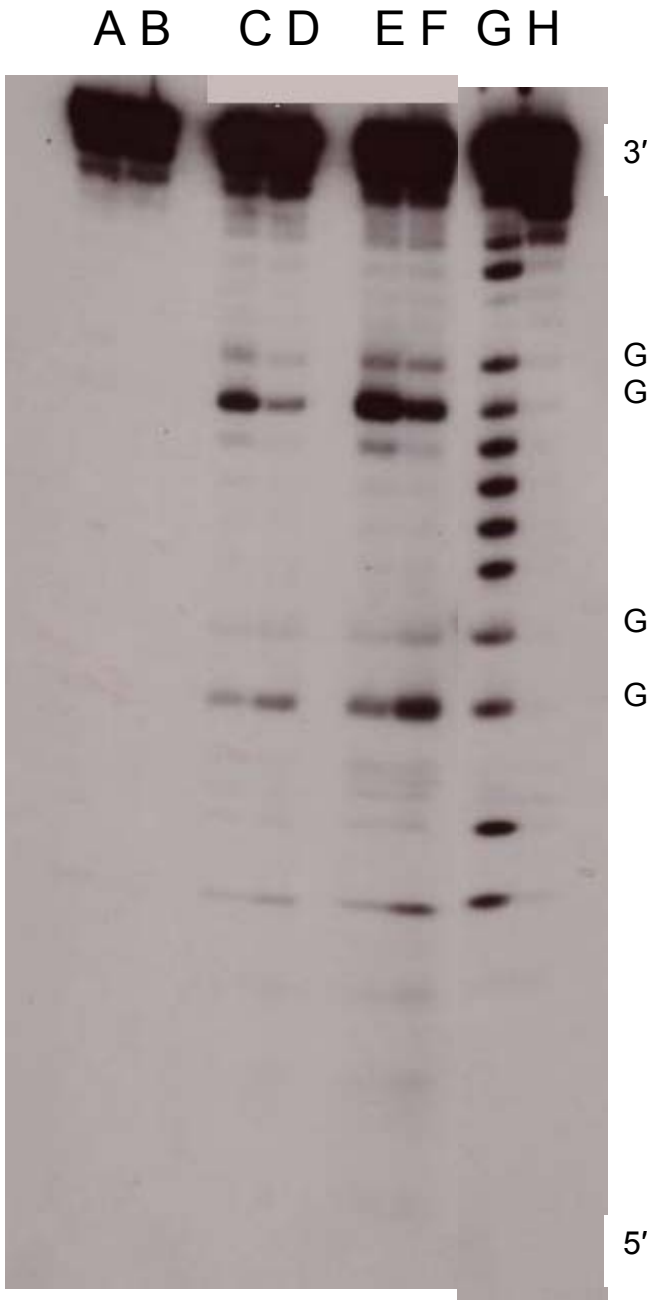

Figure 4-10 Autoradiogram of the duplex1 with and without netropsin. Experimental lanes A and B are the dark control lanes, A without netropsin and B with netropsin.

Lanes C and E are the light control lanes irradiated for 15 and 30 min respectively and lanes D and F are the experimental lanes containing netropsin in a 1:1 ratio with DNA. Lanes G and H are the A/G and T sequencing respectively.

except these samples were irradiated for 30 min as oppose to 15 min. The results of these lanes were the same as for the 15 min lanes except there was more damage seen at the GG steps because of the longer irradiation times. It appeared when netropsin is bound to the DNA it decreases the overall damage at the GG steps. These experiments were repeated several times and the results were identical within experimental error. The experiment was even run with an AQ containing strand (duplex8) just for comparison (Figure 4-11). Although there were thought to be uncontrolled variables, discussed in chapter 3, it was interesting to compare the different photosensitizer linked duplexes side by side.

Further investigation led to titrating amounts of netropsin while leaving the DNA concentration fixed. This sample set included a dark control (no netropsin), a light control, and netropsin samples containing netropsin and DNA in a 1:4, 1:2, 3:4, 1:1, 2:1, and 3:1. The result seen in the dark control experimental lanes were as expected, there was little to no damage. The light control lanes displayed results that are supported by literature[7]. Damage was detected at the 5′ G of the proximal and distal GG steps. Once again the netropsin containing lanes did not display the same results as the light control. The damage at the GG steps was decreased as the concentration of netropsin was increased. The damage seen at the GG steps seemed to resemble that of the dark control when a concentration of 2:1 was reached (Figure 4-12). There were several experiments

involving the titration of netropsin while the concentration of DNA remained constant. They all produced the same results.

There were several possibilities of what was causing these results. It was possible the radical cation was being quenched by the netropsin or the netropsin was acting as a

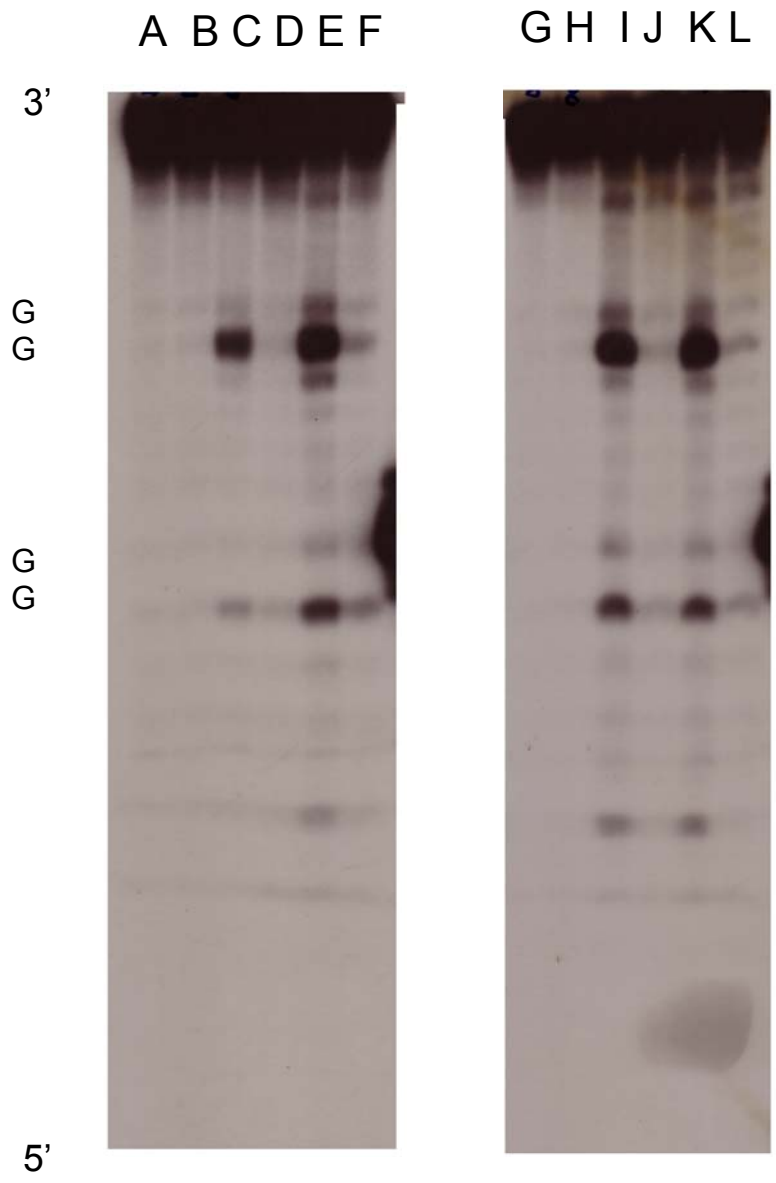

Figure 4-11. An autoradiogram showing the effects of netropsin on a TQ-linked DNA duplex and an AQ-linked DNA duplex when irradiated for 15 and 30 min. Lanes A-F are

the experimental lanes for the TQ-linked DNA and lane G-L are the experimental lanes for the AQ-linked DNA. Lanes A, B, G and H are the dark control lanes without (A and G) and with (B and H) netropsin. Lanes C and I are the light control lanes for 15 min and lanes E and K are the light control for the irradiation time of 30 min. Lanes D, F, J, and L contain netropsin in a 1:1 with DNA and are irradiated for 15 min (D and J) and 30 min (F and L).

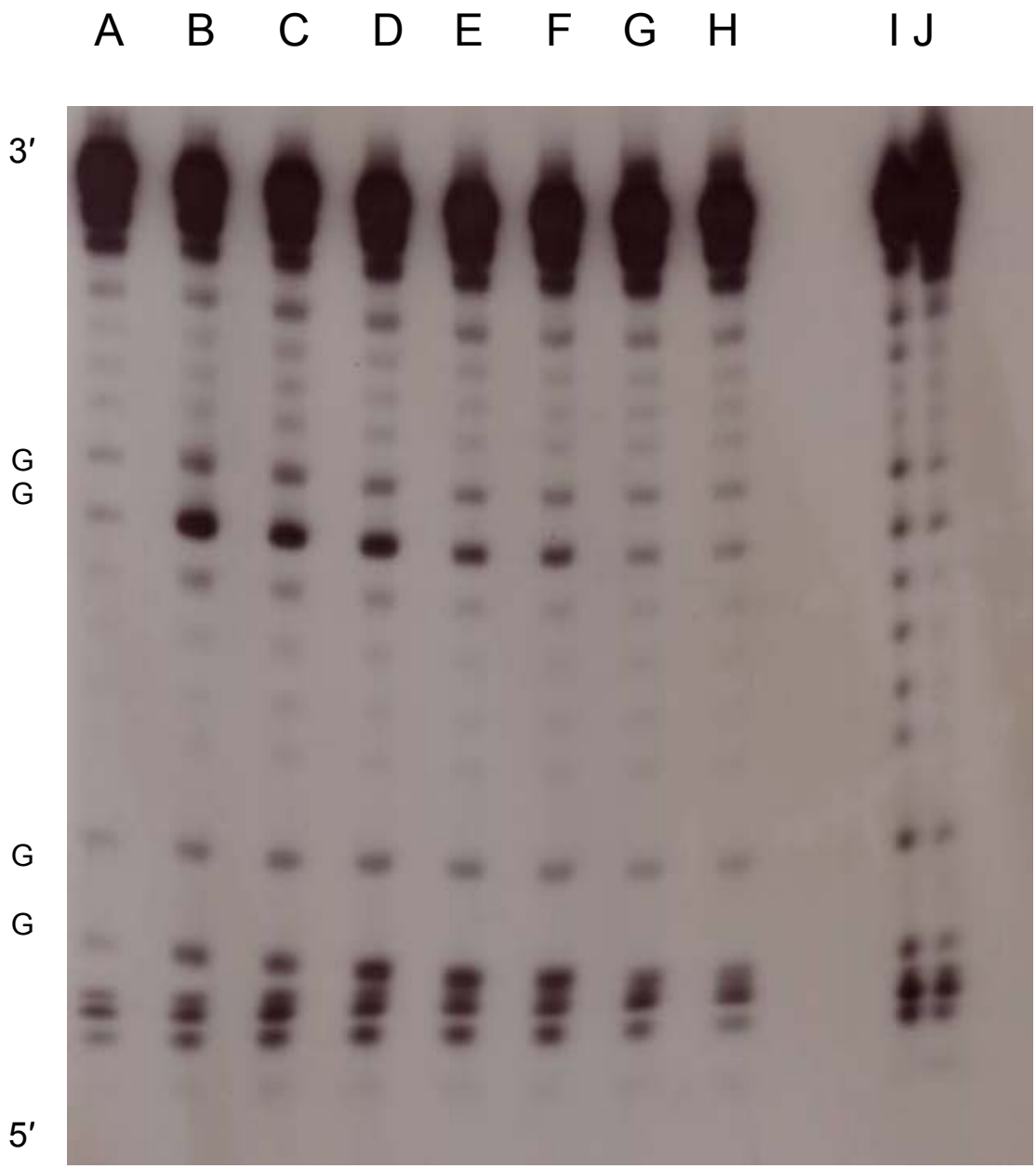

Figure 4-12 The autoradiogram of a netropsin dependence concentration study on oxidative damage for duplex1. Lane A is the experimental lane for the dark control sample. Lanes B-H are the experimental lanes for the netropsin containing samples with the concentrations ranging from 0 – 15 μM (0, 1.25, 2.5, 3.75, 5.0, 10 and 15 μM). Lanes I and J are the A/G and T sequencing respectively.

bridge for the radical cation. Knowing the netropsin possesses a lower oxidation potential than the four DNA bases, there was a great possibility the netropsin was acting as a quencher for the radical cation. The netropsin acted as a deeper trap and when the radical cation reaches the GG steps, the netropsin donates an electron to the guanine leading to the decrease at oxidative damage.

There were two directions taken, the first was to create a duplex that contained GG steps that were away from the netropsin binding site, duplex2. The second was to create a control DNA duplex3. Experiments with duplex3 should show the opposite results of those seen with duplex1.

Duplex2 was created with the 4 A netropsin binding site. The first experiments run with this duplex followed the same protocol as for duplex1. The ss4 was γ P^{32} labeled and an irradiation time test was performed to determine which time would be best for the length of irradiation. It was found 15 min was best length of time to irradiate the 30 mer in order to see a reasonable amount of damage at each GG step without going out of single hit conditions. Studies with this duplex were run several times. It was seen when netropsin was in 1:1 with DNA, damage was not decreased as effectively as it was with duplex1. This was a bit surprising and the experiment was repeated increasing the amount of netropsin added to the DNA. Several samples were prepared to test the effect the netropsin had on the sequence. The sample set included a dark control, a light control, and samples containing DNA and netropsin in 2:1, 1:1 and 1:2. The samples were, minus the dark control, were irradiated, piperidine treated and analyzed by electrophoresis and visualized by autoradiography. The dark control, experimental lane A, shows very little

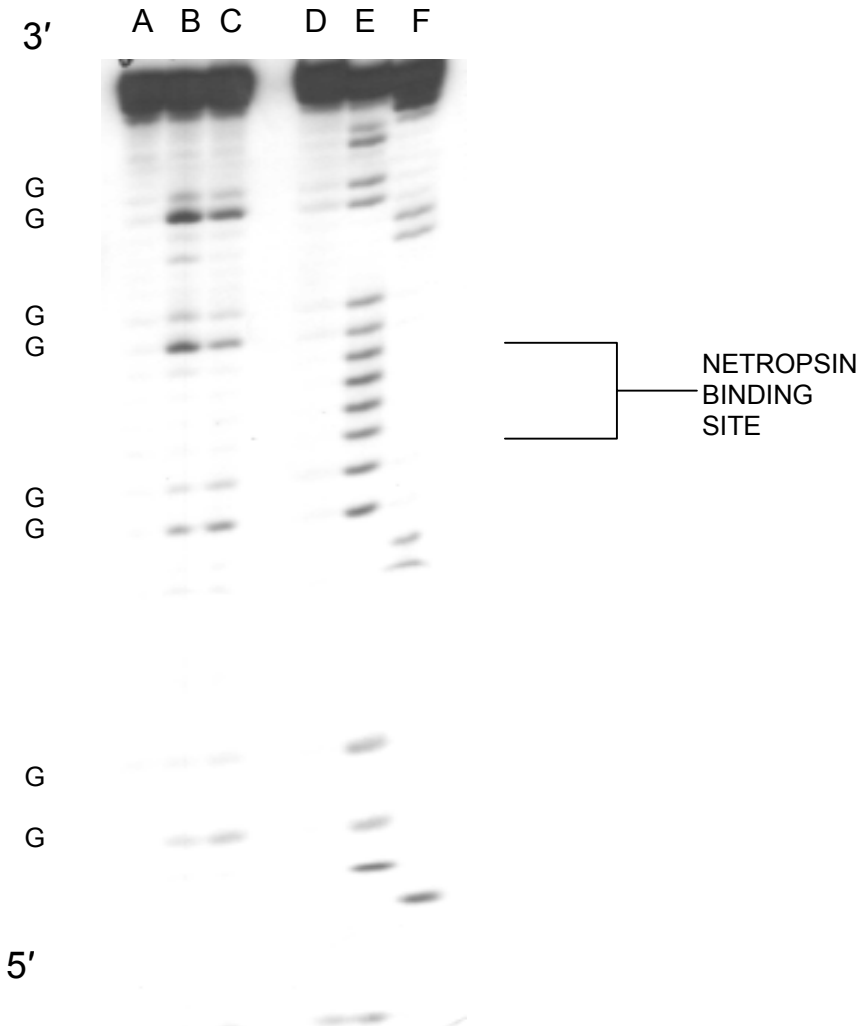

Figure 4-13 Autoradiogram for netropsin's effect on duplex2 when irradiated for 15 min. Lanes A and B are the experimental lanes for the dark and light control sample respectively. Lanes C and D contain DNA and netropsin in 1:1 and 1:2. Lanes E and F are the Maxim-Gilbert A/G and T sequencing lanes respectively.

to no damage. The light control experimental lane B (Figure 4-13) showed damage at the 5′ G of all four GG steps with a less damage at the two distal steps. This has to do with

the efficiency of charge migration through the DNA duplex. Lane C is the experimental lane for the sample containing the netropsin in 1:1 with DNA showing a decrease in damage at the first and second GG steps yet the damage seemed about the same at the two distal GG steps (Figure 4-13). The experimental lane for the sample containing 1:2 DNA to netropsin, lane D, shows results similar to those seen in the dark control lane. These results were comparable to those seen in the duplex1 yet the 1:1 ratio lanes were slightly different. Duplex1 showed less damage for the 1:1 sample than seen in duplex2. This could be because there were four GG steps instead of two, therefore less damage is seen in the case of duplex1. It could also mean there is more of an effect on GG steps closer to the binding site, which doesn't seem likely. It is also possible the free netropsin was quenching the radical cation but there is very little free netropsin in solution. Therefore free netropsin cannot be the primary source for quenching.

The results of these two experiments led to the conclusion that if damage was decreased due to netropsin binding then when netropsin was not bound, the netropsin containing lanes should resemble those of the light control. Meaning there should be no effect on oxidative damage. Therefore duplex3 was examined. It was similar to the duplex1 yet it did not contain a netropsin binding site in the middle of the two GG steps. The DNA was tested for the proper irradiation conditions. They were similar to the conditions for the dupex1. The samples were prepared in the same fashion as for duplex1 with a dark control, light control and two netropsin containing samples with a 1:1 ratio and 1:2 ratio DNA to netropsin. The results for this experiment were quite unexpected

A B C D E F

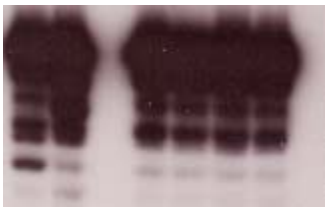

Figure 4-14 Autoradiogram for netropsin's effect on duplex3 when irradiated for 15 min. Lanes C and D are the experimental lanes for the dark and light control sample respectively. Lanes E and F contain DNA and netropsin in 1:1 and 1:2. Lanes A and B are the Maxim-Gilbert A/G and T sequencing lanes respectively.

(Figure 4-14). The dark control was the same as the other experiments with little to no damage in the experimental lane. The light control had damage at the proximal and distal d(GG) steps with equal amounts of damage. This was quite different from that of

duplex1 which had more damage at the proximal d(GG) than the distal. This is due to the efficiency of charge migration through the d(AAAA) sequence and the d(AACA) sequence[8]. It has been derived from other charge transfer studies that the polaron migration is more efficient through d(AACA) than the d(AAAA) segment. This was one difference seen between duplex1 and duplex3. The experimental lane C for the 1:1 sample showed the opposite of what was expected. There was no damage seen at either GG steps in this lane. The most surprising of this result was the damage totally stopped as oppose to duplex1 where there seemed to still be a small amount of damage present. The experimental lane D for the 1:2 sample showed no damage which is comparable to that of the 1:2 experimental lane in duplex1. These result lead to several questions, the mechanism of netropsin quenching was not entirely understood and there seemed to be more to this study than initially expected. The unbound netropsin seem to stop the damage at the GG steps more efficiently than when it was bound. This lead to several other experiments as well as the reevaluating of experiments already performed.

There was a question that maybe netropsin was partially binding to duplex3. This was remedied by the design of duplex4. Duplex4 was used as a true nonbinding site duplex. The sequence made it impossible for netropsin to bind to duplex by the incorporation of more G:C base pairs. The experiments above were repeated for duplex4 (Figure 4-15). The only change was the time of irradiation to 30 min. The sample set included a dark control, a light control, and two netropsin containing sample of 1:1 and

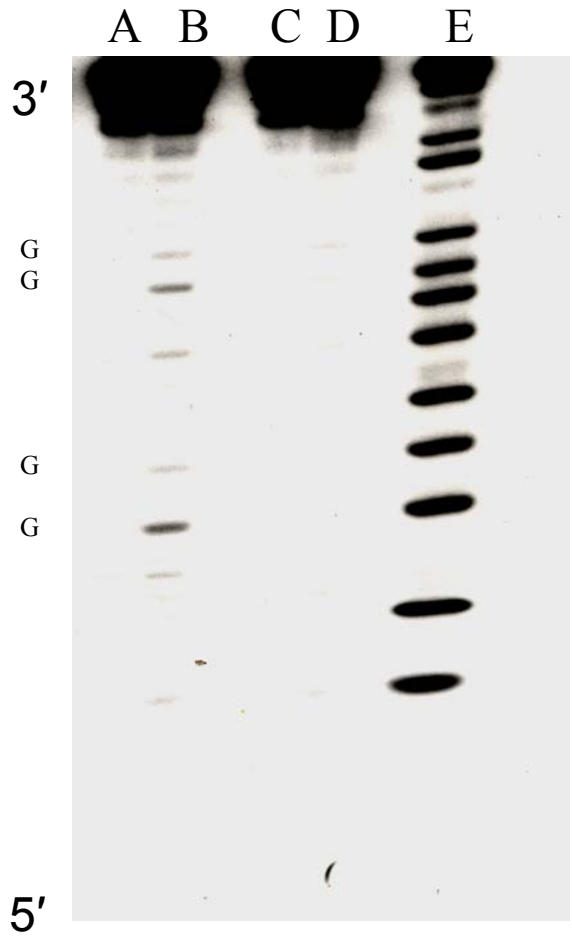

Figure 4-15 Autoradiogram for netropsin's effect on duplex4 when irradiated for 15 min. Lanes A and B are the experimental lanes for the dark and light control sample respectively. Lanes C and D contain DNA and netropsin in 1:1 and 1:2. Lane E is the Maxim-Gilbert A/G sequencing lane.

1:2 DNA to netropsin. These result seemed identical to those for duplex3. The netropsin appeared to totally quench the radical cation when the netropsin was in a 1:1 with the DNA. This was evidence that the quenching of the radical cation in duplexes 3 and 4 was

not caused by partial binding but by some other mechanism. The experiments involving duplexes 1-3 were repeated several times and always produced the same results.

This phenomenon brought up the question of possible coordination of the netropsin with the TQ charge injector. This was tested in two ways the first was by UV experimentation and the second by experiments using duplex 5. Concentrated samples of duplex1 and duplex2 were prepared in order to see the TQ absorbance peak at 420 nm clearly. They were measured by a UV-Vis spectrophotometer and the absorbance was noted. Concentrated samples of the duplexes with netropsin were also measured. If the netropsin was coordinating to the TQ, there might be a possible bathochromic shift in the absorbance a 420 nm. If this was not seen the test would be inconclusive and other measures need to be taken to determine netropsin:TQ coordination. As seen in figure 4-16 there were was no red shift of the absorbance band at 420 nm in the presence of netropsin with duplex1 or duplex3. This was still not conclusive evidence that the netropsin was or was not binding to the TQ.

This prompted the use of duplex5 to block the netropsin from coordinating with the TQ if coordination was actually occurring. If the results were positive and damage occurred upon irradiation, it could be concluded that the netropsin was quenching the TQ before charge injection could occur when it was not bound within the minor groove. If we saw the same results as seen in the case of duplex 2 and duplex 3 the result would help rule out the coordination possibility. A four T overhang strand was γ P^{32} labeled in this experiment. The results were similar to those found for duplex 3 (Figure 4-17). The sample set included a dark control, light control, DNA and netropsin in 1:1 and 1:2. The dark control was as expected there was little to no damage seen (lane A). The light

control lane B showed damage at the proximal and distal GG steps. The netropsin containing lanes, C and D, show the same results as those for duplex3. There was a decrease in damage at the proximal and distal GG steps.

Binding Site

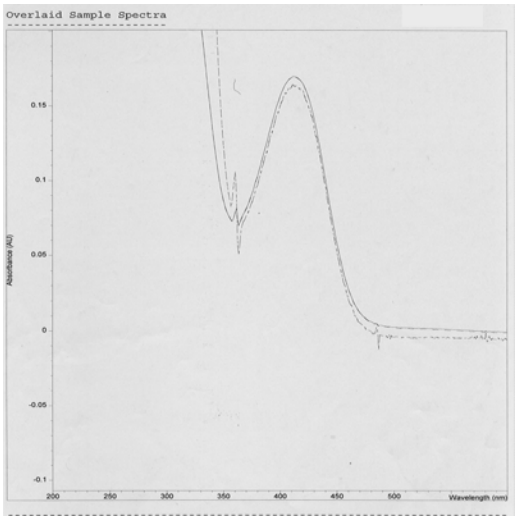

Nonbinding Site

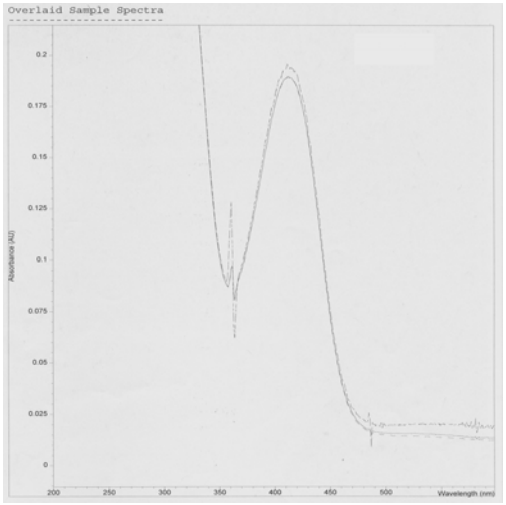

Figure 4-16 Partial UV-Vis spectra of duplex1 and duplex3 displaying the no effect on the absorbance peak representing TQ-linked DNA duplex in the presence of netropsin. Each spectrum contains the peak with and without netropsin.

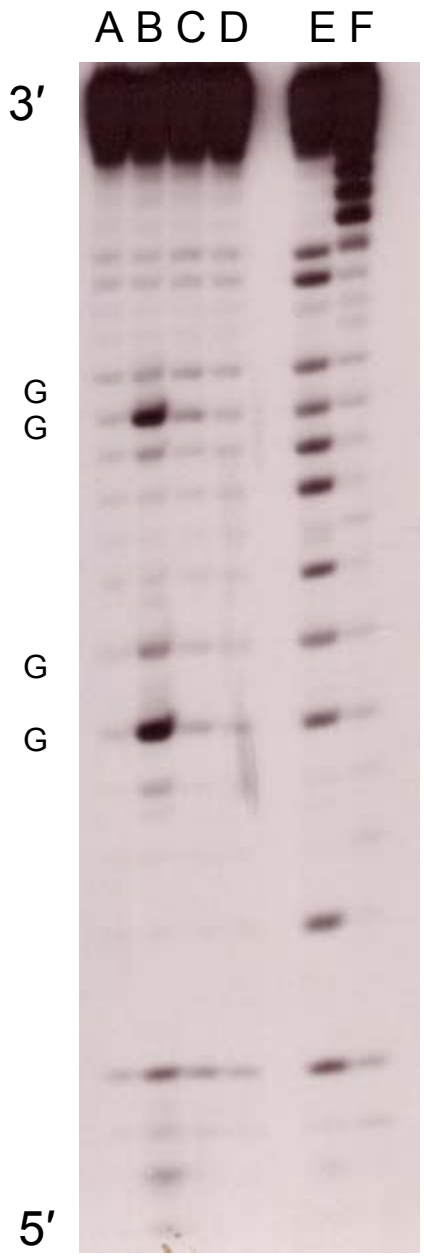

Figure 4-17 Autoradiogram for netropsin's effect on duplex5, the overhang sequence, when irradiated for 15 min. Lanes A and B are the experimental lanes for the dark and light control sample respectively. Lanes C and D contain DNA and netropsin in 1:1 and 1:2. Lanes E and F are the Maxim-Gilbert A/G and T sequencing lanes respectively.

One more avenue was taken to disprove TQ:netropsin coordination. The use UAQ containing DNA, duplex6, was studied to see if having the photosensitizer intercalate with in the strand would change the result. By the photosensitizer intercalating, the netropsin would have no way to coordinate with it. If damage occurred as opposed to an increase as seen previously in the presence of netropsin, a UTQ photosensitizer would be synthesized to explore these results further. The results seen from this experiment did not give much insight to our studies and therefore the results are not shown. The behavior of charge transfer did not seem to change by the intercalation of the AQ. Damage was decreased as netropsin was titrated into the DNA. The results of all three of these experiments ruled out the possibility of coordination with the TQ, yet it did not explain why damage was decreased whether netropsin was bound or free in solution.

It was decided to perform a simple test determining the possibility that netropsin affected the piperidine treatment. If the netropsin affected piperidine treatment, the piperidine would not be able to cleave the damage bases therefore damage would not be seen in the autoradiogram (Figure 4-18). Duplex1 and duplex3 were tested in this experiment. It was decided to focus on these two duplexes for further investigation since duplex3 and duplex4 display the same behavior. The samples sets included a dark control, a light control, a sample containing netropsin before irradiation, and a sample containing netropsin after irradiation. The lanes A- F are the experimental lanes for duplex1 and lanes G-L are the experimental lanes for duplex3. The A and G lanes for the dark controls exhibited the expected results. The B and H lanes for the light control lanes displayed the expected damage at the proximal and distal GG steps. Lanes C and I

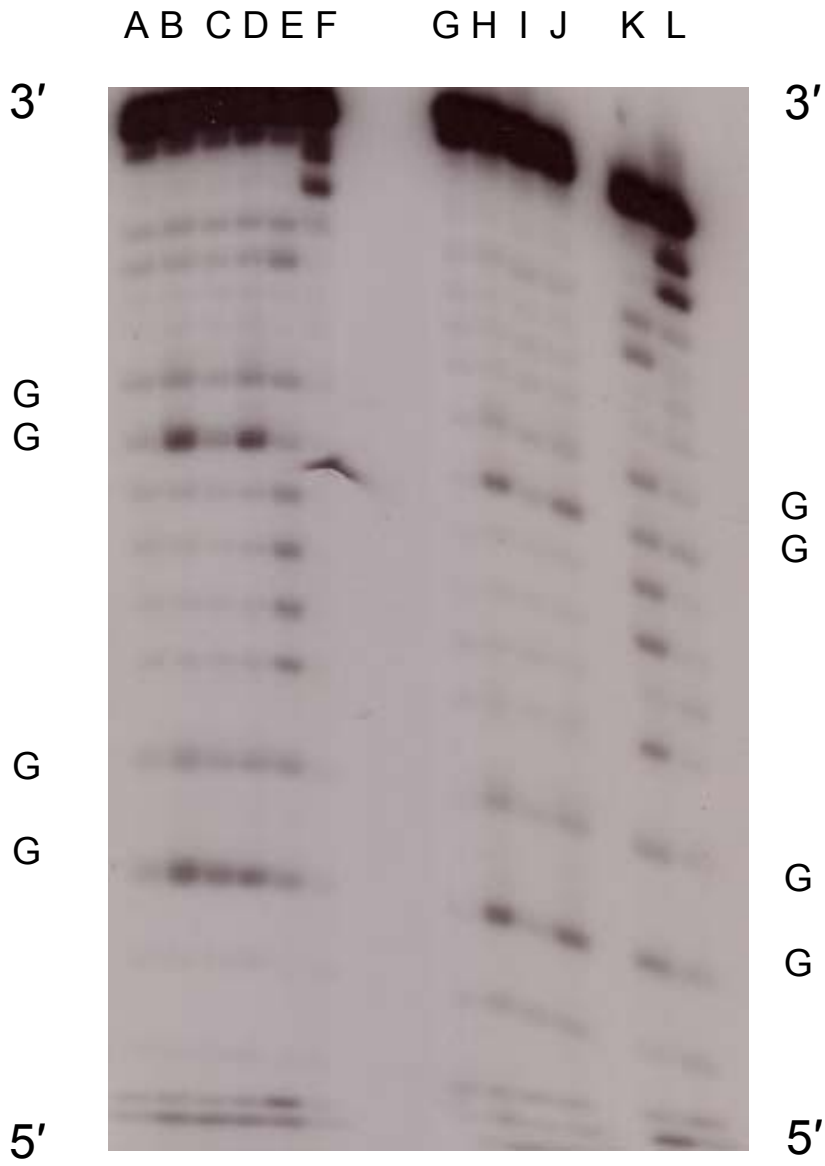

Figure 4-18 Autoradiogram testing the effect of netropsin on piperidine treatment. Lanes A-F are the experimental lanes for the binding site duplex1 and lanes G-L are for duplex3. Lanes A and G are the dark control lanes; B and H are the light control lanes; C and I contain netropsin in 1:1 with DNA before irradiation; and D and J are samples containing netropsin in 1:1 added after irradiation. Lanes E and K are the A/G sequencing lanes and F and L are the T sequencing lanes.

represented the samples with netropsin present before irradiation. The results were the same with a decrease in damage at the GG steps. The lanes for D and J, represented the addition of netropsin after irradiation, these lanes resembled the experimental lanes for the light control. There was damage seen in at the GG steps. Lanes E, F, K, and L are the A/G and T sequencing lanes. The result show netropsin has no effect on piperidine treatment and the results are directly due to reactions during irradiation. Although it was unlikely for the netropsin to have an effect, it was important to examine all avenues.

Therefore another unlikely possibility was studied, the effect of the concentration of DNA. In all experiments DNA has a concentration of 5 μM. A question was raised of possible aggregation in the presence of netropsin. Duplex1 and duplex3 were studied in these experiments. The concentration of DNA was changed and samples sets were made to have concentrations of 0.5 μM, 1 μM, and 5 μM of DNA. Netropsin samples were composed of the DNA in these concentrations with netropsin in the same concentrations. The autoradiogram displays the results of this experiment (Figure 4-19 and Figure 4-20). The results for each concentration were the same. Each light control sample displayed damage at the proximal and distal d(GG) steps. The only difference was the damage intensity for each concentration. The netropsin containing experimental lanes were similar. A decrease in damage was seen. These experiments proved there was no effect of concentration on the results. It showed no matter the concentration netropsin decreases the oxidative damage.

Considering all the above experiments, literature states netropsin has electrostatic interactions with the DNA. The positively charged netropsin may not be binding to the minor groove but it may be interacting with the negatively charged DNA backbone. It

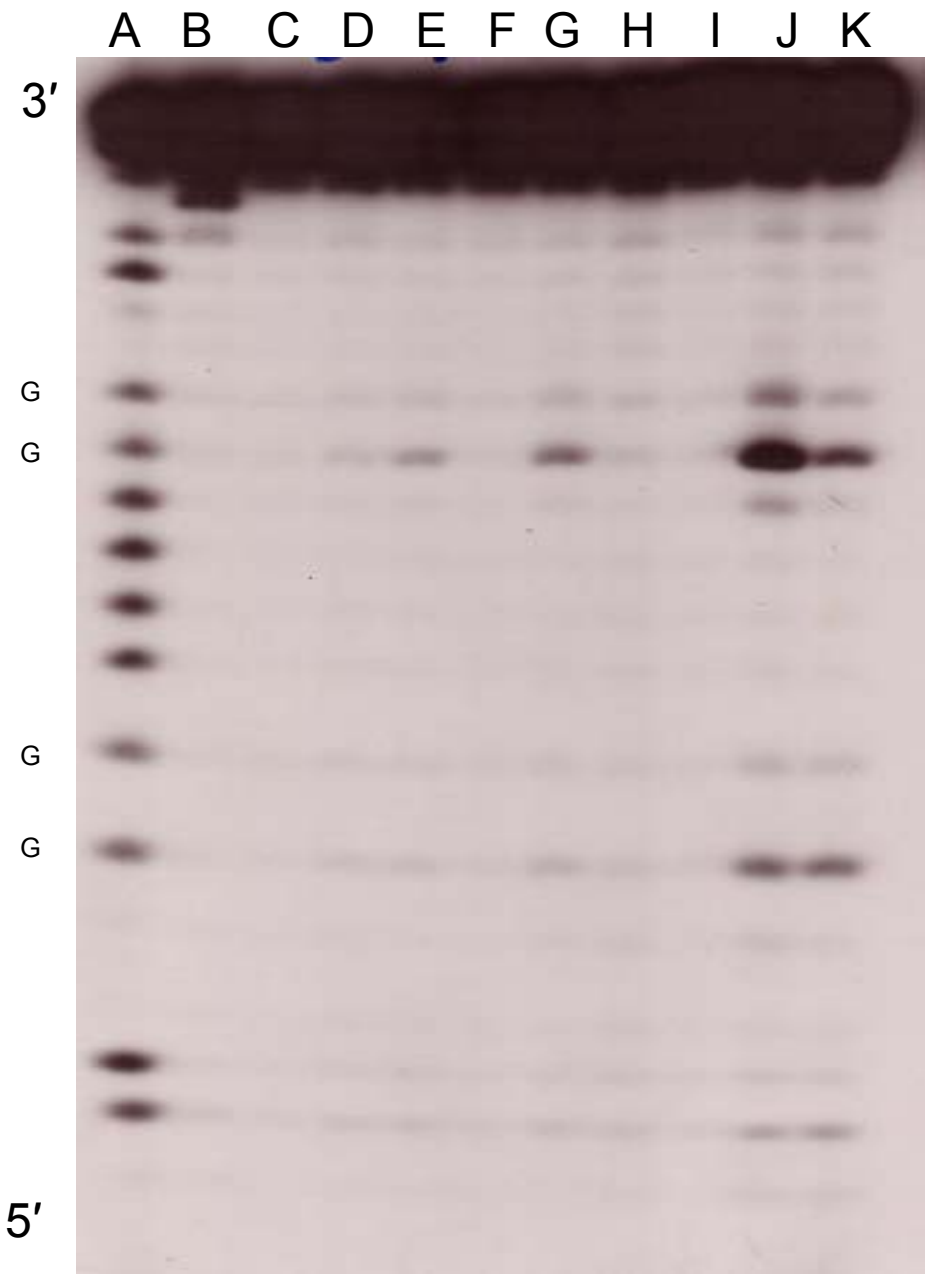

Figure 4-19 Autoradiogram of the DNA concentration dependence study on charge transfer for duplex1. Lanes A and B are the A/G and T sequencing lanes respectively. Lane C-E contain DNA with a concentration of 0.5 uM with experimental lanes for a dark control, light control and a netropsin containing sample in a 1:1 respectively. Lane F-H contain DNA with a concentration of 1.0 uM with experimental lanes for a dark control, light control and a netropsin containing sample in a 1:1 respectively. Lane I-K contain DNA with a concentration of 5.0 uM with experimental lanes for a dark control, light control and a netropsin containing sample in a 1:1 respectively.

could be these secondary interactions that are causing the decrease in damage in the cases of the nonbinding duplexes. This possibility prompted the use of spermine as a possible deterrent from this type of interaction. Spermine is a polycation that can bind non specifically to DNA. It has been seen to interact with the phosphate backbone as well as can interact with the bases[9]. It has been determined to have no effect on one electron oxidation of DNA[10]. When spermine is introduced in a 20-fold excess, in the case of duplex3, netropsin should be displaced by spermine and unable to interact with the DNA. If this is the case, netropsin should not be able to affect the oxidative damage of the DNA if in fact decrease in damage is due to netropsin binding in the minor groove. Therefore the lanes containing the DNA, netropsin, and spermine should resemble the light control if the decrease in oxidative damage is indeed attributed to netropsin binding. Duplex1 and duplex3 were tested in this experiment. The sample set contained a dark and a light control for each duplex, samples containing spermine with a concentration of 100 uM for each duplex, samples containing DNA:netropsin:spermine in 1:1:20 and samples with 1:2:20 (Figure 4-21). Lanes A-I are the experimental lanes for duplex3 and lanes J-S are the experimental lanes for duplex1. The results for the experiment showed the expected results for the dark and light control. The lanes C and L with spermine actually increased the damage rather than have no effect on the proximal GG step. The spermine itself had an effect on the DNA but this effect was not evaluated during the course of this study. This study's main focus was on the netropsin effect. The experimental lanes containing netropsin once again showed a decrease in oxidative damage at the proximal and distal GG steps. These results did not give any conclusive evidence because there is still the

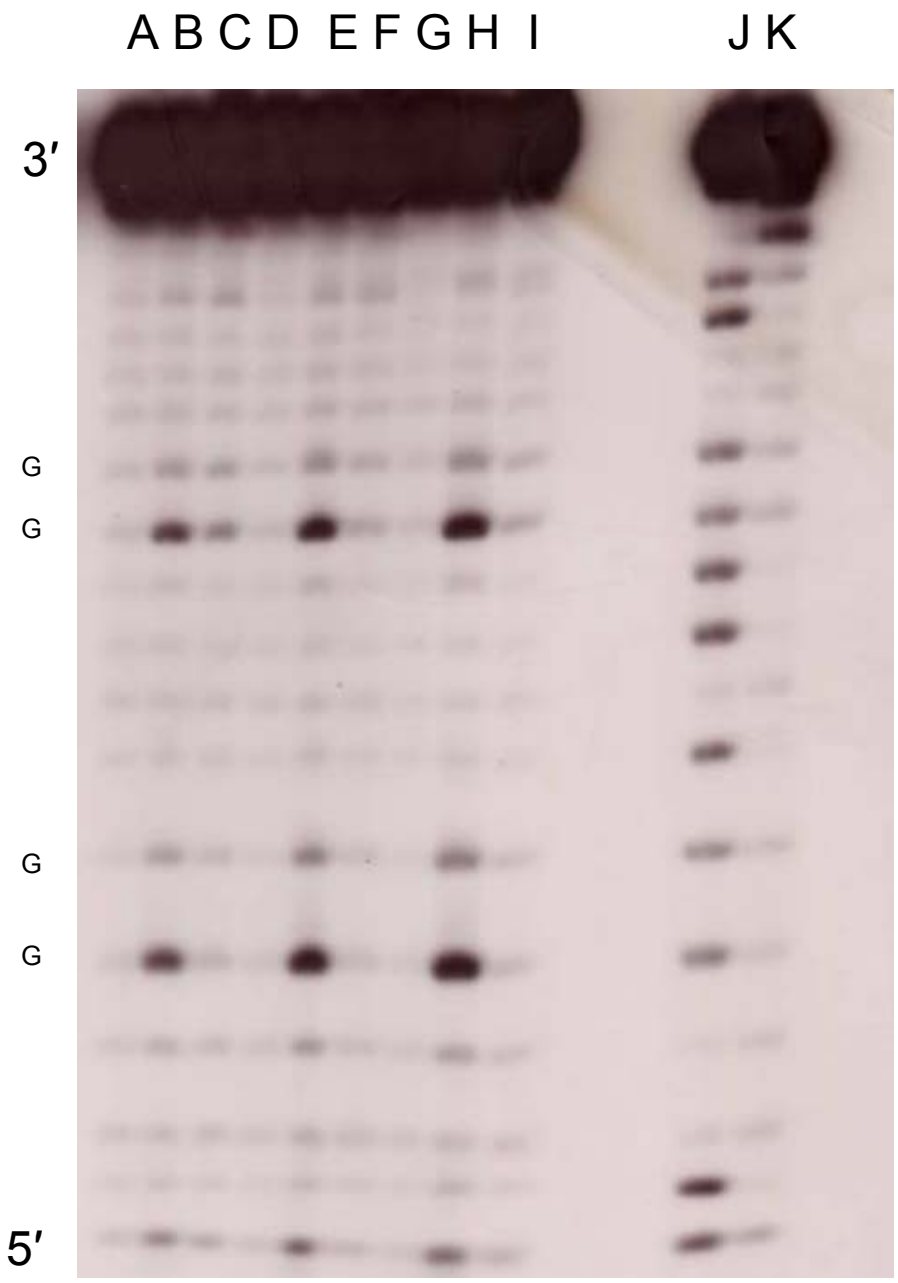

Figure 4-20 Autoradiogram of the DNA concentration dependence study on charge transfer for duplex3. Lane A-C contain DNA with a concentration of 0.5 uM with experimental lanes for a dark control, light control and a netropsin containing sample in a 1:1 respectively. Lane D-F contain DNA with a concentration of 1.0 uM with experimental lanes for a dark control, light control and a netropsin containing sample in a 1:1 respectively. Lane G-I contain DNA with a concentration of 5.0 uM with experimental lanes for a dark control, light control and a netropsin containing sample in a 1:1 respectively. . Lanes J and K are the A/G and T sequencing lanes respectively.

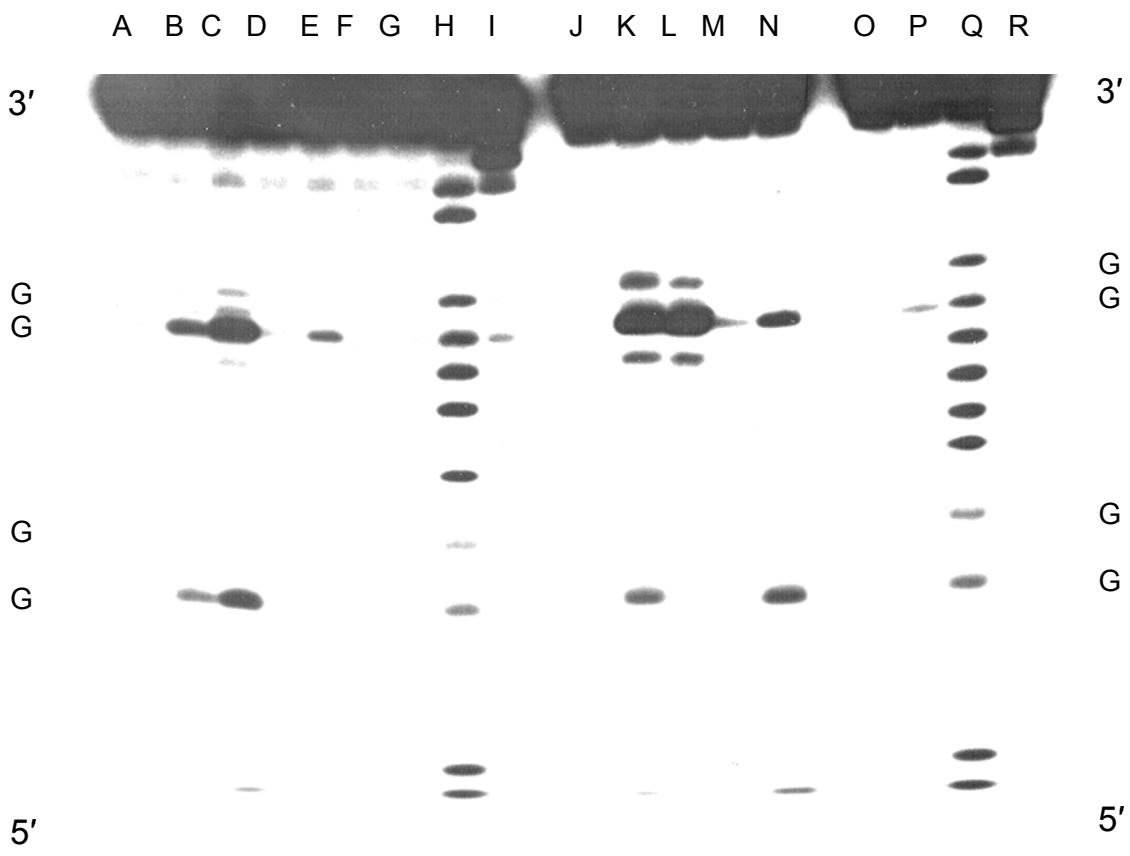

Figure 4-21. An autoradiogram containing the experimental results for duplex1 and duplex3 with binding of spermine and netropsin. The A-I experimental lanes contain the duplex3 samples and J-R are the experimental lanes for duplex1 samples. Lanes A & J, dark controls; B & K, light controls; C & L contain 20 : 1 spermine to DNA; D & M, 1:1 netropsin to DNA; E & N 20:1:1 spermine : netropsin : DNA; F & O – 2:1 netropsin : DNA; G & P – 20: 2 :1 spermine:netropsin: DNA; H& Q - A/G sequencing; I & R – T sequencing.

possibility that even an excess of spermine could not hinder the netropsin from interacting with the DNA. If it in fact it did stop the netropsin from binding to the DNA, this was evidence that supports the presence of netropsin was enough to affect oxidative damage and is a quencher for the radical cation whether specifically bound or not.

Before this theory was concluded one more theory needed to be addressed. There was speculation the netropsin was able to intercalate. This theory has not been proven but all possibilities need to be examined. Duplex7 was designed to act a duplex for the netropsin to intercalate within. If in fact the netropsin could intercalate it would more than likely have an affinity to intercalate within duplex7 over duplex3. The duplex was first evaluated by UV melting studies. The melting temperature was taken in and out of the presence of netropsin. The T_m results show the same results in and out of the presence of netropsin. If the netropsin was actually intercalated the melting temperature might indeed increase because of possible π-stacking but this is not always the case with intercalators. Therefore these experiments did not prove or disprove the intercalation theory.

Duplex7 was used in irradiation experiments to act as a deterrent for intercalation within duplex1 and duplex3. If the netropsin was indeed intercalating with the duplexes, an excess of duplex7 should stop this from occurring. Duplex1 and duplex3 were both studied for this set of experiments. The sample sets included a dark control; a light control; a sample including 100 μM of duplex7 with 5 μM duplex1 or duplex3; a sample containing DNA and netropsin in 1:1, a sample containing duplex7, duplex1 or 3, and netropsin in 20:1:1; a sample containing DNA and netropsin in 1:2; and a sample

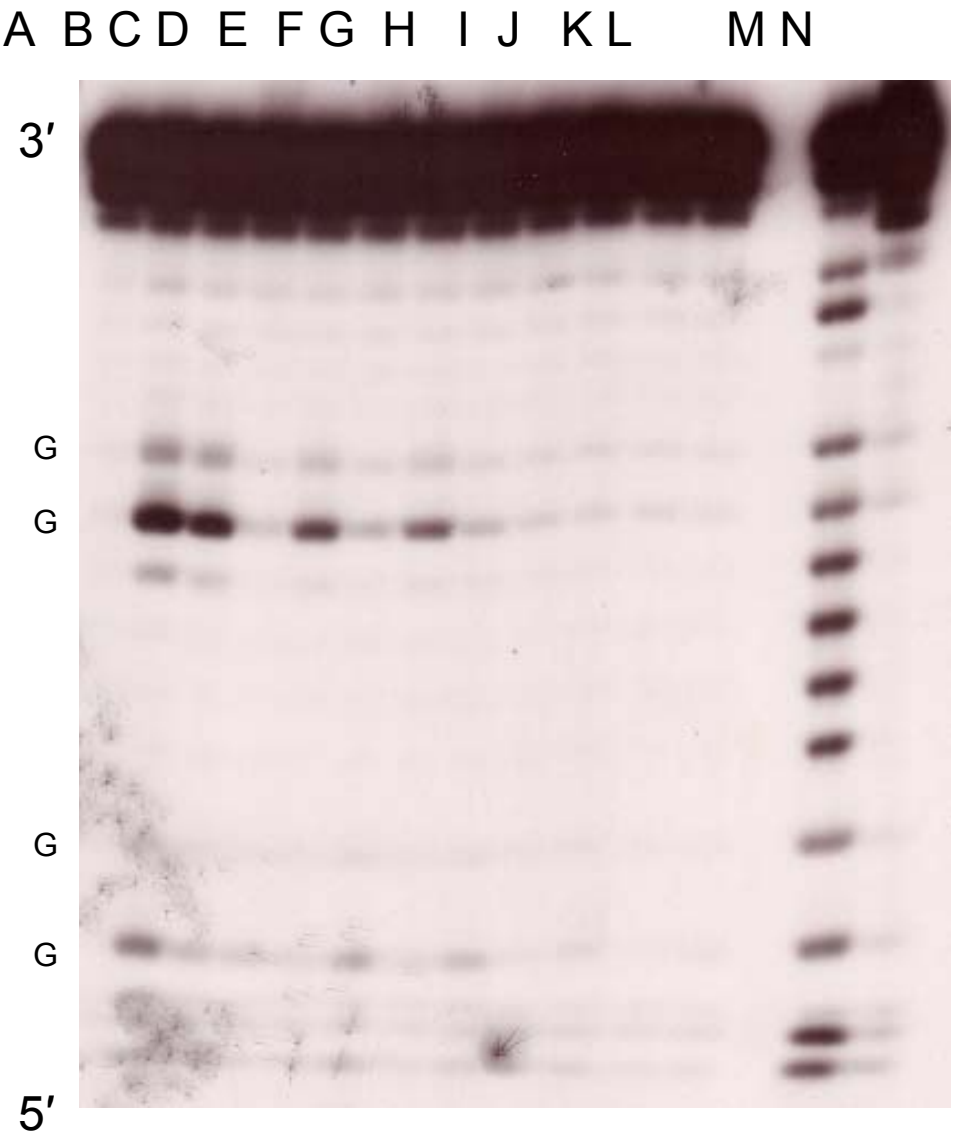

Figure 4-22 Autoradiogram for the effect of the titration of duplex7 to oxidative damage on duplex1 in and out of the presence of netropsin. The sample set contains a dark control (A), a light control (B), duplex1 and duplex7 in 5:1 (C), duplex1, duplex7 and netropsin in 5:1:5 (D), duplex1 and duplex7 in 1:1 (E), duplex1, duplex7 and netropsin in 1:1:1 (F), duplex1 and duplex7 in 1:2 (G), duplex1, duplex7 and netropsin in 1:2:1 (H), duplex1 and duplex7 in 1:10 (I), duplex1, duplex7 and netropsin in 1:10:1 (J), duplex1 and duplex7 in 1:20 (K), and duplex1, duplex7 and netropsin in 1:20:1 (L). Lanes M and N are the Maxim-Gilbert sequencing lanes for A/G and T respectively.

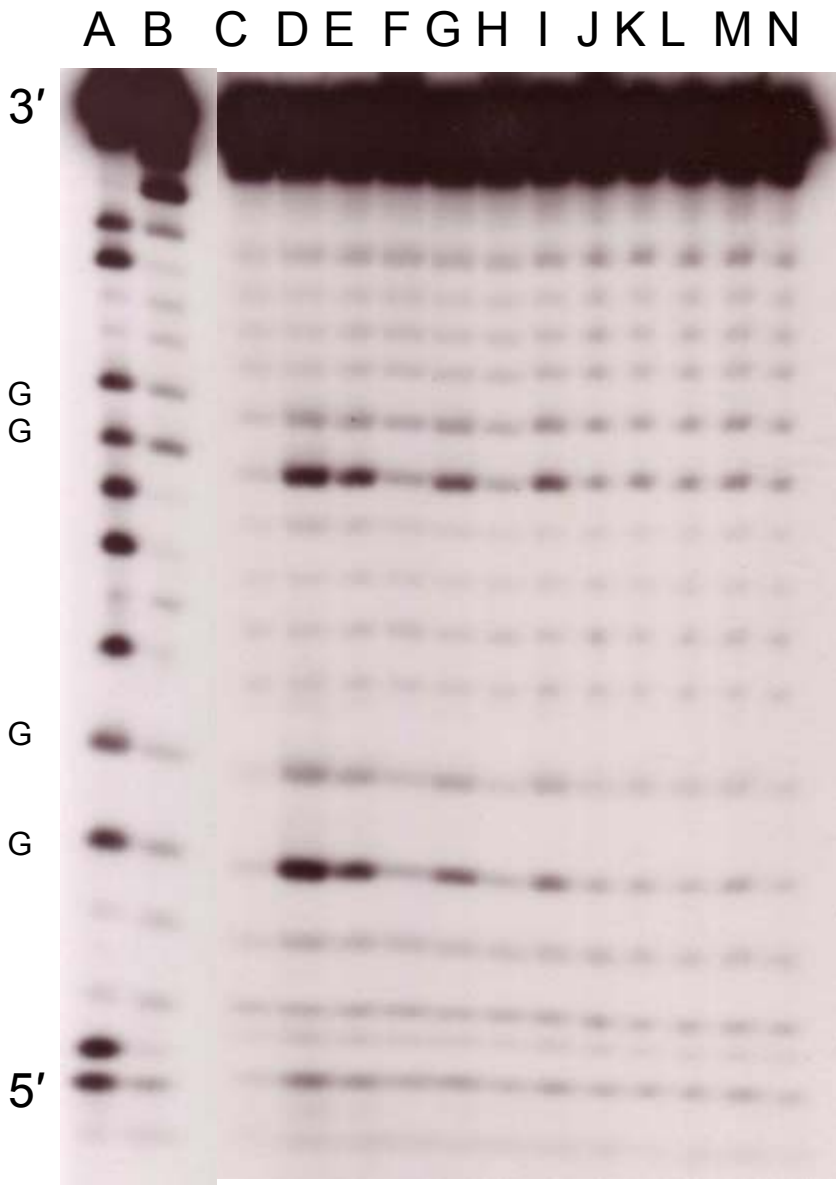

Figure 4-23 Autoradiogram for the effect of the titration of duplex7 to oxidative damage on duplex3 in and out of the presence of netropsin. The sample set contains a dark control (C), a light control (D), duplex3 and duplex7 in 5:1 (E), duplex3, duplex7 and netropsin in 5:1:5 (F), duplex3 and duplex7 in 1:1 (G), duplex3, duplex7 and netropsin in 1:1:1 (H), duplex3 and duplex7 in 1:2 (I), duplex3, duplex7 and netropsin in 1:2:1 (J), duplex3 and duplex7 in 1:10 (K), duplex3, duplex7 and netropsin in 1:10:1 (L), duplex3 and duplex7 in 1:20 (M), and duplex3, duplex7 and netropsin in 1:20:1 (N). Lanes A and B are the Maxim-Gilbert sequencing lanes for A/G and T respectively.

containing duplex7, duplex1 or 3, and netropsin in 20:1:2. The autoradiograms can be found in figure 4-22 for duplex1 and figure 4-23 for duplex3. The experiment did not turn out as expected. The samples containing the duplex7 seemed to have hindered oxidative damage of duplex1 and 3 and raised more questions. There was no damage seen at the proximal and distal d(GG) steps when excess of duplex7 was present. These results lead to more experiments to determine why this was occurring. It was possible duplex7 was being damaged instead of duplex1 and duplex3. The TQ could be intercalating into duplex causing charge transfer to occur. Duplex7 was studied and it was found that this was not occurring. We reexamined duplex1 and duplex3 by titrating amounts of duplex7 into the samples to determine if the lack of oxidative damage was due to the concentration of excess duplex7. The amounts were varied from 0-100 μM. The results showed a lack of oxidative damage after 10 μM of duplex7. At 5 μM the oxidative damage decreased from what was seen in the light control sample. We concluded from this series of experiments that adding an excess amount of duplex7 causes aggregation of the DNA and hinders charge transfer. It was not expected for duplex7 to affect duplex1 results because the minor groove binding interaction is preferred over any secondary interactions. We also determined it was highly unlikely the netropsin intercalates and abandoned this theory.

It was observed that when netropsin was studied with the nonbonding duplexes 3 and 4 the decrease in damage was more efficient and comparable with the dark control at a 1:1 ratio. In terms of duplex 1 comparison with the dark control was not reached until netropsin was added in ~ a 2:1 mixture with the DNA. It was concluded that the netropsin quenched the radical cation and decreased the damage observed whether bound or

unbound and created a quenching sphere around the DNA. To determine the quenching sphere for netropsin quenching of the radical cation, concentration dependence experiments were performed. The DNA concentration was held constant as the concentrations of netropsin were varied from 0 to 2 times the amount of DNA. There was a constant decrease in the damage seen as more netropsin was added. In the case of duplex1, damage comparable to the damage observed in the dark control was lane was seen after a ratio of about 1.75: 1 was reached netropsin to DNA (Figure 4-24). In the cases of duplex 3 and 4, this was observed at about 0.75-1:1, netropsin to DNA (Figure 4-25 and 4-26). It appeared that damage was stropped at lower concentrations of netropsin in the cases of duplex 3 and 4 than with duplex 1. The results of the concentration dependence studies were plotted using the Perrin Formulation (Plot 1 - duplex1, Plot 2 – duplex3, and Plot 3 – duplex4)[11] .

$$\text{Perrin Formulation} \quad Y = NV[Q] \qquad (1)$$

Where Y is ln (I_o/I) (I is intensity and I_o is the intensity in the absence of quencher), N is Avagodro's Number, V is Volume, [Q] is the quencher Concentration. The gels were analyzed by Fuji imaging and the intensity counts were recorded. This data was then plotted and the radius quenching cylindrical sphere was extracted. This was accomplished by solving for the volume and then using the volume to solve for the radius of a cylinder.

$$r = (V/h\pi)^{1/2} \qquad (2)$$

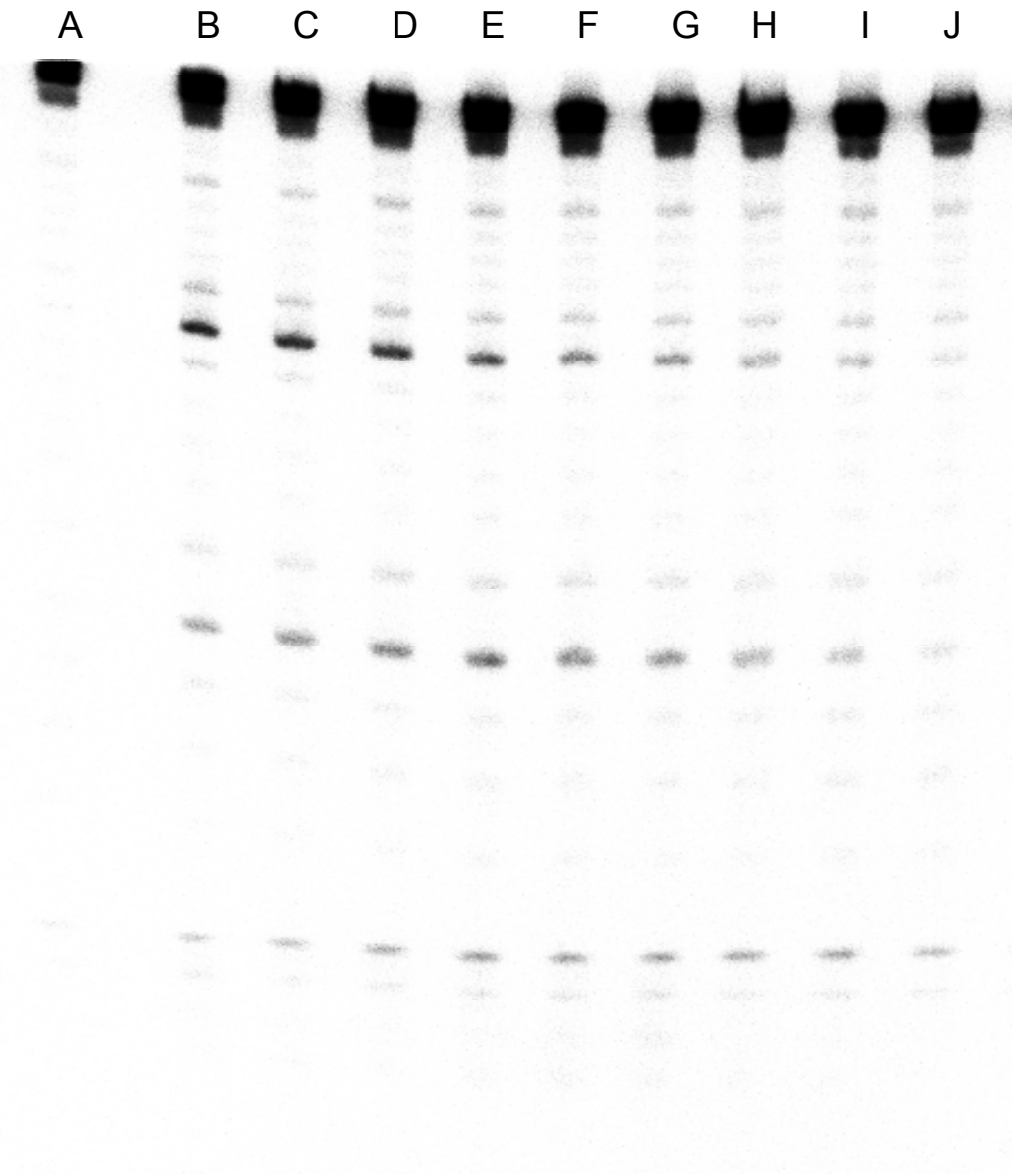

Figure 4-24 Autoradiogram of the netropsin concentration dependence studies on duplex1. The concentrations of netropsin range from 0- 10 μM in 1.25 μM increments and concentration of DNA remains at 5 μM. The experimental lane A contains the dark control sample and lanes B-J contain the netropsin containing samples from 0 to 10 μM.

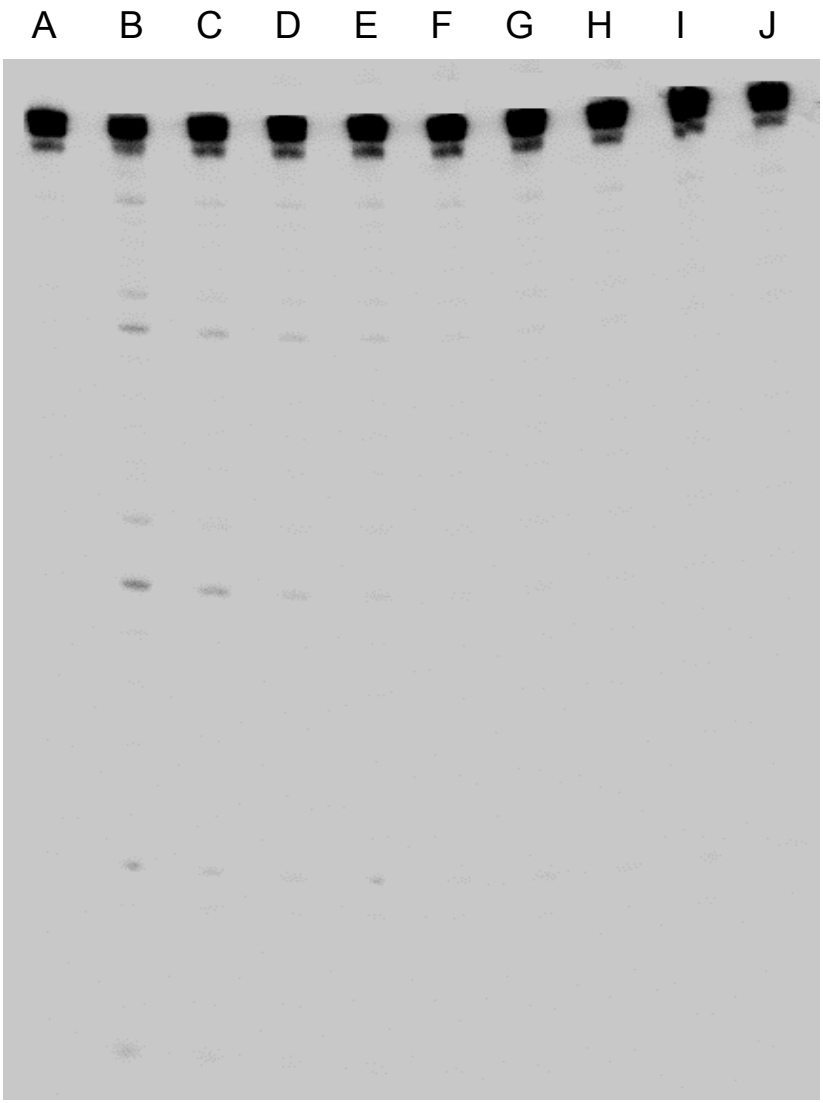

Figure 4-25 Autoradiogram of the netropsin concentration dependence studies on duplex3. The concentrations of netropsin range from 0- 10 μM in 1.25 μM increments and concentration of DNA remains at 5 μM. The experimental lane A contains the dark control sample and lanes B-J contain the netropsin containing samples from 0 to 10 μM.

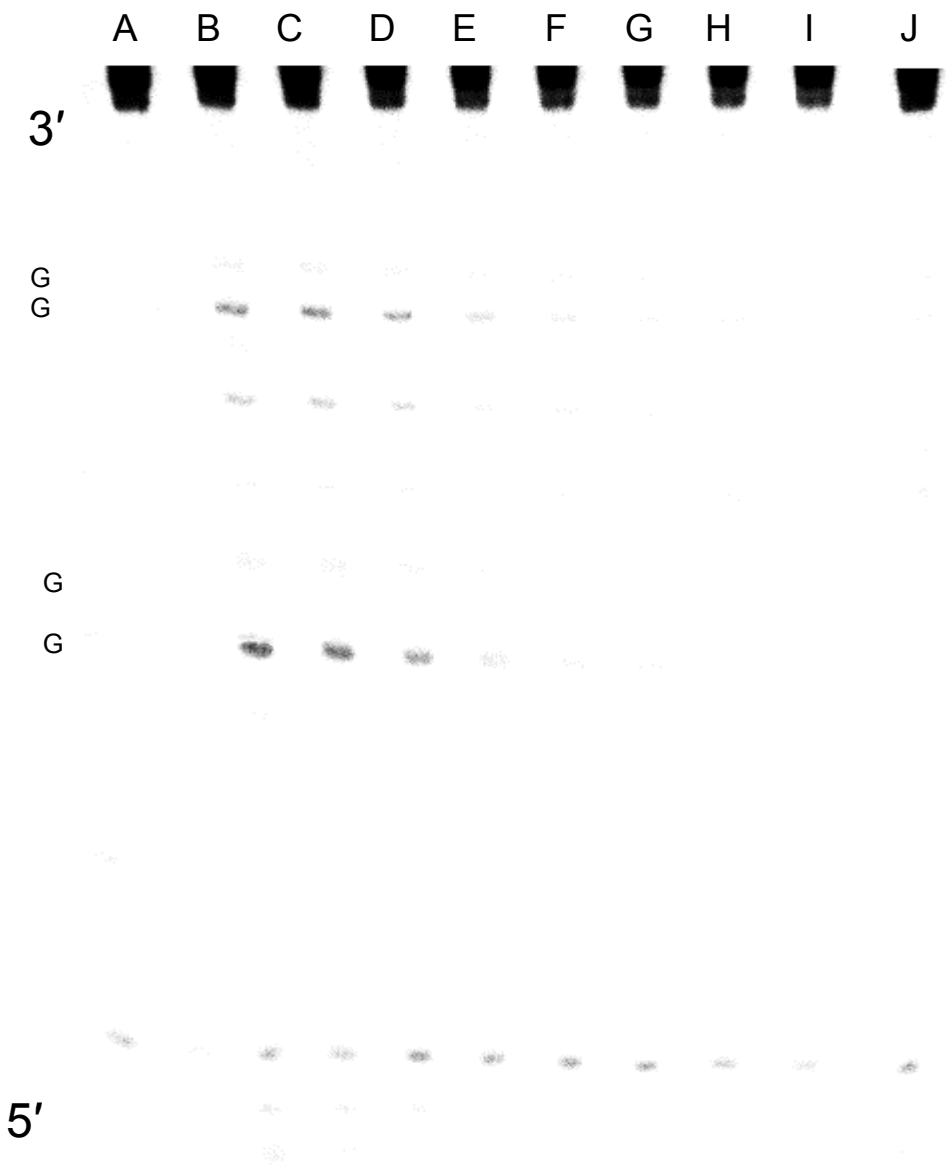

Figure 4-26 Autoradiogram of the netropsin concentration dependence studies on duplex4. The concentrations of netropsin range from 0- 10 μM in 1.25 μM increments and concentration of DNA remains at 5 μM. The experimental lane A contains the dark control sample and lanes B-J contain the netropsin containing samples from 0 to 10 μM.

Table 4-2 The calculated values for the quenching radii of the three main DNA duplex 1, 3 and 4 using the Perrin Formulation.

DNA (Duplex)	Radius
Duplex (1)	1132 Å
Duplex (3)	1370 Å
Duplex (4)	1380 Å

The cylinder equation was used because of DNA's cylindrical shape. Duplex 1 had a radius of 1132 A and duplex 2 and 3 are 1370 and 1380 Å respectively (Table 4-2). The radius for the nonbinding DNA is slightly larger than that of the binding DNA duplex showing that specific binding of the netropsin to the DNA is not required for it to exert its protective effect.

Discussion

During the course of this study we have looked at the effect a molecule that seems to have no effect or no significant interaction with the π-stacking in DNA has on one electron oxidation of DNA. Under normal charge injection conditions, a photosensitizer is excited and receives an electron from the neighboring base of the DNA duplex. The photosensitizer may be covalently linked at the end of the duplex strand or may be intercalated within the duplex. Once electron transfer occurs it creates a radical anion and radical cation pair. The radical cation or the "hole" in the DNA is delocalized over a

set a bases, usually 3 or 4, creating a distortion (polarons) of relatively low potential sites[12]. These polarons move adiabatically through the DNA until it reaches an area of low energy. This is commonly an area of $d(G)_n$ (n=2 or 3) steps where the radical cation is trapped and is quenched with water or O_2 creating damage in that area of the strand. When treated with hot piperidine, the DNA strand is cleaved and damage is revealed by analytical techniques. We have identified this mechanism for long distance charge transfer in DNA as phonon-assisted polaron hopping and is supported by experimental observations and theoretical considerations[8]. Depending on the sequence of the DNA duplex, the polaron has a different rate of hopping (k_{hop}) and trapping (k_{trap}). These rates also determine the amount of damage seen at each d(GG) step. In the case where k_{trap} is faster than k_{hop}, more damage is seen at the proximal steps than the distal steps. In the reverse case damage would seem to be equal at each d(GG) step. This seemed to be the case in duplex1 and duplex3. Although the only difference lie in a base pair change within the binding site, this was enough to change these rates and the amount of damage seen at the d(GG) steps.

The netropsin seemed to have stopped oxidative damage whether it is bound within the minor groove of DNA or floating around free in solution. Under normal circumstances (without netropsin), upon irradiation of TQ-DNA, damage was seen as expected at the 5′ G of the d(GG) steps. The netropsin appears to protect the DNA from oxidative damage just by being present in the DNA containing sample. Experiments were done to ensure the results seen during the course of the study were not attributed to netropsin quenching the TQ by forming a ground state complex before charge injection occurred.

Netropsin has a lower E_{ox} than the four DNA bases and donates an electron in order to quench the radical cation returning the DNA to its unoxidized state. An electron transfer reaction restores the DNA oligomer and results in oxidation of the netropsin. "Spermine disulfide" is capable of electron transfer to oxidized DNA because the disulfide group has a lower E_{ox} than guanine, this provides substantial protection[10]. This is explanation for netropsin's protective behavior, but it does not account for the observation that DNA oligomers with and without specific netropsin binding sites behave similarly or more interestingly why when free the protective behavior appears more efficient.

The results from the titration of netropsin were used to determine the mechanism of quenching. The first model is based on an assumption of random diffusional encounters between the netropsin and oxidized DNA. It is characterized by Stern-Vollmer behavior where the ratio of the reaction efficiency in the absence of quencher to the amount of reaction in its presence is directly proportional to the concentration of quencher. With a lifetime of the DNA radical cation in the microsecond domain, and a diffusion rate constant in water of ca. 10^9 M^{-1} s^{-1}, Stern-Vollmer behavior could account for the observed protective effect of netropsin. Experimentation giving quantitative data showing the effect of netropsin concentration is not consistent with the Stern-Vollmer equation[13].

Original Equation Stern-Vollmer Equation

$$I_o/I = (1 + K_{sv}[Q]) \qquad (3)$$

Stern-Vollmer Equation For Binding Quenchers

$$I_o/I = (1 + K_{eq}[Q]) * (1+K_{sv}[Q]) \qquad (4)$$

The second model was the model for static quenching known as Perrin quenching to determine the "quenching sphere" or in this case cylinder netropsin creates around the DNA. In this case, the model defines an interaction distance between oxidized DNA and netropsin[11]. Quenching occurs if the two partners are within this interaction distance. If the partners are not within the interaction distance, there is no quenching. This model predicts an exponential dependency between the ratio of the reaction efficiency in the absence of quencher to the amount of reaction in its presence and the concentration of quencher. As shown in Figures 4-26, 4-27 and 4-28, the protection of DNA from oxidative damage appears to follow the expected Perrin exponential behavior. The interaction distance (a radius) defines a volume. In the present case, we assume that that the volume is a cylinder with the DNA as its axis. The estimated volume of the quenching cylinder for the oxidative protection of DNA by netropsin is ca. 5.8×10^8 Å^3, independent of whether the DNA contains a specific netropsin binding site.

The Perrin model offers an explanation for the observed binding site independence. Roughly, the diffusion of the DNA oligomers is relatively slow and within the microsecond lifetime of the DNA oligomer it can be assumed to be static. Based on the estimation of the netropsin quenching volume, at a concentration of netropsin of ca. 7 μM, statistically, there will be on average one netropsin molecule in the quenching cylinder around the DNA oligomer whether there is a specific binding site or not. This is the concentration, essentially 1:1 with the DNA, where the protective effect of the netropsin is observed. Thus, a netropsin molecule is expected to be within the quenching volume of oxidized DNA whether or not there is a binding site.

Another probable explanation for the difference in quenching radius is a separate mechanism for quenching for binding duplexes and nonbinding duplexes. We observed a more efficient quenching in the cases of duplex3 and duplex4, non specific binding duplexes, where damage appeared to be stopped when netropsin was in a 1:1 with DNA. In this case the netropsin is quenching the DNA by the electron transfer mechanism. On further reexamination of duplexes containing binding sites, it was observed the distal damage seemed to have increased when the netropsin was bound. There was still an overall decrease in damage to the DNA but this lead us to believe that maybe netropsin is acting in a dual role. The first role was the actual quenching by electron transfer. The second role could affect the k_{trap}. Netropsin disturbs the "spine of hydration" when it binds in the minor groove displacing the water[14]. When this occurs, it is likely the water that normally reacts with radical cation is not able to react as efficiently slowing down the k_{trap}. This leads to more damage at the distal d(GG) step. This mechanism would account for the difference in quenching radius. Although this is a possibility, it was not explored during the course of this study.

Conclusion

Netropsin protects DNA against oxidative damage by creating a quenching cylinder derived from the Perrin Formulation. Although this theory is not specifically for molecules in solution, it can be applied as a possible explanation for our results. If netropsin is anywhere within this quenching cylinder, it is able to protect the DNA by quenching the radical cation. Our results have proven netropsin protects the damage caused by one-electron oxidation of DNA.

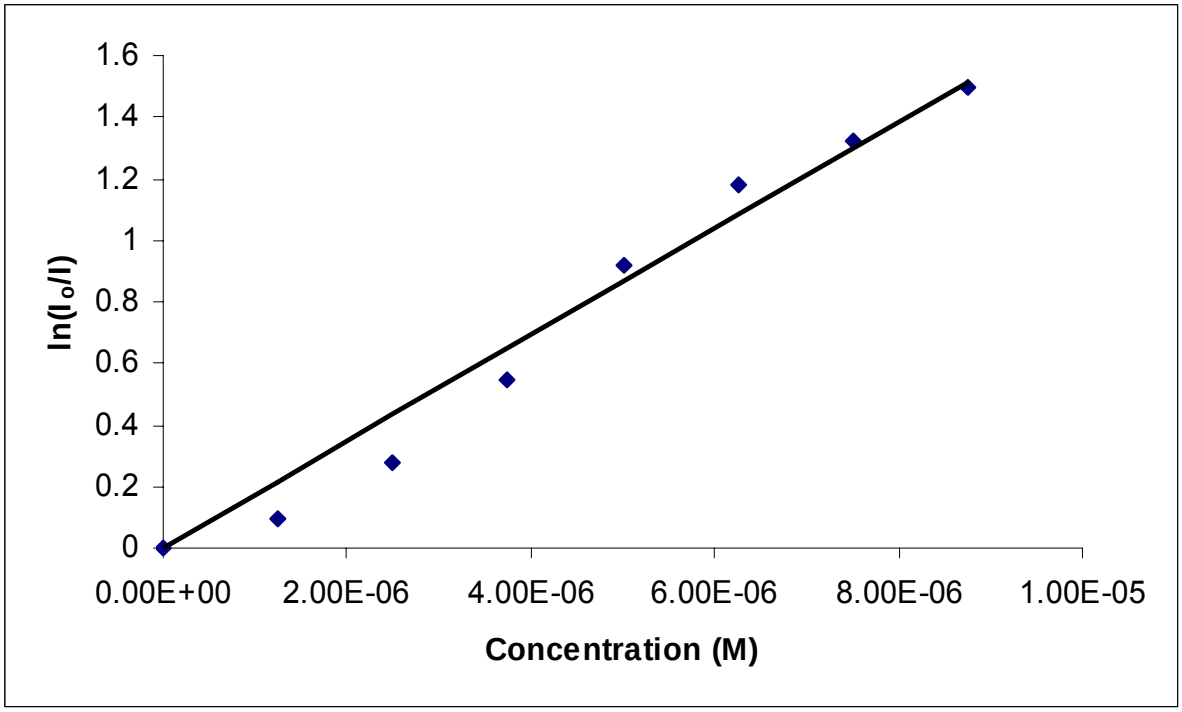

Figure 4-27 The semilog plot of data obtained from the concentration dependence of netropsin on duplex1 study.

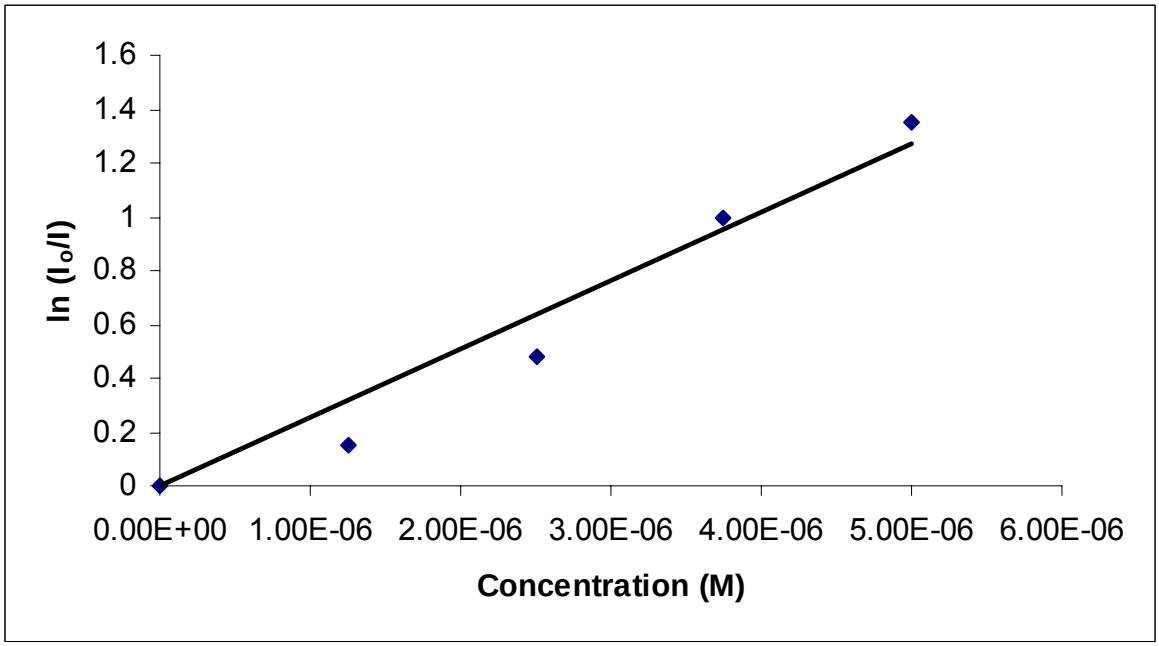

Figure 4-27 The semilog plot of data obtained from the concentration dependence of netropsin on duplex3 study.

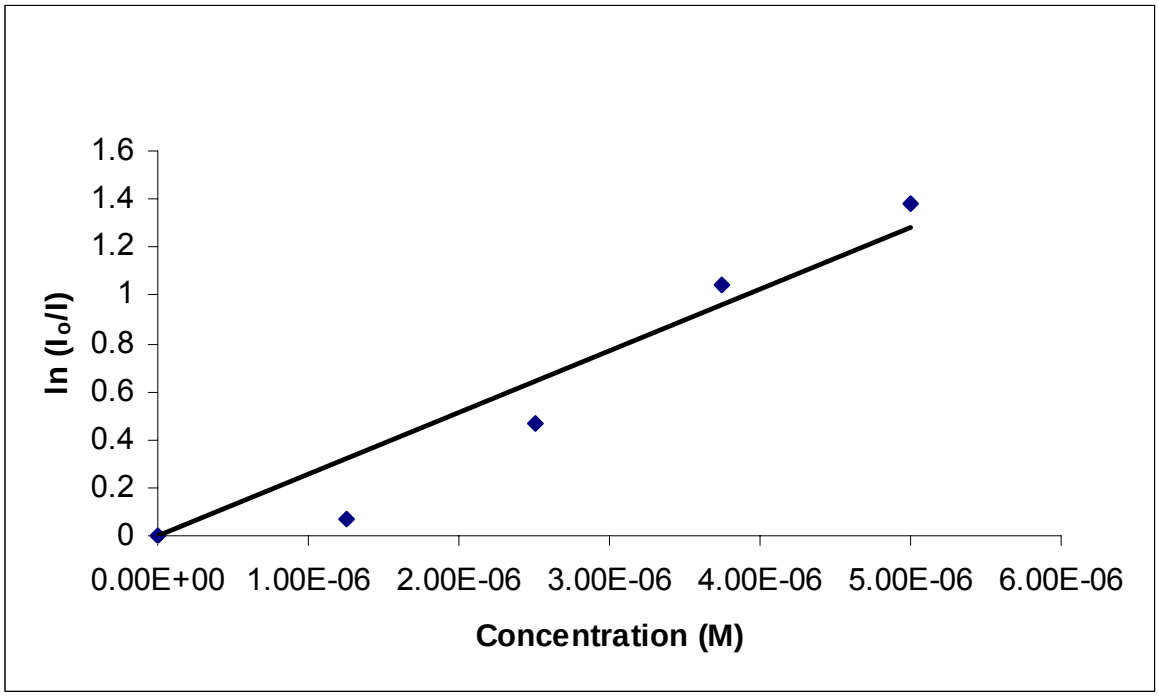

Figure 4-28 The semilog plot of data obtained from the concentration dependence of netropsin on duplex4 study.

Materials and Methods

DNA was prepared using Applied Biosystems Expidite Nucleic Acid Synthesis System. Each strand was deprotected and purified with HPLC using an acetonitrile and TEAA buffer solvent system. The DNA was desalted using Sep Pak cartridges. DNA concentrations were performed by dissolving the DNA in nanopure water. An aliquot of DNA solution was added to an UV cell blanked with nanopure water to obtain the absorbance. The concentration was calculated with an extinction coefficient obtained by the Schepartz Lab Biopolymer Calculator.

Netropsin was purchased from Fluka. The netropsin was dissolved in nanopure water to make a 50 μM solution fresh before use. Netropsin's integrity and concentration was measured using UV. A 50 uM solution was prepared and the concentration was verified using the extinction coefficient at 260 nm, 21500.

Melting temperature A 2.5 μM solution was of the TQ-DNA and its complement in 10 μM phosphate buffer was prepared. The melting curve was monitored at an absorbance of 260 nm as the temperature was ramped from 15 to 90 ^{o}C. The melting temperatures were measured on a Cary 1E UV-Vis Spectrophotometer.

Circular Dichroism (CD). CDs were run on a J720 Jasco Spectropolarimiter with a 2.5 μM sample of hybridized DNA.

Cyclic Voltammetry. The CVs were taken on CH Instruments model 660 Electrochemical Workstation with Ag/AgCl as the reference electrode, carbon as the working electrode and silver wire as the auxillary electrode. The first set of cyclic voltammetry measurements measured of netropsin were taken on a. Netropsin was dissolved in a 0.1 M solution of NaCl. Sweep range were from -1.2 V - 1.2 V and the sweep rate ranged from 100 mV to 500 mV/s.

20% Denaturing Polyacrylamide Gel. In order to label the DNA, a small purification gel was prepared. A solution of 50 mL of PAGE, 438 uL of 10% APS, and 21.9 uL of TEMED was made. The solution was injected in between the two small plates of a Hoefer electrophoresis apparatus.

Labeling of DNA. The DNA strand complement to the charge injector linked DNA was γ-P^{32} labeled. An aliquot of 10μL of DNA was added to a micro centrifuge tube followed by 5 μL of water, 2 μL of NEBuffer for T4 Polynucleotide Kinase and 2 μL of T4 Polynucleotide Kinase enzyme. A 1 μL amount of P^{32} was added to the sample. The samples were incubated 37^{o}C for 45 minutes. This radiolabelled the DNA strands. A volume of 10 μL of dye was added to bring the mixture to 30 μL. The radiolabelled samples were purified on 20% denaturing polyacrylamide gel. This separates all labeled strands by size. Voltage to run the purification gel was set at 400 V. Once separation was completed, visualized DNA bands were cut from the gel developed by using radiography on Kodak film, and placing the developed film below the gel plate to see where the bands were located. An amount 800 μL of standard elution buffer was added

to the gel containing DNA and incubated for no less than 4 h at 37°C. The elution buffer is a mixture of 0.5 M ammonium acetate (NH_4OAc), 10 mM of magnesium actate (MgOAc), 1 mM EDTA, 0.1%SDS

Precipitation of DNA. The tubes containing the DNA were centrifuged for a minute. The eluent was removed with a thin tip pipet and added to each tube. To each of the samples, 600 μL of cold ethanol and 1 μL of glycogen were added. The radioactivity of the eluent was checked with a Geiger counter to ensure the labeled DNA was present in the solution. The samples were vortexed for at least 30 s and placed in a below -80 °C freezer on dry ice for 30 min. The samples were centrifuged for 30 min and the supernatant was checked for activity and discarded. An aliquot of 100 μL of 80% ethanol was added; and, the samples were centrifuged five minutes. The supernatant was discarded and this was repeated once more. The samples were then dried on low heat for twenty minutes or until dry. Nanopure water (20 μL) was added to the samples until they contained 10,000 cpm.

Hybridization. The DNA duplex was formed by adding the labeled DNA (~10,000 cpm) to the corresponding TQ-DNA (5 μM) and unlabeled complementary DNA (5μM). The samples were heated to 90 °C for 5 min and allowed to cool to room temperature. Appropriate amounts of netropsin were added to the hybridized samples and allowed to incubate at room temperature for 30 min. A dark control (not irradiated and without netropsin) and a light control (without netropsin) samples were prepared under similar conditions.

All the samples, except the dark control, were irradiated using eight 420 nm lamps (eight 350 nm lamps for AQ containing samples) in a Rayonet Photoreactor. The samples were precipitated using cold ethanol and glycogen, dried and treated for 30 min with 100 μL of 1 M piperidine at ~90 ^{o}C and dried. The piperidine treated samples were analyzed by 20% denaturing PAGE. The gels were dried and the cleavage bands were visualized by autoradiography and quantified using Fuji phosphorimager.

A/G Sequencing. In a micro centrifuge tube, 3.0 μL γ-P^{32} DNA, 1.0 μL CT DNA and 12 μL water were added followed by 4.0 μL piperidine formate. The mixture was incubated at 37 ^{o}C for 30 min. Then, 1 μL of glycogen and 100 μL of cold ethanol were added; and, the mixture was vortexed. The samples were placed on dry ice for thirty minutes then centrifuged for 30 min. The supernatant was discarded and 100 μL of 80% ethanol to the pellet and centrifuged for 5 min. This was repeated; and, the pellet was dried for 5 min in speedvac at low heat. The pellet was then treated with piperidine and the steps from the irradiated samples were followed.

T Sequencing. In a micro centrifuge tube, 3.0 μL γ-P^{32} DNA, 1.0 μL CT DNA and 15.5 μL water were added followed by 0.5 μL $KMnO_4$. The mixture was incubated at room tmperature for 1 min. Then, 1 μL of glycogen and 100 μL of cold ethanol were added; and, the mixture was vortexed. The samples were placed on dry ice for thirty minutes then centrifuged for thirty minutes. The supernatant was discarded and 100 μL of 80% ethanol to the pellet and centrifuged for five minutes. This was repeated; and, the pellet

was dried for five minutes in speedvac at low heat. The pellet was then treated with piperidine and the steps from the irradiated samples were followed.

A/G Sequencing In a micro centrifuge tube, 3.0 μL γ-P^{32} DNA, 1.0 μL CT DNA and 12 μL water were added followed by 4.0 μL piperidine formate. The mixture was incubated at 37 ^{o}C for 30 min. Then, 1 μL of glycogen and 100 μL of cold ethanol were added; and, the mixture was vortexed. The samples were placed on dry ice for thirty minutes then centrifuged for thirty minutes. The supernatant was discarded and 100 μL of 80% ethanol to the pellet and centrifuged for five minutes. This was repeated; and, the pellet was dried for five minutes in speedvac at low heat. The pellet was then treated with piperidine and the steps from the irradiated samples were followed.

Footprinting. A 1.1 μL volume of 10 X DNase I reaction buffer was added to preincubated DNA-netropsin sample followed by 1 μL of Dnase 1 (U/μL). The sample was digested for 5 min. at 5 ^{o}C followed by the addition of cold ethanol. The sample was placed in the -80 ^{o}C or, freezer for thirty minutes; the procedure for precipitation was followed. Studies were done varying DNase I buffer from 1.1 to 4.4 and DNase I from 1 to 4 to obtain the best condition for footprinting in these in experiments.

Perrin Plot Calculation. Samples were prepared as described above. To determine the quenching cylinder of the DNA, experiments were run varying the concentration of netropsin from 0 μM to 10 μM and holding the DNA concentration constant at 5 μM. The samples were irradiated at 420 nm for the predetermined time for each duplex. The irradiated samples along with a dark control for each duplex were precipitated, treated

with piperidine and analyzed by electrophoresis. The gels obtained were quantified using a Fuji Phosphorimager. The results were plotted as ln (I_o/I) vs. the concentration of netropsin, where I_o is the intensity (radioactive count) in the absence of netropsin and I is the intensity in the presence of netropsin. The slope obtained was used in the Perrin formulation (17) to calculate the quenching radius.

$$Y = NV\,[Q] \qquad \text{Eq. (1)}$$

Where Y is ln I_o/I, N is Avogadro's number, V is Volume, and [Q] is the quencher concentration. The equation for the volume of a cylinder was used to solve for the radius.

Reference

(1) Sanii, L., Schuster, G.B. *J. Am. Chem. Soc.* **2000**, *122*, 11545-11546.

(2) Abu-Daya, A., Brown, P. M., Fox, K. R. *Nucleic Acids Res.* **1995**, *23*, 3385-3392.

(3) Sartor, V., Boone, E., Schuster, G. B. *J. Phys. Chem. B* **2001**, *105*, 11057-11059.

(4) Rentzeperis, D., Marky, L. A., Dwyer, T. J., Geierstanger, B. H., Pelton, J. G., Wemmer, D. E. *Biochemistry* **1995**, *34*, 2937-2945.

(5) Baguley, B. C. *Mol. Cell. Biochem* **1982**, *43*, 167-181.

(6) Fish, E. L., Lane, M. J., Vournakis, J. N. *Biochemistry* **1988**, *27*, 6026-6032.

(7) Schuster, G. B. *Acc. Chem. Res.* **2000**, *33*, 253-260.

(8) Liu, C., Schuster, G. B. *J. Am. Chem. Soc.* **2003**, *125*, 6098-6102.

(9) Haworth, I. S., Rodger, A., Richards, W. G. *Proc. R. Soc. Lond. B* **1991**, *244*, 107-116.

(10) Kanvah, S., Schuster, G. B. *J. Am. Chem. Soc.* **2002**, *124*, 11286-11287.

(11) Turro, N. J. *Modern Molecular Photochemistry*; The Benjamin/Cummings Publishing Co., Inc.: Menlo Park, 1978.

(12) Liu, C., Hernandez, R., Schuster, G. B. *J. Am. Chem. Soc.* **2004**, *126*, 2877-2884.

(13) Jones, R. M., Lu, L., Helgeson, R., bergstedt, T. S., McBranch, W., Whitten, D. G. *Proc. Natl. Acad. Sci. USA* **2001**, *98*, 14769-14772.

(14) Neidle, S. *Nat. Prod. Rep.* **2001**, *18*, 291-309.

Chapter V: Distamycin effect on One-Electron oxidation

Another minor groove binder was also tested in order to determine if the effects on oxidative damage seen in the case with netropsin holds true for other minor groove binders. Distamycin A was used in charge transfer experiments to compare the results to what was found with netropsin. Although an extensive study was not performed with distamycin, results found in this chapter coincide with results found in chapter 3.

Distamycin A

Distamycin A is an antibiotic that binds to tracts of four of more A:T base pairs[1,2]. It is closely related to netropsin in structure as well as in its binding to DNA characteristics (Figure 5-1). It contains three methyl pyrrole groups as oppose to netropsin's two. It also has a carboxyl group as oppose to the guanidinium group found in netropsin. This gives distamycin a monocationic character instead of the dicationic character on netropsin. This also affects the way distamycin binds in the minor groove of the DNA duplex.

Distamycin can bind within the minor groove of a DNA duplex in by a 1:1 mode as well as side by side in a 2:1, distamycin:DNA[3-5]. The molecules run anti-parallel to one another so that the charged ends are on opposite ends of the binding site. Therefore the likely-hood of repulsion is minimized. There have been several renderings reporting the binding mode for distamycin to DNA[1]. In some cases, the hydrogens on the amide

groups as well as the hydrogens from the pyrrole groups contribute to the binding within the minor groove. They all seem to have differences in the way distamycin binds. In actuality the binding mode should be dependent on the A:T sequence. The hydrogen on the pyrrole and the hydrogen on its neighboring amine form H-bonds with the same DNA base. In the case netropsin, each of the amide hydrogens form two bonds with two different DNA bases as explained in chapter 3.

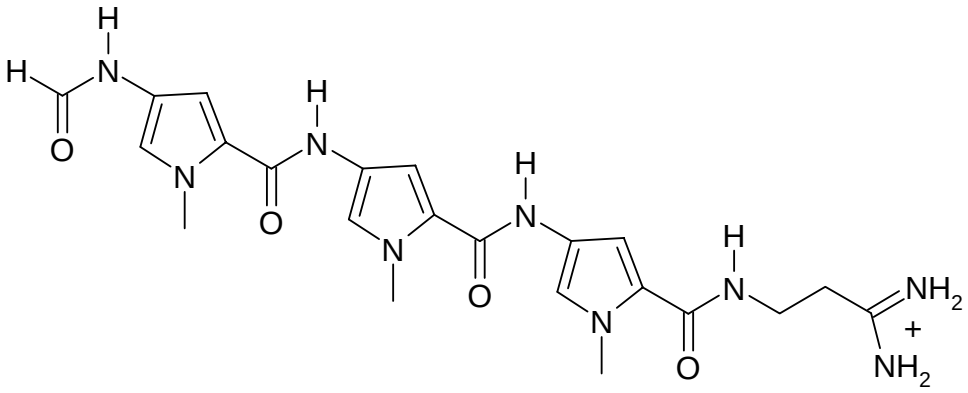

Figure 5-1 The distamycin A structure.

The monocationic character of the distamycin gives it the ability to bind in the minor groove in a side by side fashion[6]. Due to netropsin's dicationic character netropsin is not able to bind in this way because the positive charges repel one another. The distamycin molecules can stack in the minor groove anti parallel to one another. When there is a narrow minor groove, the 1:1 mode is preferred and when the minor groove is wider the 2:1 (distamycin:DNA) is often found[7].

Distamycin binding constants are slightly higher than that of netropsin when in a 1:1 with DNA[8]. Like the binding experiments involving netropsin, these values reported in literature range from 10^6 to 10^9 because of the different experimental conditions used by different research groups [7,9]. When in a 2:1 ratio (distamycin:DNA), its reported association constant is 10^{16} M^{-1}. The the kon for distamycin and DNA in 1:1 is 7 * 107 M-1 s-1 and the k_{off} ranges from 10 – 100 M-1 s^{-1} showing the most of the distamycin will be bound the DNA at any given time [10]. The difference between the

distamycin and netropsin binding constants can be contributed to the third pyrrole group causing a more stabilizing affect of the DNA duplex[11]. There are more hydrogen bonds created between the distamycin and the DNA bases allowing for slightly stronger binding. Overall the binding constants are of the same order.

Distamycin Concentration Studies

The DNA duplex studied in the distamycin experiments are duplex1 and duplex3 from chapter 4. Concentration dependent studies were performed that were similar done for netropsin. The distamycin concentrations used were verified by UV-vis spectroscopy by using the extinction coefficient 37000 and 303 nm[8]. The same experimental method was used as explained in the previous chapter. Netropsin's concentration was varied

from 0 – 20 μM with a fixed concentration of DNA (5 μM). The concentrations were doubled due to 2:1 binding mode of the distamycin.

The results show that distamycin displays the same effects as netropsin. As distamycin is titrated in, the amount of overall damage at the d(GG) steps was decreases (Figure 5-3). In the case of the duplex1, the binding 10 μM concentration was enough to stop the damage as seen in netropsin. Damage seen in duplex3 was ceased when distamycin reached 5 μM in concentration.

The data obtained from phosphorimagery was used to determine the quenching radius of distamycin for duplex1. Due to the lack of data this was not performed for duplex3. A semilog plot of the intensity was created and the quenching radius was calculated from the data.

Discussion

Although distamycin appeared to have the same effect on electron oxidation as netropsin, a difference in mechanism of quenching was observed. It appeared the distamycin did not have the affect of increasing the damage seen at the distal step as seen in the cases of netropsin when in 1:1 concentration with DNA. This could be caused by the distamycin not totally displacing all the water in the minor groove therefore not affecting the rate of trapping.

The quenching cylinder for the distamycin was calculated to be 5.0 * 10 $Å^3$. This was slightly lower than that of the netropsin quenching cylinder. The radii of the two duplexes were the same within experimental error.

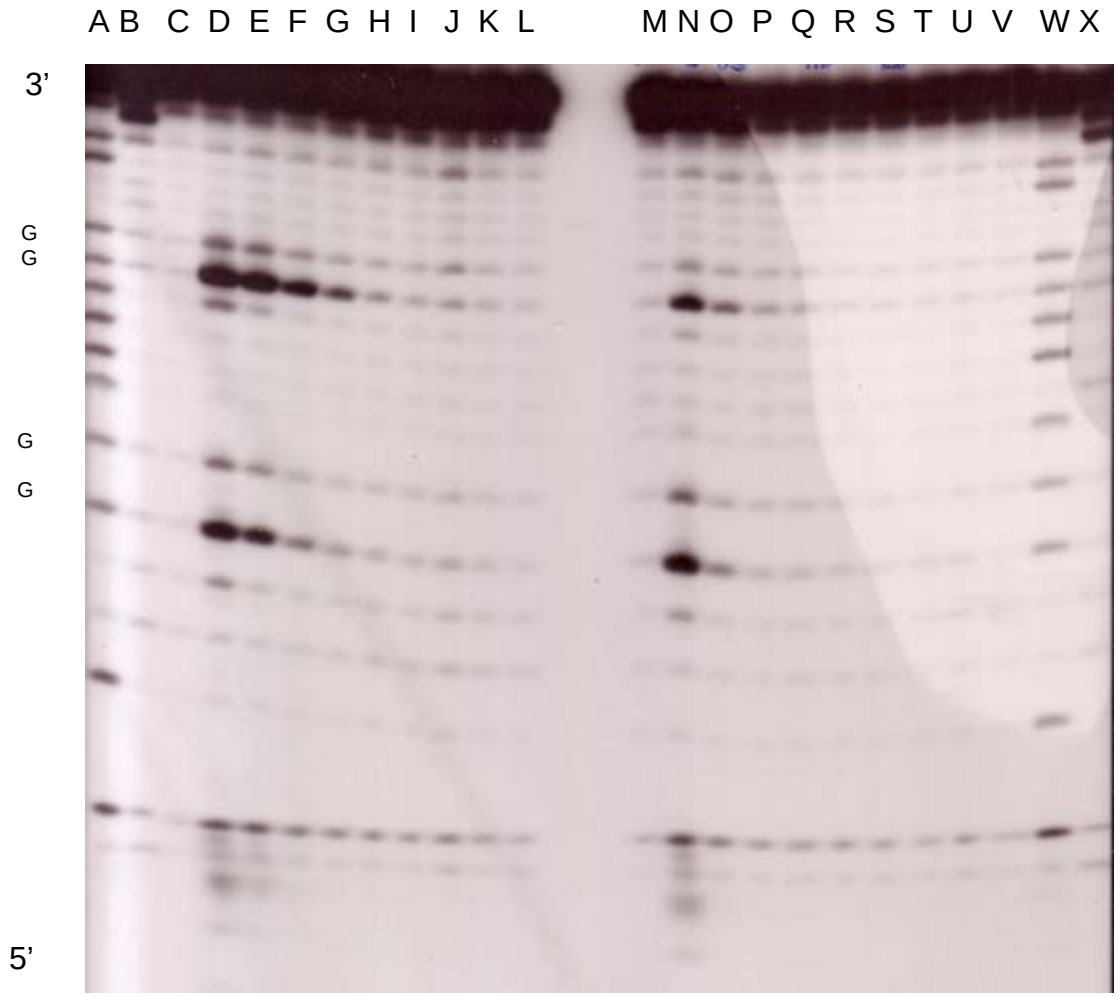

Figure 5-3. The autoradiogram of the distamycin concentration dependence study. The effect of distamycin on oxidative damage when titrate in duplex1 and duplex3. The concentration was varied from 0-20 μM of distamycin (in 0.5 μM increments) with a fixed concentration of DNA at 5 μM The A-L experimental lanes contain the duplex1 samples and M-X are the experimental lanes for duplex3 samples. Lanes C & M, dark controls; D & N, light controls. Lanes E and O 0.5:1); F and P (1:1); G and Q (1.5:1); H and R (2:1); I and R (2.5:1); J and S (3:1); K and T (3.5:1); and L and U (4:2). Lanes A and B are the A/G and T sequencing for duplex1 and W and X are for duplex3.

Conclusion

The results found for this set of experiments have shown that distamycin not only similar in structure and binding mode but also has similar electrochemical properties as netropsin. When protecting DNA against oxidative damage these two minor groove binders can be interchanged to give the desired effect. If further investigation was done and the peak potential of distamycin was taken, we would more than likely see a three peak potential due to the pyrrole or possibly a lower potential than that of netropsin. In conclusion the netropsin and distamycin have the ability to protect DNA from oxidative damage when it is in a certain range to the DNA duplex.

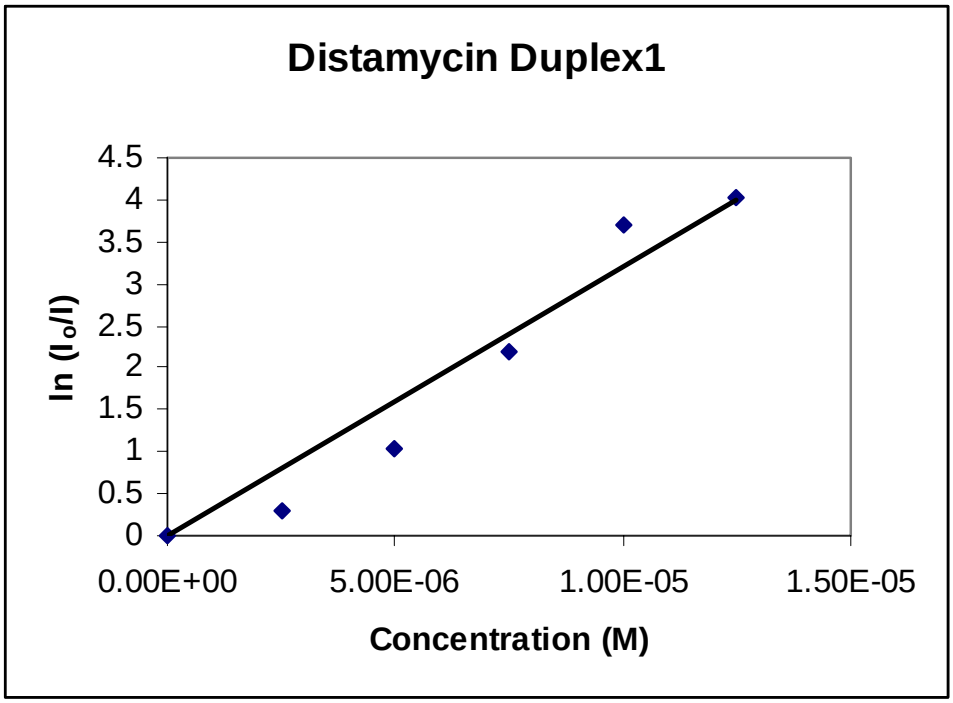

Figure 5-4. The semilog plot of data obtained from the concentration dependence of distamycin on duplex1 study.

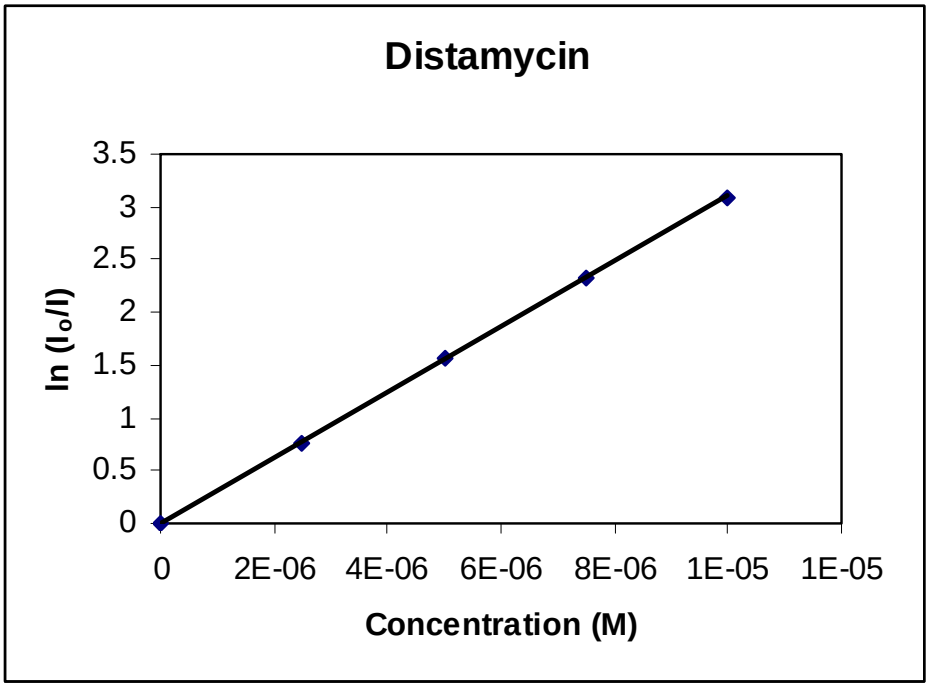

Figure 5-5. The semilog plot of data obtained from the concentration dependence of distamycin on duplex3 study.

Table 5-1 The calculated values for the quenching radii of the three main DNA duplex 1 and 3 using the Perrin Formulation.

DNA (Duplex)	Radius
Duplex (1)	1500 Å
Duplex (3)	1500 Å

References:

(1) Pelton, J. G., Wemmer, D. E. *Biochemistry* **1988**, *27*, 8088-8096.

(2) Rentzeperis, D., Marky, L. A., Dwyer, T. J., Geierstanger, B. H., Pelton, J. G., Wemmer, D. E. *Biochemistry* **1995**, *34*, 2937-2945.

(3) Pelton, J. G., Wemmer, D. E. *Proc. Natl. Acad. Sci. U.S.A.* **1989**, *86*, 5723-5727.

(4) Pelton, J. G., Wemmer, D. E. *J. Am. Chem. Soc.* **1990**, *112*, 1393-1399.

(5) Pelton, J. G., Wemmer, D. E. *J. Biomol. Struct. & Dyn.* **1990**, *8*, 81-97.

(6) Chen, X., Ramakrishnan, B., Sundaralingam, M. *J. Mol. Biol.* **1997**, *267*, 1157-1170.

(7) Lah, J., Vesnaver, G. *Biochemistry* **2000**, *39*, 9317-9326.

(8) Fish, E. L., Lane, M. J., Vournakis, J. N. *Biochemistry* **1988**, *27*, 6026-6032.

(9) Browne, K. A., He, G., Bruice, T. C. *J. Am. Chem. Soc.* **1993**, *115*, 7072-7079.

(10) Baliga, R., Crothers, D. M. *Proc. Natl. Acad. Sci. U.S.A.* **2000**, *97*, 7814-7818.

(11) Klevit, R. E., Wemmer, D. E., Reid, B. R. *Biochemistry* **1986**, *25*, 3296.